High Resolution Identification of Bioparticle Subpopulations with Electrophysical Properties

by

Yameng Liu

A Dissertation Presented in Partial Fulfillment
of the Requirements for the Degree
Doctor of Philosophy

Approved March 2020 by the
Graduate Supervisory Committee:

Mark Hayes, Chair
Chad Borges
Xu Wang

ARIZONA STATE UNIVERSITY

May 2020

ABSTRACT

There is increasing interest and demand in biology studies for identifying and characterizing rare cells or bioparticle subtypes. These subpopulations demonstrate special function, as examples, in multipotent proliferation, immune system response, and cancer diagnosis. Current techniques for separation and identification of these targets lack the accuracy and sensitivity needed to interrogate the complex and diverse bioparticle mixtures. High resolution separations of unlabeled and unaltered cells is an emerging capability. In particular, electric field-driven punctuated microgradient separations have shown high resolution separations of bioparticles. These separations are based on biophysical properties of the un-altered bioparticles. Here, the properties of the bioparticles were identified by ratio of electrokinetic (EK) to dielectrophoretic (DEP) mobilities.

As part of this dissertation, high-resolution separations have been applied to neural stem and progenitor cells (NSPCs). The abundance of NSPCs captured with different range of ratio of EK to DEP mobilities are consistent with the final fate trends of the populations. This supports the idea of unbiased and unlabeled high-resolution separation of NSPCs to specific fates is possible. In addition, a new strategy to generate reproducible subpopulations using varied applied potential were employed for studying insulin vesicles from beta cells. The isolated subpopulations demonstrated that the insulin vesicles are heterogenous and showed different distribution of mobility ratios when compared with glucose treated insulin vesicles. This is consistent with existing vesicle density and local concentration data. Furthermore, proteins, which are accepted as

challenging small bioparticles to be captured by electrophysical method, were concentrated by this technique. Proteins including IgG, lysozyme, α-chymotrypsinogen A were differentiated and characterized with the ratio factor. An extremely narrow bandwidth and high resolution characterization technique, which is experimentally simple and fast, has been developed for proteins. Finally, the native whole cell separation technique has also been applied for *Salmonella* serotype identification and differentiation for the first time. The technique generated full differentiation of four serotypes of *Salmonella*. These works may lead to a less expensive and more decentralized new tool and method for transplantation, proteomics, basic research, and microbiologists, working in parallel with other characterization methods.

ACKNOWLEDGEMENTS

To my research advisor, Prof. Mark A. Hayes, I would love to express my sincere appreciation not only for your professional instructions on my research, but also for the great time and efforts you devoted in training me without reservation. I acknowledge your generosity of offering me precious opportunities to widen my vision. Your profound experience and insightful persistence on research always direct me towards success when I am confused. Thank you for considering me to be one of your students. That is the luckiest thing ever happened to me after traveling 18 h by flight from one continent to another. The 4 and half years spent in our group is fruitful and these valuable memories will be the best gift for my whole life.

To my committees, Prof. Borges and Prof. Wang, thanks for taking this responsibility for helping with my academic progress. Prof. Borges, thanks for your approachable and reliable response whenever I have a question. Your class is always the best and in great details. Prof. Wang, thanks for providing useful tips on my research during poster session each year. Your wisdom and erudition impress me very often.

To my parents, thanks for all the love and encouragement, which motivates me to go forward and gives me reasons to help others. I am always proud of being rich in love because of you.

To Hayes lab members, so glad to meet each of you in my life. Dr. Fanyi Zhu, thanks for the accompany and help in both my life and research. Where you are makes me safe and rooted. Dr. Claire Crowther, thanks for all the research talks to help me improve. You made me brave enough to share my thoughts. Dr. Shannon Hilton, thank

you for your help on my oral exam. Dr. Jie Ding, I appreciate all the possibility you created for me and interesting ideas you shared. Jerry Sheu, I am so happy that you joined our group and thanks for making my stressful days easier. Your intelligence and concentration characteristics always make you outstanding and unique. Alex Ramirez, thanks for your help and suggestions on my English writings. Your maturation and consideration provided a lot of support to each of us.

To my friends and roommates, Hangkun, Minxi, Yue, Qi, and Shan, thanks for making my life lively and less lonely.

Thanks to ASU, this is an amazing experience!

TABLE OF CONTENTS

LIST OF FIGURES

CHAPTER 1

INTRODUCTION

The separation, isolation, and concentration of bioparticles has been the subject of decades of research across several disciplines. There is an emerging interest in subpopulation studies for their special function within basic and clinical research and biotechnology development. Separation is an essential step for characterizing bioparticle subpopulations to access accurate proteomic profiles. Current techniques for separating subpopulations are lacking accuracy and can be time consuming. More importantly, they are inadequate to understand the complexity and diversity of the bioparticle subpopulations. There is an increasing demand for developing appropriate tools and methods for subpopulation identification and separation. Here, a high-resolution separation method based on biophysical behaviors of the bioparticles is introduced. It aims to develop an unbiased isolation and characterization method for segregating and identifying subpopulations with higher resolution for further biochemical characterization.

Bioparticle subpopulation refers a type of subset population in complex biological tissues and fluids. Cells that are currently considered to be of the same population have subtypes that are differ in their abundance, propagation ability and localization [1]. Rapid, efficient methods are required to separate the cell subtypes for cellular biology, diagnostics and therapeutics. The accurate identification, characterization and separation of cell subpopulations contributes not only to basic research on how cell evolves, but also to biotechnology and clinical applications on developing transplantation strategies [2-3].

1.1 Significance of Bioparticle Subpopulation Studies

Subpopulations have their unique role in tumor relapse, immune system response, and metabolic control. Various types of bioparticle subpopulations have been described [4-6]. Examples of these studies include cancer stem cells for cancer diagnosis, progenitors with different proliferation activity, and cells with slower metabolism potential for transplant.

Stems cells are a widely studied rare subpopulation in cancer cells. Cancer stem cells have been identified in melanomas, ovarian cancer, hepatocellular carcinoma, pancreatic cancer, and colorectal cancer. They are a minority subset of cancer cells, retaining their self-renew and multipotent differentiation properties, contributing to tumor growth and propagation. Their multipotent properties result in the cellular heterogeneity generation, suggesting a need for separation towards investigating them [6-12]. They could be recognized and selected by specific common antigens or incubation preferences. The development of effectively targeting type of subpopulation for eradication will provide new approach for the detection and prevention of tumors.

For bone marrow cells, a plastic-adherent cells subpopulation was indicated to have greater potential for their multipotent capability and gene/cell therapy [13]. A subpopulation of small round cells was found in marrow stromal cells that are more likely to differentiate when compared to large cells. They also expressed different surface epitopes when compared to the larger cells. The subpopulation of interest showed negative CD 117 and Stro-1. The cells were sorted by culturing, showing rapid growth

and retention of their ability to differentiate. The potential of their use in marrow cell and gene therapies highlights the possible use of the separated subpopulations.

The cell subpopulations also exist in immune system which benefit transplantation. A subpopulation of mouse dendritic cells shows potential for significantly reduced T-cell stimulatory [14]. Satellite cells contain a subpopulation with lower metabolic activity than other cells in adult skeletal muscle stem cells. They were characterized and by $B220^{+}$ and separated by immunomagnetic technique. The results indicate that this type of separated cells is nonresponsive for T-cells recognition based on antigen specificity. The subpopulation studies provide an opportunity for better understanding of immune system response [15].

1.2 Techniques for Characterizing and Separating Bioparticle Subpopulations

Different techniques arise in concentrating, identifying, separating the subpopulations from complex and diverse bioparticle samples for studying their biology and mechanism. Some commonly used techniques for cell subpopulations sorting includes magnetic-activated cell sorting (MACS), fluorescent-activated cell (FACS) sorting gradient centrifugation, and microfluidic cell expression. For immunophenotyping techniques (such as MACS, FACS), the separation is based on particular surface antigens and markers were used for cell subpopulation characterization. For example, CD 133, CD 44, surface immunoglobulin were common antigens for detecting the levels of cell maturity by the presence or absence [16]. Gradient centrifugation is a cell density sorting method and has been applied to suspended particles using a nontoxic density medium. This method provides a tool for cell analysis and enrichment. Microfluidic cell sorting

has also emerged as a low-cost tool for accurate detection for cell populations with high complexity [1]. The separation is based on flow and forces the bioparticles experience. To explore how bioparticles are separated, multiple techniques for subpopulations isolation are introduced.

1.2.1 Flow cytometry

Flow cytometry is considered the "gold standard" for cell sorting [17]. This method separates single cells with multi-parameters for discrimination. The cell population after separation show high selection accuracy and purity. Multiple characteristics for the fluorescently-labeled bioparticles are distinguished by optical and fluorescence response. Markers are mostly bound to DNA/RNA or antibodies. These binding sites are located either on the surface membrane or in the cytoplasm of the bioparticles. Bioparticles are suspended as single particles and interrogated by light source. The optical signal at different angles were captured and analyzed. The single cells were sorted according to specific patterns of the different signals. This method has been applied to blood, bone marrow, urine, and body tissue samples. These include some clinical uses in immunology, blood banking, and genetic disorders. Flow cytometry is popular because of its fast and reproducible for cell sorting [18].

Early works identified a specific population of apoptotic cells in mouse thymocytes by flow cytometry through determining the percentage of apoptotic nuclei. The results were consistence with those obtained from electrophoretic and colorimetric methods. The work showed that flow cytometry can be a simple, rapid method for cell populations identification for tissues with heterogenous populations [19].

Holyoake et al. obtained a quiescent subpopulation of leukemic cells from bone marrow cells by fluorescence-activated cell sorting (FACS). This rare subset is a fraction of $CD34^+$ cells distinguished by labeling with Hoechst 33342 and Pyronin Y. This work demonstrated the existence of subset which contributed to a leukemic clone [20].

Flow cytometry was also used to isolate a subpopulation in head and neck squamous cell carcinoma samples. The isolation was based on the expression of CD10 surface marker [21]. This subpopulation was shown to be more likely to form spheres and tumors after transplanting into mice *in vivo*. Also, they are more resistance to medical treatment and radiation when compared with CD10-negative cells.

Li et al. identified a tumorigenic subpopulation by the expression of cell surface markers CD24, CD44 and epithelial specific antigen (ESA) in pancreatic cancer cells [12]. The mice with injected subsets after enrichment are 100-fold more likely to form tumors than controlled mice with negative-expressed cells injected. It may provide a new way for pancreatic cancer therapy and inform future works focused on cancer stem cell growth mechanisms.

1.2.2 Magnetic cell sorting

Magnetic cell sorting is an efficient, gentle cell sorting technique used for separation of rare cell populations from heterogenous mixtures with high throughput. Colloidal cells to be separated are labeled with magnetic nanoparticles through antibodies against antagonists on the cell surface [22]. High gradient magnetic filtration was used for cell sorting where unlabeled particles are eluted from the column. After removal of magnetic forces, the labeled particles are eluted and thereby isolated from the mixture.

The two types of cell enrichment are positive selection and negative selection. Positive selection is the collection of target cells. Negative selection is the depletion of non-targeted cells. The technique relies upon the accuracy and quality of the antibodies used to attach the magnetic particles to the cells, and common problems of cell aggregation and biological debris can limit the effectiveness of the technique. When compared to FACS, it has larger capacity and simpler sample preparation procedures. The FACS technique analyzes cells one-by-one which both increases the complexity of the sample suspension preparation and lowers the amount analyzed per unit time. Magnetic sorting can distinguish up to 10^{11} cells with in 30 min, compared to 10^{8} cells in 6 hours for FACS. The low forces which the cells experience in the magnetic field also allow the recovery of viable cells after sorting. The acceleration of cells in the nozzle by FACS is considered more to be more harmful than the force exerted on cells in MACS. One drawback of magnetic cell is that it provides only one parameter for cell sorting and this has been solved by MACS-MultiSort [23, 24]. This technique has been applied to a variety of cells enrichment and characterization, such as red blood cells, cancer stem cells, plant cells, and bacteria [25-30].

With regards to the cancer stem cells, in human oral squamous cell populations, the cancer stem cells result in higher chemoresistance. Qunzhou Zhang et al. identified a small subpopulation by magnetic cell sorting by isolating $CD133^{+}$ and $CD133^{-}$ phenotype cells. The $CD133^{+}$ showed higher clonogenicity and demonstrated resistance to chemotherapy [31].

Similar to cancer stem cells with multipotent differentiation capability, progenitors were also separated by MACS. Hematopoietic progenitor cells that are more committed in contrast to primary cells have been separated with immunomagnetic methods. These bone marrow cells were discriminated by expression of CD34. This separation gave higher enrichment (2000-fold) and recovery of the cells than other works, indicating the feasibility of using MACS to improve purification by other methods [32].

MACS has also been applied to separating cells related to nervous system. Jan Manent et al. enriched Schwann cells to 99% purity from peripheral nerves by MACS. The cells were conjugated to expression of $p75^{NGFR}$. After sorting the cells, they were plated and propagated indicating that the recovery and viability of the cells after enrichment. This was taken as supporting evidence of the gentler nature of the separation method [33]. They concluded that a highly efficient purification method for enriching Schwann cells has been established.

Cells with magnetic labeling can also be fluorescent labeled and thus magnetic cell sorting can be combined with flow cytometry to achieve further purification or characterization [22]. Magnetic cell sorting was used to characterize cancer stem cells in human brain tumors. Sheila K. Singh and co-workers labelled cells with microbeads and purified a subpopulation of $CD133^{+}$ cells combined with flow cytometry. The assay showed the cells initiate tumors while 1000-fold CD 133^{-} cells did not [34]. These results showed that magnetic cell sorting efficiently distinguished brain tumor stem cells from other tumor cells.

1.2.3 Cell culture selection

Cell culture has been widely applied for selecting subpopulations of viruses and mammalian and plant cells. The investigation of the cultivation contributes to our knowledge on the genetic and molecular levels. It also facilitates cell growth to expected tropism [35].

The selection of cells can be controlled by the design of the cell culture conditions. A 3D scaffold was used to select cancer stem cell subpopulations based on creating microenvironments similar to tumor growth conditions. Mouse renal adenocarcinoma cells were studied and incubated in macrobeads with diameters of 6 to 8 mm. The selected cells had increased metabolic status, demonstrating that the macrobeads approach is selective towards identifying cancer stem cell subpopulation in culture [36].

Cell subpopulations can also be selected by their adherent conditions. Dong Fang et al. found a subpopulation of melanoma cells showing nonadherent spheres propagation. The subset is able to self-renew and demonstrated more tumorigenic behaviors. The suspended spheroid cells were separated from mixed cultures. Flow cytometry indicated the expression of CD20. The culturing method selectively separated cell subpopulations with same surface antigens based on their behaviors in culturing medium [11].

Culture selection of subpopulations has also been applied to virus. Influenza B virus cultured in eggs gives a subpopulation that contains monoclonal antigen 238 while those cultured in mammalian cells has antigen 209 [37]. The work showed evidence of

subpopulation selection by different host cells and has significance for vaccine safety and efficacy development.

1.2.4 Gradient centrifugation

Gradient centrifugation was first introduced by Myron K. Brakke in 1951 and it has been the predominant method used for suspended particle separations [38]. Mixed particles samples are introduced in solution at the top of a density gradient. Gradient density solution selection is dependent upon the particles to be separated. Early works took advantage of sucrose solutions with different densities for potato yellow-dwarf virus concentration and purification. A more-developed medium for gradient centrifugation includes Iodixanol. Iodixanol has advantages of low toxicity and forms gradient by itself. Gradient centrifugation based on Iodixanol has been shown to separate organelles including lysosomes, peroxisomes, and mitochondria from mouse liver cells. This work showed a higher resolution separation than previous methods used for organelle isolations [39, 40].

Separation parameters of gradient centrifugation used to separate particles are dependent on different operational methods. With continued centrifugation, the particles progress until they reach an equilibrium density. The separation is based on density of the particle. With a shorter time of the centrifugation, the separation is related with the sedimentation rates, not only density, but also ratios of mass to frictional constant. With osmotic pressure gradient, the separation factor has identical osmotic pressure as an extra factor. Aggregation of solution droplets causes sedimentation and lead to the spreading of

the separation zone. The convenience and efficiency of this method has enabled to be applied to separation of virus, bacteria, DNA, mammal cells, and organelles.

Human natural killer (NK) cells were characterized and enriched by gradient centrifugation [41]. The NK were separated from lymphocytes and activity against leukemic K-562 cell line peak was found in low density fraction and absent in high density fraction. This work established an efficient method for enriching human NK cells when compared to other methods based on membrane properties.

Another use of gradient centrifugation was applied to cell organelles [42]. Schwitzguebel et al. purified peroxisomes and mitochondria from spinach by Percoll, which is compose of colloidal silica particles covered with polyvinylpyrrolidone. The method established the conditions for purifying plant organelles.

Bacteria has also been separated by gradient centrifugation. Urografin was used to separate *Bacillus megaterium* spores and vegetative cells. The density differences are related to the ability to be activated and resistance to death caused by increasing temperature. Gradient centrifugation can be used as a measurement of bacteria culture degree and efficiency [43].

Small molecules such as DNA were also fractionated by a solution of Cs_2SO_4-Ag^+ by the differences of their density. Three components were separated with similar G+C contents. This work successfully separated DNA related with buoyant density, CsCl bands and melting curves [44].

1.2.5 Microfluidic cell sorting

Recent interest in studying cell identification and the complexity of cell populations has increased the popularity of microfluidic cell sorting, especially for rare cell subpopulations. Microfluidics have reduced sample consumption and reagent waste. The microfluidic devices are portable. More importantly, the method can be label-free for bioparticles. Comparatively, flow cytometry strategies are inefficient for identifying rare cell subpopulations or the genetic differences between cells [45]. Microfluidic control systems and platform have been used for cell sorting and single cell analysis based on phenotype for diagnostic applications. The improvement of the platforms enables the high throughput of the single cell analysis [46].

Magnetic-bead based immunoassay microfluidic devices has been applied for purifying hematopoietic stem cells [47]. Target stem cells were bound with magnetic beads and the work has a high efficiency resulting in 88% purification. This work provided a more accurate and less bulky method for isolating hematopoietic cells.

Microfluidic adhesion-based process is one of the commonly used applications for cell subpopulation analysis. The microfluidic devices are coated with antibodies which can interact with specific antigens on the surface of the cells. The capture of a subpopulations of the cells are based on their common membrane properties and this cause the adhesion of the subpopulation. Controlled flow rate and firm adhesion are required [46]. DNA aptamer adhesive device was used for enrichment of three types of cancer cells. The enrichment of the subpopulations is as high as 135-fold. When evaluated by flow cytometry, the purification was as high as 96% [48]. After isolation,

the cells showed comparable propagation rate as the control cells. The adhesive-based microfluidics has been used for the isolation of rare cells from heterogeneous cell mixtures.

Furthermore, microchips based on DEP has also been used for viable and nonviable cell sorting [49]. This was applied on living and nonliving yeast cells. With varying flow rate, yeast cells were purified with high efficiency (97.3% and 74.3%).

Subpopulation separation techniques including flow cytometry, MACS, cell culture selection, gradient centrifugation, microfluidic cell sorting were used, aiming at complementing the profiles of bioparticle populations. They are providing useful tools to help to understand the diversity and complexity of tissues or cell populations.

1.3 Dissertation Overview

This dissertation shows the identification and characterization of bioparticle subpopulations by direct current insulator-based dielectrophoresis (DC-iDEP). Chapter 1 describes the overview of bioparticle subpopulations, including the recent types of subpopulation studied, significance and techniques for characterization the subsets. Chapter 2 introduces dielectrophoresis technique, composed of the definition of dielectrophoresis, high resolution characteristics of the technique, the forces bioparticle experience and bioparticle concentration theory in a microfluidic device based on dielectrophoresis.

In Chapters 3 and 4, the subpopulations of neural stem and progenitor cells and insulin vesicles from beta cells were studied by DC-iDEP, respectively. In Chapter 3, neural stem and progenitor cells were identified according to their biophysical properties

and showed a relative heterogeneity than control HEK 293 cells. The final fate trends are consistent with the cells detected in the microfluidic devices according to the composition of specific stage cells. In Chapter 4, insulin vesicles subpopulations were concentrated and isolated using high resolution separation based on DC-iDEP. Several subpopulations were identified with consistent biophysical properties with varying voltages applied. The decreasing voltages applied isolated some low ratio mobility subpopulations mixed at high voltages. Furthermore, insulin vesicles from glucose-treated beta cells showed distinguishing behaviors comparable to previous studies.

Chapter 5 demonstrates an application of protein differentiation based on a newly developed theory for dielectrophoresis. Proteins include immunoglobin G, α−chymotrypsinogen A, and lysozyme, which were concentrated and characterized by their biophysical properties. Four serotypes of *Salmonella* were characterized and distinguished for the work presented in Chapter 6. This is the first-time concentration and characterization of *Salmonella* has been accomplished by dielectrophoresis. The four strains show different ratios of electrokinetic to dielectrokinetic mobilities and individually with electrokinetic mobility.

Chapter 7 summarized the work in the dissertation and explicit future directions based on the work has been done.

1.4 References

[1] Darzynkiewicz, Zbigniew, et al. *Recent Advances in Cytometry, Part B: Advances in Applications*. Academic Press, 2011.

[2] Prince, M. E., et al. "Identification of a subpopulation of cells with cancer stem cell properties in head and neck squamous cell carcinoma." *Proceedings of the National Academy of Sciences* 104.3 (2007): 973-978.

[3] Holyoake, Tessa, et al. "Isolation of a highly quiescent subpopulation of primitive leukemic cells in chronic myeloid leukemia." *Blood, The Journal of the American Society of Hematology* 94.6 (1999): 2056-2064.

[4] Flow cytometry Thomas A. Fleisher, João Bosco de Oliveira, in Clinical Immunology (Third Edition), 2008

[5] Delves, Peter J., and Ivan Maurice Roitt. *Encyclopedia of immunology*. Academic Press, 1998.

[6] Pang, Roberta, et al. "A subpopulation of CD26+ cancer stem cells with metastatic capacity in human colorectal cancer." *Cell stem cell* 6.6 (2010): 603-615.

[7] Wicha, Max S., Suling Liu, and Gabriela Dontu. "Cancer stem cells: an old idea—a paradigm shift." *Cancer research* 66.4 (2006): 1883-1890.

[8] Prince, M. E., et al. "Identification of a subpopulation of cells with cancer stem cell properties in head and neck squamous cell carcinoma." *Proceedings of the National Academy of Sciences* 104.3 (2007): 973-978.

[9] Suetsugu, Atsushi, et al. "Characterization of CD133+ hepatocellular carcinoma cells as cancer stem/progenitor cells." *Biochemical and biophysical research communications*351.4 (2006): 820-824.

[10] Zhang, Shu, et al. "Identification and characterization of ovarian cancer-initiating cells from primary human tumors." *Cancer research* 68.11 (2008): 4311-4320.

[11] Fang, Dong, et al. "A tumorigenic subpopulation with stem cell properties in melanomas." *Cancer research* 65.20 (2005): 9328-9337.

[12] Fang, Dong, et al. "A tumorigenic subpopulation with stem cell properties in melanomas." *Cancer research* 65.20 (2005): 9328-9337.

[13] Colter, David C., et al. "Rapid expansion of recycling stem cells in cultures of plastic-adherent cells from human bone marrow." *Proceedings of the National Academy of Sciences*97.7 (2000): 3213-3218.

[14] Martín, Pilar, et al. "Characterization of a new subpopulation of mouse CD8alpha+ B220+ dendritic cells endowed with type 1 interferon production capacity and tolerogenic potential." *Blood* 100.2 (2002): 383-390.

[15] Rocheteau, Pierre, et al. "A subpopulation of adult skeletal muscle stem cells retains all template DNA strands after cell division." Cell 148.1-2 (2012): 112-125.

[16] Terstappen, L. W., Meredith Safford, and Michael R. Loken. "Flow cytometric analysis of human bone marrow. III. Neutrophil maturation." *Leukemia* 4.9 (1990): 657-663.

[17] Bhagat, Ali Asgar S., et al. "Microfluidics for cell separation." *Medical & biological engineering & computing* 48.10 (2010): 999-1014.

[18] Brown, Michael, and Carl Wittwer. "Flow cytometry: principles and clinical applications in hematology." *Clinical chemistry*46.8 (2000): 1221-1229.

[19] Nicoletti, I., et al. "A rapid and simple method for measuring thymocyte apoptosis by propidium iodide staining and flow cytometry." *Journal of immunological methods* 139.2 (1991): 271-279.

[20] Holyoake, Tessa, et al. "Isolation of a highly quiescent subpopulation of primitive leukemic cells in chronic myeloid leukemia." *Blood, The Journal of the American Society of Hematology* 94.6 (1999): 2056-2064.

[21] Fukusumi, T., et al. "CD10 as a novel marker of therapeutic resistance and cancer stem cells in head and neck squamous cell carcinoma." *British journal of cancer* 111.3 (2014): 506-514.

[22] Radbruch, Andreas, et al. "High-gradient magnetic cell sorting." *Methods in cell biology*. Vol. 42. Academic Press, 1994. 387-403.

[23] Owen, Charles S., and Norman L. Sykes. "Magnetic labeling and cell sorting." *Journal of immunological methods* 73.1 (1984): 41-48.

[24] Thiel, Andreas, Alexander Scheffold, and Andreas Radbruch. "Immunomagnetic cell sorting—pushing the limits." *Immunotechnology* 4.2 (1998): 89-96.

[25] Hansel, Trevor T., et al. "An improved immunomagnetic procedure for the isolation of highly purified human blood eosinophils." *Journal of immunological methods* 145.1-2 (1991): 105-110.

[26] Schmitz, Jürgen, and Andreas Radbruch. "Distinct antigen presenting cell-derived signals induce Th cell proliferation and expression of effector cytokines." *International immunology* 4.1 (1992): 43-51.

[27] Kato, Kimitaka, and Andreas Radbruch. "Isolation and characterization of CD34+ hematopoietic stem cells from human peripheral blood by high-gradient magnetic cell sorting." *Cytometry: The Journal of the International Society for Analytical Cytology* 14.4 (1993): 384-392.

[28] Vollenweider, Peter, et al. "Differential effects of hyperinsulinemia and carbohydrate metabolism on sympathetic nerve activity and muscle blood flow in humans." *The Journal of clinical investigation* 92.1 (1993): 147-154.

[29] Irsch, Johanns, et al. "Switch recombination in normal IgA1+ B lymphocytes." *Proceedings of the National Academy of Sciences* 91.4 (1994): 1323-1327.

[30] Kronick, Paul, and Richard W. Gilpin. "Use of superparamagnetic particles for isolation of cells." *Journal of biochemical and biophysical methods* 12.1-2 (1986): 73-80.

[31] Zhang, Qunzhou, et al. "A subpopulation of CD133+ cancer stem-like cells characterized in human oral squamous cell carcinoma confer resistance to chemotherapy." *Cancer letters*289.2 (2010): 151-160.

[32] Servida, Federica, et al. "Functional and morphological characterization of immunomagnetically selected CD34+ hematopoietic progenitor cells." *Stem Cells* 14.4 (1996): 430-438.

[33] Manent, Jan, et al. "Magnetic cell sorting for enriching Schwann cells from adult mouse peripheral nerves." *Journal of neuroscience methods* 123.2 (2003): 167-173.

[34] Singh, Sheila K., et al. "Identification of human brain tumour initiating cells." *nature* 432.7015 (2004): 396-401.

[35] Hoffmann, Beate, et al. "A new Medicago truncatula line with superior in vitro regeneration, transformation, and symbiotic properties isolated through cell culture selection." *Molecular plant-microbe interactions* 10.3 (1997): 307-315.

[36] Smith, Barry H., et al. "Three-dimensional culture of mouse renal carcinoma cells in agarose macrobeads selects for a subpopulation of cells with cancer stem cell or cancer progenitor properties." *Cancer research* 71.3 (2011): 716-724.

[37] Schild, G. C., et al. "Evidence for host-cell selection of influenza virus antigenic variants." *Nature* 303.5919 (1983): 706-709.

[38] Brakke, Myron K. "Density gradient centrifugation: a new separation technique1." *Journal of the American Chemical Society* 73.4 (1951): 1847-1848.

[39] Ford, T., J. Graham, and D. Rickwood. "Iodixanol: a nonionic iso-osmotic centrifugation medium for the formation of self-generated gradients." *Analytical biochemistry* 220.2 (1994): 360-366.

[40] Graham, J., T. Ford, and D. Rickwood. "The preparation of subcellular organelles from mouse liver in self-generated gradients of iodixanol." *Analytical biochemistry* 220.2 (1994): 367-373.

[41] Timonen, T., and E1 Saksela. "Isolation of human NK cells by density gradient centrifugation." *Journal of immunological methods* 36.3-4 (1980): 285-291.

[42] Schwitzguebel, Jean-Paul, and Paul-André Siegenthaler. "Purification of peroxisomes and mitochondria from spinach leaf by Percoll gradient centrifugation." *Plant Physiology* 75.3 (1984): 670-674.

[43] Tamir, Hadassah, and Charles Gilvarg. "Density gradient centrifugation for the separation of sporulating forms of bacteria." *Journal of Biological Chemistry* 241.5 (1966): 1085-1090.

[44] Filipski, Jan, Jean-Paul Thiery, and Giorgio Bernardi. "An analysis of the bovine genome by Cs2SO4—Ag+ density gradient centrifugation." *Journal of molecular biology* 80.1 (1973): 177-197.

[45] Autebert, Julien, et al. "Microfluidic: an innovative tool for efficient cell sorting." *Methods* 57.3 (2012): 297-307.

[46] Reece, Amy, et al. "Microfluidic techniques for high throughput single cell analysis." *Current opinion in biotechnology* 40 (2016): 90-96.

[47] Wu, Huei-Wen, et al. "An integrated microfluidic system for isolation, counting, and sorting of hematopoietic stem cells." *Biomicrofluidics* 4.2 (2010): 024112.

[48] Xu, Ye, et al. "Aptamer-based microfluidic device for enrichment, sorting, and detection of multiple cancer cells." *Analytical chemistry* 81.17 (2009): 7436-7442.

[49] Doh, Il, and Young-Ho Cho. "A continuous cell separation chip using hydrodynamic dielectrophoresis (DEP) process." *Sensors and Actuators A: Physical* 121.1 (2005): 59-65.

CHAPTER 2

DIELECTROPHORESIS THEORY AND BACKGROUND

2.1 Dielectrophoresis Theory

The properties of particles dispersed in a buffer or solvent in the presence of an external electric field exhibit behavior directly according to their physical makeup. In this dissertation, biophysical behaviors are identified within a DC-iDEP device by the applied voltage and location of cell or bioparticle capture. The DC-iDEP process captures particles in a microfluidic channel based on electrokinetic and dielectrophoretic effects and provides a deterministic biophysical characterization of those particles.[25-27] The electrokinetic force is a combination of electrophoretic force and electroosmotic flow effect. The electrophoretic force can be expressed as:

$$\vec{F}_{EP} = 6\pi r \varepsilon_m \zeta_p \vec{E} \qquad (1)$$

where r is the radius of the particle, ε_m is the dielectric constant of the solution, $\vec{E}$ is the electric field intensity, and ζ_p is the zeta potential of the particle. The electroosmotic flow effect is the motion of the liquid in a microfluidic channel as a result of the Debye layer. This effect is a function of the viscosity (η), the permittivity, and the zeta (ζ_m) of the medium/wall system. Reflecting these processes, EK mobility (μ_{EK}) is defined by

$$\mu_{EK} = \mu_{EP} + \mu_{EOF} \qquad (4)$$

where μ_{EP} is EP mobility and μ_{EOF} is EOF mobility. And they can be described by

$$\mu_{EP} = \frac{\varepsilon_m \zeta_p}{\eta} \qquad (5)$$

$$\mu_{EOF} = \frac{-\varepsilon_m \zeta_m}{\eta} . \qquad (6)$$

Dielectrophoretic force ($\vec{F}_{DEP}$) is caused by the interaction between a non-uniform electric field and a dielectric particle of radius, *r*:

$$\vec{F}_{DEP} = 2\pi\varepsilon_m r^3 f_{CM} \nabla \left| \vec{E} \right|^2 \qquad (2)$$

where, $\nabla |\vec{E}|$ is the gradient of the electric field and f_{CM} is the Clausius-Mossotti factor. Higher order electrophysical effects are described by DEP mobility, μ_{DEP}, and can be expressed as [1, 2, 3]:

$$\mu_{DEP} = \frac{\varepsilon_m r^2 f_{CM}}{3\eta} \qquad (3)$$

DEP and EK effects exerted on a single cell or bioparticle were used to determine the properties of the particles by trapping them at different positions in a DEP device.

The particles are captured when velocity along the field line is zero such that EK velocity is equal to DEP velocity. The capture condition is described as following [26,28]:

$$\vec{J} \cdot \vec{E} = 0 \qquad (7)$$

$$\frac{\nabla |\vec{E}|^2}{E^2} \cdot \vec{E} \geq \frac{\mu_{EK}}{\mu_{DEP}} \qquad (8)$$

where $\vec{J}$ is particle flux. Theoretical estimates and previous studies suggest extremely high-resolution separation of DC-iDEP.[27] The ratio of the electrokinetic mobility over the dielectrophoretic mobility ($\frac{\mu_{EK}}{\mu_{DEP}}$, electrokinetic mobility ratio, EKMr) can be used to quantify subtle electrophysical differences of particles.

2.2 Microfluidic Device and Fabrication

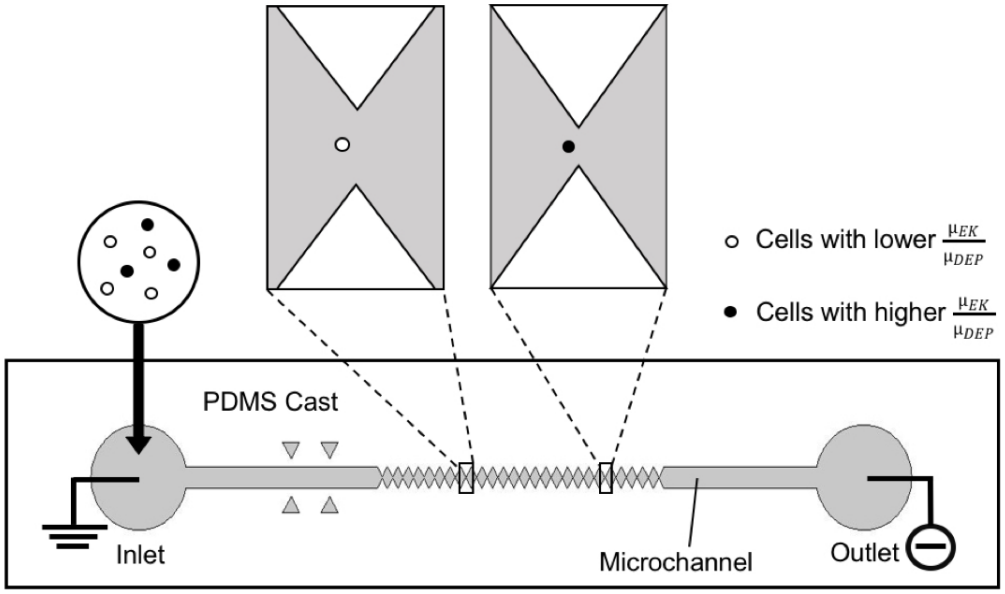

Figure 2.1. Schematic of DC-iDEP device and capture behavior of bioparticles. The channel (grey) was constricted by an increasing size of paired triangular (gate) insulator material (white), creating decreasing pitch width ranging from 945 μm to 27 μm for V1 type channel and 73 μm to 25 μm for V2 type channel. Samples were introduced from the inlet and a direct current potential was applied between the inlet and outlet of the channel. Bioparticles with lower EKMr (white circle) are captured with larger width gates and bioparticles with higher EKMr (black circle) are captured with smaller gates. Dotted lines in the upper illustration represent centerline for computational simulations. The length of V1 and V2 channel is 4.2 cm and 3.5 cm. All the recordings for V1 channel was at 27 μm gate.

Two designs of DC-iDEP devices were used for the work presented in this thesis. The design and fabrication methods were described in prior works [4]. Both were constituted by a sawtooth channel with a depth of approximately 20 μm and a length of 4.2 cm (V1 type) and 3.5 cm (V2 type) from inlet to outlet respectively (Figure 2.1). The distance between two paired triangle tips (gates) decreases from 945 μm to 27 μm (V1) and 73 μm to 25 μm (V2) in the channel. For V1 type, the gate size decreases

approximately 40 μm after every 6 repeats. V2 type, the gate size decreases approximately 5 μm after every 3 repeats. V1 channel has been applied for data collection in Chapter 5 and Chapter 6 to study the behaviors of different samples. V2 channel was used to study and separate subpopulations of neural stem and progenitor cells in Chapter 3 and insulin vesicles in Chapter 4. Direct current was applied for both type of the devices between inlet and outlet. The potentials were between 0 – 3000 V for testing.

The microfluidic devices were fabricated by standard soft lithographic technique and has been described in previous works [4]. The designs of the channels were created by AutoCAD (Autodesk, Inc., San Rafael, CA) and were used for fabricating photomask. The channel was created by exposing AZ P4620 positive photoresist (AZ Electronic Materials, Branchburg, NJ) on Si wafer CEM388SS (Shin-Etsu MicroSi, Inc., Phoenix, AZ) by contact lithography. The photoresist is sensitive to light exposure and weakens the material to be more soluble. Extra materials were removed from the Si wafer. A weight of 22 g of polydimethylsiloxane (PDMS, Sylgard 184, Dow/Corning, Midland, MI) was used to fabricate four channels simultaneously. The PDMS mixture was placed on Si wafer template and let stand for 30 mins to allow bubbles to dissipate and then were baked for 1 h at a temperature of 80 °C. Holes of 2.5 mm diameter were punched for inlet and outlet reservoirs. Each channel was capped with a glass microscope slide to fabricate the enclosed channels after cleaning and activation by plasma cleaner (Harrick Plasma, Ithaca, NY, USA) with a voltage of 50 kV.

2.3 Imaging and Simulations

Images and recordings were taken by an Olympus IX70 inverted microscope with ×4 and ×10 objectives. A mercury short arc lamp (H30102 w/2, OSRAM) and a triple band pass cube (Olympus, Center Valley, PA) were used for sample illumination in Chapter 4 and 5.

Finite element modeling (COMSOL, Inc., Burlington, MA) of the distribution of the electric field in the microchannel was performed as previously detailed [5]. The *AC/DC module* was used to interrogate the $\vec{E}$, $\nabla\left|\vec{E}\right|^2$, and $\frac{\nabla|\vec{E}|^2}{E^2}\cdot\vec{E}$ in an accurately scaled 2D model of the microchannel (Figure 2.2).

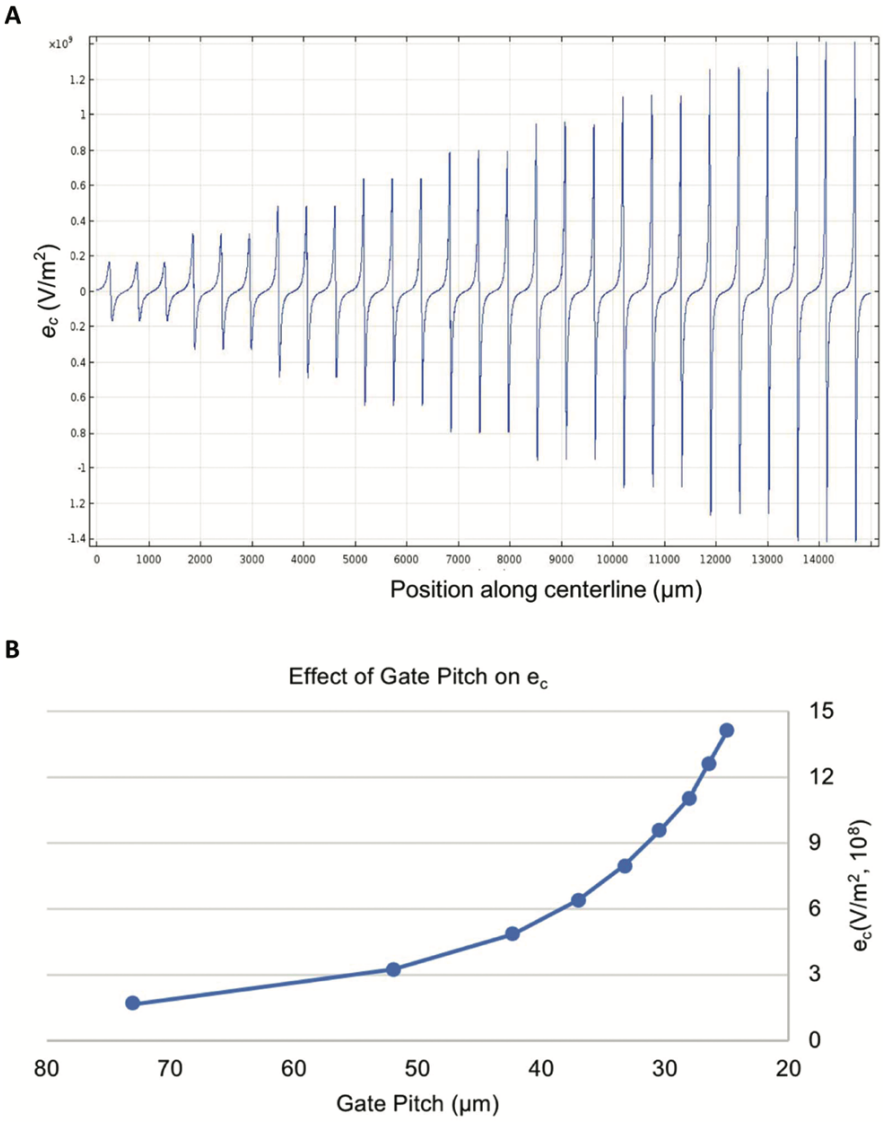

Figure 2.2. Calculated $\frac{\nabla|\vec{E}|^2}{E^2} \cdot \vec{E}$ (e_c) values in the DC-iDEP device. (A) e_c intensity along centerline (see Figure 2.1) in the microchannel. Position along centerline started from the beginning of the sawtooth design to the end of the last (narrowest) gate. Peak-valley pairs correspond to e_c value distributions about each gate. The e_c value was positive on the left side of the gate tip and negative on the right side of the gate tip. (B) Effect of gate pitch on e_c. Values increase as gate pitch size decreases from the inlet to the outlet in the microchannel. The voltage is modeled at 90 V applied global voltage of V2 type channel.

2.4 Application of Dielectrophoresis to Bioparticle Subpopulation Separation

Dielectrophoresis has been a valuable tool for subpopulation assessment because of its continuous separation, label-free, and some designs enable the separation of varied subpopulations all at once [6]. Subpopulations within different cell types were studied and separated by dielectrophoresis.

Some DEP works are focused on cancer stem cells. They are based on the physiological status of the bioparticles, especially membrane capacitance differences of subpopulations. Peter R. C. Gascoyne et al. found the average plasma membrane capacitance of a type (MDA-231) of human breast cancer cell subpopulation is significantly larger than that of resting cells. Taking advantage of distinguishing DEP forces, cancerous cells were enriched to maximum 10^5 compared to normal cells. The isolation of human cancer cells subpopulations was demonstrated by microfluidic cell sorting [7].

Some other DEP separation works are related to functioning stem cells. Human mesenchymal stem cells and their progeny cells osteoblasts were isolated by a cell sorting device [8]. The progenies experience larger DEP force than multipotent stem cells. The efficiency of stem cell and osteoblasts purification was more than 80%. This work demonstrated the feasibility of DEP application on sorting stem cells and their progenies. DEP was also used to isolate different progenitor subpopulations from stem cells. Based on whole-cell membrane capacitance, DEP was also used for separating neurogenic progenitors and astrogenic progenitors. Each subpopulation was enriched and

demonstrated that cell biophysical behaviors such as membrane characteristics could be used for distinguishing progenitor cells [9].

2.5 References

[1] Jones, Thomas B., and Thomas Byron Jones. *Electromechanics of particles*. Cambridge University Press, 2005.

[2] Nili, Hossein, and Nicolas G. Green. "Higher-order dielectrophoresis of nonspherical particles." *Physical Review E* 89.6 (2014): 063302.

[3] Hilton, Shannon Huey, and Mark A. Hayes. "A mathematical model of dielectrophoretic data to connect measurements with cell properties." *Analytical and bioanalytical chemistry* 411.10 (2019): 2223-2237.

[4] Staton, Sarah JR, et al. "Characterization of particle capture in a sawtooth patterned insulating electrokinetic microfluidic device." *Electrophoresis* 31.22 (2010): 3634-3641.

[5] Crowther, Claire V., et al. "Isolation and identification of Listeria monocytogenes utilizing DC insulator-based dielectrophoresis." *Analytica chimica acta* 1068 (2019): 41-51.

[6] Vahey, Michael D., and Joel Voldman. "An equilibrium method for continuous-flow cell sorting using dielectrophoresis." *Analytical chemistry* 80.9 (2008): 3135-3143.

[7] Gascoyne, Peter RC, et al. "Dielectrophoretic separation of cancer cells from blood." *IEEE transactions on industry applications* 33.3 (1997): 670-678.

[8] Song, Hongjun, et al. "Continuous-flow sorting of stem cells and differentiation products based on dielectrophoresis." *Lab on a Chip* 15.5 (2015): 1320-1328.

[9] Nourse, J. L., et al. "Membrane biophysics define neuron and astrocyte progenitors in the neural lineage." *Stem Cells* 32.3 (2014): 706-716.

CHAPTER 3

IDENTIFICATION AND SEPARATION OF NEURAL STEM AND PROGENITOR CELL SUBPOPULATIONS

3.1 Introduction

The cell is the most fundamental functional element for living organisms. Natural sources of cells, as opposed to cell lines, are heterogeneous mixtures. Often only a subset of cells in this mixture are useful for any given research purpose or therapeutic application. In other cases, all the sub-populations in the mixture need to be individually fully identified and characterized. In any case, there are numerous circumstances where high-resolution isolation and concentration of similar cell types is needed. Stem cells are a good example, as they are heterogenous populations that have potential for use in clinical therapies and basic science. Unfortunately, it currently is not clear how each cell type in stem cell populations contribute to repair or to normal function. Understanding the functional capability of the different cell types in stem cell populations is a necessary first step towards improving the use of these cells in transplantation [1-4]. New capabilities in high resolution cell separations provided by direct current insulator based dielectrophoresis (DC-iDEP) provides a novel method to characterize cells according to their native biophysical properties, which can be related to their cell identity and function, and ultimately their final fate.

A main driving force for scientists and physicians who study stem cells is their desire to understand and exploit the potential of the cells to regenerate and renew damaged tissues. Neural stem and progenitor cells (NSPCs) give rise to the central

nervous system (brain and spinal cord). They are capable of self-renewing and differentiating into neurons, astrocytes and oligodendrocytes. The intermediate immature cells generated during differentiation are progenitor cells. These cells may be used as the basis of treatments for CNS injuries such as stroke damage, traumatic brain and spinal cord injury, and degenerative brain conditions (including Alzheimer's disease and Parkinson's disease) [5-8].However, a major unsolved problem in the stem cell field is low reproducibility of transplants due to the heterogeneity of NSPC cultures expanded for transplant. Cellular heterogeneity in NSPC cultures is currently not well described qualitatively, much less quantitatively. This was recently highlighted by the inability of scaled-up cultures of NSPCs used for clinical trials to match the effectiveness of research-grade NSPC cultures in animal models of spinal cord injury and Alzheimer's disease [9-11].

Cultures of NSPCs contain undifferentiated stem cells as well as progenitors tied to differentiated cell fates. The ratios of progenitors in NSPC cultures can vary across different NSPC batches, be affected by external cues such as culture conditions, and change over time in culture [1, 12-15]. Differing ratios of progenitors generate heterogeneity in the types of differentiated cells that form after transplantation. Further, differing ratios of undifferentiated stem cells, progenitors and differentiated cells produce variation in secretion of growth factors, exosomes, cytokines, etc., affecting survival and function of both host and transplanted cells [16,17].All these factors will contribute to variability in cell survival, migration, and differentiation after transplantation into pre-clinical or therapeutic models, making it imperative to address heterogeneity of NSPC

transplants. To achieve an effective and stable long-term therapy using NSPCs by transplantation, predicting the final fates of progenitor cells are of great importance. Other benefits of full accounting of stem cell populations are that sorted cells could also be used to reduce the risks of introducing tumor cells into transplanted patients and the identification and isolation of the NSPCs with distinguished final cell types could increase the efficiency of basic research studies [18].

Dielectrophoresis has proven to be a valuable tool to assess heterogeneity of cells without the need for cell-type specific labels. Analysis of cells with AC-based dielectrophoresis (AC-DEP) systems can depict the heterogeneity of stem cell populations. Neuron-biased and astrocyte-biased populations can be enriched in AC-DEP by adjusting the applied frequency [19, 20]. These studies showed that distinct progenitors could be defined and isolated by electrophysiological properties that serve as a metric of their fate potential. While AC-DEP can be used to enrich distinct cell types from NSPCs, it is hypothesized that higher resolution separations are possible using a different type of DEP that allows several cell types to be characterized simultaneously.

Direct current insulator-based dielectrophoresis (DC-iDEP) is capable of introducing large field gradients using a low voltage and separating several cell types with high-resolution. The technique juxtaposes electrophoretic and dielectrophoretic forces induced on individual cells such that very subtle physical differences can be discerned. This juxtaposition is the reason such high-resolution separation can be achieved and is based on gradient steady state separation techniques. Electrophoretic forces generally reflect surface charge of the cell and dielectrophoretic forces probe both

internal and surface features. The DC-iDEP devices are easy to fabricate and robust. The technique has been applied to a wide variety of cells and bioparticles including blood cells, bacteria, viruses, and nanoparticles [21-23]. As an extreme example of very high-resolution cell separation, Jones et al. separated gentamicin resistant and susceptible strains of *Staphylococcus epidermidis* using DC-iDEP [23].

This work presents a high-resolution analysis of NSPCs populations in a DC-iDEP device. A cell population used as control, human embryonic kidney (HEK) 293 cells, showed relatively homogeneous dielectrophoretic properties. Three populations of NSPCs that differed in fate potential were tested that were chosen because there should be subtle but identifiable differences in the sub-populations. The three populations were 1) neuron-biased NSPCs from early in cerebral cortical development, 2) the same population of NSPCs treated with N- acetylglucosamine (GlcNAc) to induce an astrocyte-biased population [24], and 3) astrocyte-biased NSPCs from a later stage in cerebral cortical development.

3.2 Theory

High-resolution unbiased determinations of sub-populations from complex cell mixtures has not been attempted, even though several needs have been identified for highly refined stratification of these cells. The relatively new technique of DC-iDEP promises extremely high-resolution separations based on small differences in the native, unlabeled biophysical properties of cells. The high-resolution capability is the result of applying the principles gradient steady state separations exploiting large fields and gradients induced on the microdevice. The deterministic biophysical property of the cells

which is measured by DC-iDEP is EKMr and is determined by the location of capture for a defined device and applied voltage [27,29,30].

The decreasing gate pitches of the device create larger $\frac{\nabla|\vec{E}|^2}{E^2} \cdot \vec{E}$ (=e_c) values at successive gates and provide unique conditions for the capture of cells [23]. According to classic theory, the EKMr reflects the conductivity, the radius and the zeta potential of the particles (among other physical factors) [29,31].

The value of e_c is determined by numerical models describing the electric field within the device and these values were used to quantify the EKMr. Specifically, the value of e_c was simulated along the centerline of the DC-iDEP channel (see Figures 2.1 and 2.2). The increasingly large positive-negative deviation pairs of e_c value occur near the gates along the channel, with the positive values immediately before the gate and negative values immediately after the gate. The single cells were all captured before the gates and was recorded as positive values. The e_c peak values (the value of the positive peaks) increased with decreased pitch width from the inlet toward the outlet (Figure 2.2 B). With the applied voltage of the simulation at 90 V, the e_c peak values ranged from 1.66×10^8 to 1.41×10^9 V/m^2. Each cell will pass a 'last gate' prior to being captured. This allows of the values of the e_c to be bracketed between the two values. According to the capture condition mentioned in theory section:

$$\frac{\nabla|\vec{E}|^2}{E^2} \cdot \vec{E} \geq \frac{\mu_{EK}}{\mu_{DEP}} \qquad (5)$$

as the cell properties define the capture location established by the electric field structure, cells with an EKMr value higher than e_c value of the last gate it passes through and is smaller or equal to the e_c value of the gate of capture. The width of each capture zone is

defined by the value of e_c at the two closest gates. For the device used in these studies, at 90 V (for NSPC studies) applied global voltage, bin widths are ~1.5×10^8 V/m^2 and are spaced somewhat evenly across the range. The values generated from the cells were binned together and histograms created.

3.3 Materials and Methods

3.3.1 Cell culture

HEK 293 (Passage 60) cells were cultured and passaged in Dulbecco's Modified Eagle Medium (DMEM) with 10% fetal bovine serum (FBS). Trypsin-EDTA (0.25% (w/v) was used to lift the cells off the culture plate, following which they were centrifuged at 253 g for 5 min and washed with DEP buffer solution (8.5% (w/v) sucrose (Mallinckrodt Baker, Inc., Paris, Kentucky, USA), 0.3% (w/v) dextrose (HiMedia Laboratories, Pvt. Ltd., Dindori, Nashik, India), 0.75% (v/v) Roswell Park Memorial Institute 1640 medium (HyClone, Logan, Utah, USA)), then centrifuged and washed again. The concentration was adjusted to about 10^5 cells/mL prior to use. All reagents were obtained from Life Technologies, Grand Island, NY, USA unless otherwise specified.

NSPCs were dissected from cerebral cortical regions of wild-type CD1 mice on embryonic days 12 and 16 (E12 and E16). The culture media for E12, E12 GlcNAc treated and E16 cells was DMEM, B27, N2, 1 mM sodium pyruvate, 2 mM L-glutamine, 1 mM N-acetylcysteine, 10 ng/mL FGF, 20 ng/mL EGF, and 2 μg/mL heparin, as described in previous works [1]. The E12 cells were treated with 80 mM GlcNAc (Sigma-Aldrich, St. Louis, MO, USA) for 3 days to obtain E12 GlcNAc treated cells. The

cells were incubated at 37℃ in 5% CO2. NSPCs were cultured as neurospheres then dissociated once spheres reached approximately 150 μm in diameter. NeuroCult Chemical Dissociation Kit (Stem cell Technologies, Vancouver, BC, Canada) was used to dissociate neurospheres into single cells. Dispersed cells were centrifuged at 253 g for 5 min and washed with DEP buffer solution, then centrifuged and washed again. The concentration was adjusted to about 10^5 cells/mL prior to use.

3.3.2 Experimental procedure

The device was flushed with 5% (w/v) BSA (bovine serum album) in PBS (10 mM phosphate-buffered saline) (pH 7.6) solution and then DEP buffer solution before introducing cell samples. Dielectrophoresis tests were monitored with an Olympus IX70 inverted microscope with a ×4 or ×10 objective. Images and videos were recorded by QICAM cooled CCD camera (QImaging, Inc., Surrey, BC) and Streampix III image capture software (Norpix, Inc., Montreal, QC). A voltage of 70 V was applied to platinum electrodes (0.404-mm external diameter, 99.9% purity, Alfa Aesar, Ward Hill, MA) connected to the inlet (+) and outlet (ground) to capture HEK cells. 90 V global voltage were used for the capture of NSPCs.

3.4 Results and Discussion

3.4.1 Dielectrophoretic behaviors of controlled HEK 293 cells

The system was calibrated using the biophysical behavior of a well-established cell population, the human embryonic kidney cell line HEK 293 [32]. Previous separations based on frequency-based trapping efficiency using this cell line indicate that it is more homogeneous than primary cultures of neurons and NSPCs [1]. The

biophysical behavior of HEK 293 cells were examined and single HEK cells reacted to the system in a fashion consistent with previous work, demonstrating stable, reproducible and interpretable results (n = 33). They were captured in the microchannel with μ_{EK}/μ_{DEP} values from 1.3×10^8 to 6.2×10^8 V/m^2 (Figure 3.1) with a distribution centered around the average value. The weighed mean (± standard deviation, SD) of the cell ratio mobilities is $4.2 \pm 1.1 \times 10^8$ V/m^2.

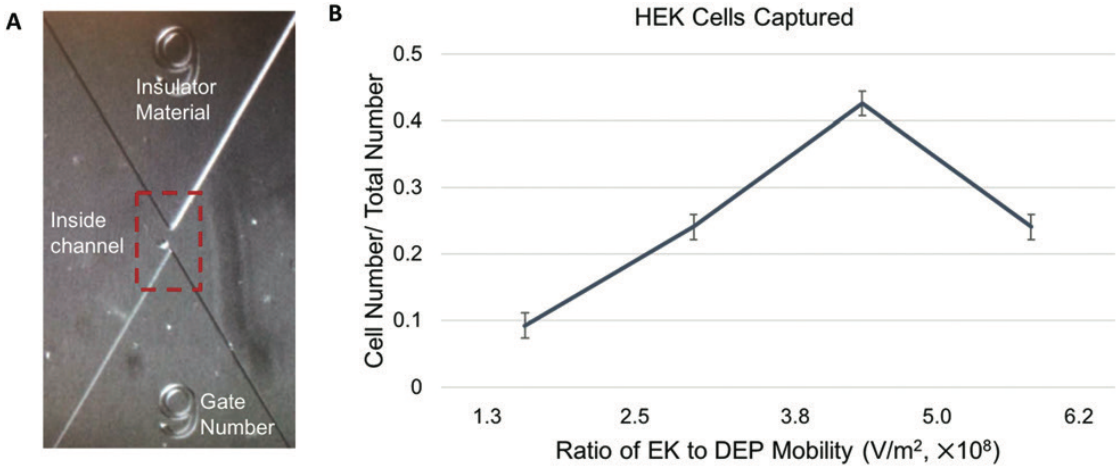

Figure 3.1. The electrophysical behaviors of HEK 293 cells. (A) The image of capturing a HEK 293 cell at gate 9 was recorded. Channel area, insulator material and gate area are labeled in the image. (B) The normalized cell number at different ratio of EK to DEP mobility. The EKMr distribution of HEK 293 cells has an average of 4.2×10^8 V/m^2 with a standard deviation of 1.1×10^8 V/m^2. Error bars are based on SEM.

3.4.2 NSPCs subpopulations high resolution separation

Three unique sets of NSPCs were introduced to the DC-DEP microchannel individually for EKMr identification. NSPCs isolated from earlier (E12) and later (E16) embryonic stages of cerebral cortex development have different fate biases. E12 NSPCs are more neurogenic and form more neurons than the more astrogenic E16 NSPCs [14]. High-resolution determinations have been carried out on these complex cell populations (Figure 3.2 A), generating a distributed pattern of values ranging from 1.3×10^8 to $1.3 \times$

10^9 V/m^2 that appeared to be unique to each population. Recent studies showed that the treatment of E12 NSPCs with GlcNAc influences the fate potential of E12 cells by the formation of branched N-glycans [24]. The treatment gives rise to the generation of more astrocytes at the cost of neurons upon differentiation. In order to control for the fact that E12 and E16 cells are from different developmental stages, E12 control and E12 GlcNAc treated cells were assessed (Figure 3.2 B). These cells from same developmental stage but differ in fate bias because GlcNAc treatment increases cell surface highly branched N-glycans and promotes astrocyte fate.

Compared with measurements of the HEK 293 cell line, all three NSPC populations demonstrated higher EKMr and exhibited significantly greater heterogeneity. Higher EKMr value indicates that either μ_{EK} increased or μ_{DEP} decreased. Increased electrokinetic effects are caused by an increase in surface charge density (changing the zeta potential), a decreased surface viscosity (also described as 'surface softness') [31, 33] and, much more subtly, a change in the overall multipole moment of the cell. A decrease in dielectrophoretic effects is caused by (according to classic theory) an increase in particle conductivity for the negative dielectrophoresis force present here. The change in conductivity is caused by a change in zeta potential, an altered conductivity of any of the cell membranes or a change in the overall multipole moment of the cell [31]. The percent relative standard deviation (%RSD) increased from 27% (1.1 V/m^2 SD) for the HEK 293 measurements to values of 47% (3.9 V/m^2 SD), 56% (3.8 V/m^2 SD), and 48% (3.4 V/m^2 SD) for the NSPCs. These values indicated a 3.1- to 3.5-fold increase compared to the control population. These results are consistent with the existence of

heterogenous subpopulations in NSPCs, supporting previous studies revealing NSPCs contain multipotent stem cells and more committed progenitor cells [20].

Visual inspection of the various cell population histograms of EKMr suggests the pattern for the three NSPC values are, to varying degrees, different. To help understand precisely how different the cell populations varied from each other, the two-sample Cramer-Von Mises criterion were applied to compare the distributions between paired NSPC samples [34]. The variance of the NSPC distributions were statistically analyzed. Briefly,

$$T = \left[\frac{NM}{(N+M)^2}\right]\{\sum_{i=1}^{N}[F_N(x_i) - G_M(x_i)]^2 + \sum_{j=1}^{M}[F_N(y_i) - G_M(y_i)]^2\}$$

$F_N(x)$ and $G_M(x)$ are the empirical distribution functions of the samples to be compared. $x_1, x_2, \ldots, x_N$ and $y_1, y_2, \ldots, y_M$ are the observed values in each sample.

The E12 and GlcNAc treated E12 samples are shown to be very different by this assessment. The T value between E12 and GlcNAc treated E12 is 1.53 – thus there is 99.98% chance that these two samples come from the same distribution can be rejected. This rather unnatural phrase is result of the construct of the statistical approach based on the null hypothesis which presumes no significant difference exists between populations. In more natural, but less exacting terms, this approximately means that there is nearly an 100% chance that these populations differ. The other comparison was between the E12 and E16 populations. They are also significantly different to the 99.92% confidence level based on T value of 1.21, and similarly they are very likely different.

Significantly and in contrast, there is only 23.0% confidence level (T= 0.067) that the distributions of GlcNAc treated E12 and E16 cells, which are both rich in astrogenic progenitor cells, differ. This analytical assessment of the patterns generated by high-resolution biophysical cell determinations is consistent with known properties of these various cell populations. Significant differences were observed in populations known to differ and similar populations gave results suggesting a high probability of sameness.

Identifying the fate potential of cells with specific EKMr values would be ideal. However, limitations in cell transport and single cell bioanalytical methods prevent this approach. Fortunately, there exists a good deal of knowledge about the distribution of the ultimate fate of these cell populations and these data can be compared to the biophysical data generated here. One of the reasons that these cell populations where chosen was for this very reason, E12, E12 GlcNAc-treated and E16 NSPCs are all relatively well characterized [14,24]. E12 and E16 are ideal populations to study neurogenic progenitors and astrogenic progenitors because of the existence of few oligodendrocyte progenitors in these stages in the cerebral cortex. Oligodendrocytes are primarily generated in the ganglionic eminence and migrate to the cortex at later embryonic stages, E18 [24].

The patterns for the various NSPCs appeared to vary more so before or after 8.0×10^8 V/m^2. Noting this observation, both the paired populations (Figures 3.2 A and 3.2 B) was defined with EKMr values greater than 8.0×10^8 V/m^2 as the higher band and less than 8.0×10^8 V/m^2 as the lower band. Compared to E12 cells, a larger number of cells captured in both GlcNAc treated E12 and E16 populations were in the higher EKMr band.

A

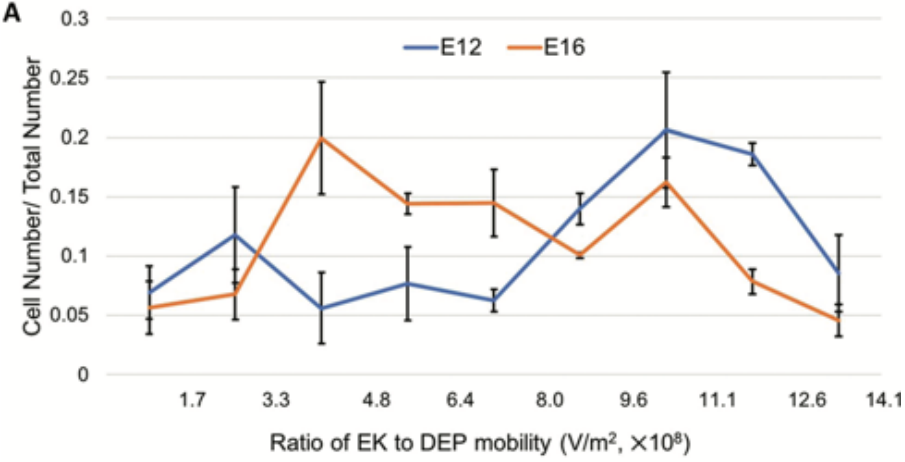

B

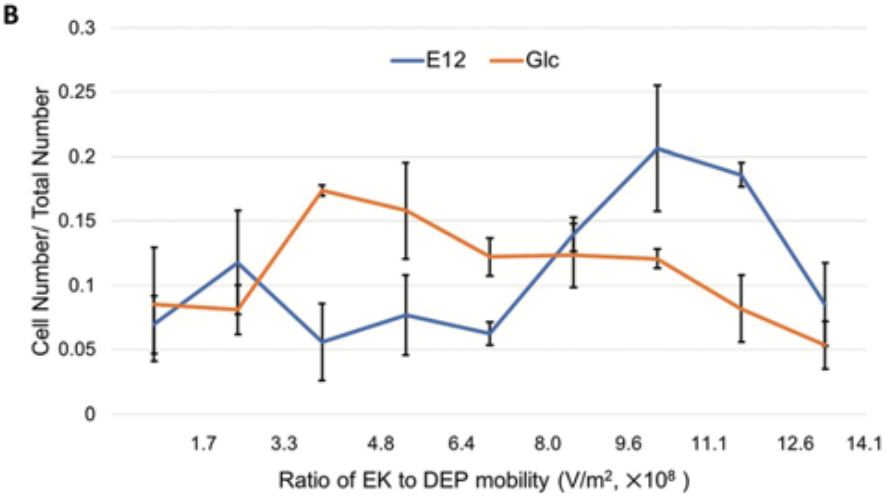

C

Cell Type	Average (10^8 V/m^2)	Standard Deviation (SD, 10^8 V/m^2)	% RSD
HEK 293	4.2	1.1	27.2
E12	8.2	3.9	47.4
Glc	6.8	3.8	56.4
E16	7.0	3.4	48.5

Figure 3.2. The biophysical behaviors of NSPCs. Three types of NSPCs of different final fate, E12, Glc-treated E12 and E16 cells, were captured and compared. E12 cells are rich in neurogenic progenitor cells; E16 and Glc-treated E12 cells contains more astrogenic progenitor cells than E12 cells. (A) Comparison of EKMr distribution differences between E12 and E16 NSPCs. (B) Comparison of EKMr distribution differences between E12 and Glc treated NSPCs. (C) An EKMr average, standard deviation (SD), % relative standard deviation (RSD) comparison between HEK293 cells, E12, Glc-treated E12, E16 NSPCs. All three types of NSPCs are showing larger average EKMr values and larger SD and %RSD than controlled HEK 293 cells. Error bars are based on SEM.

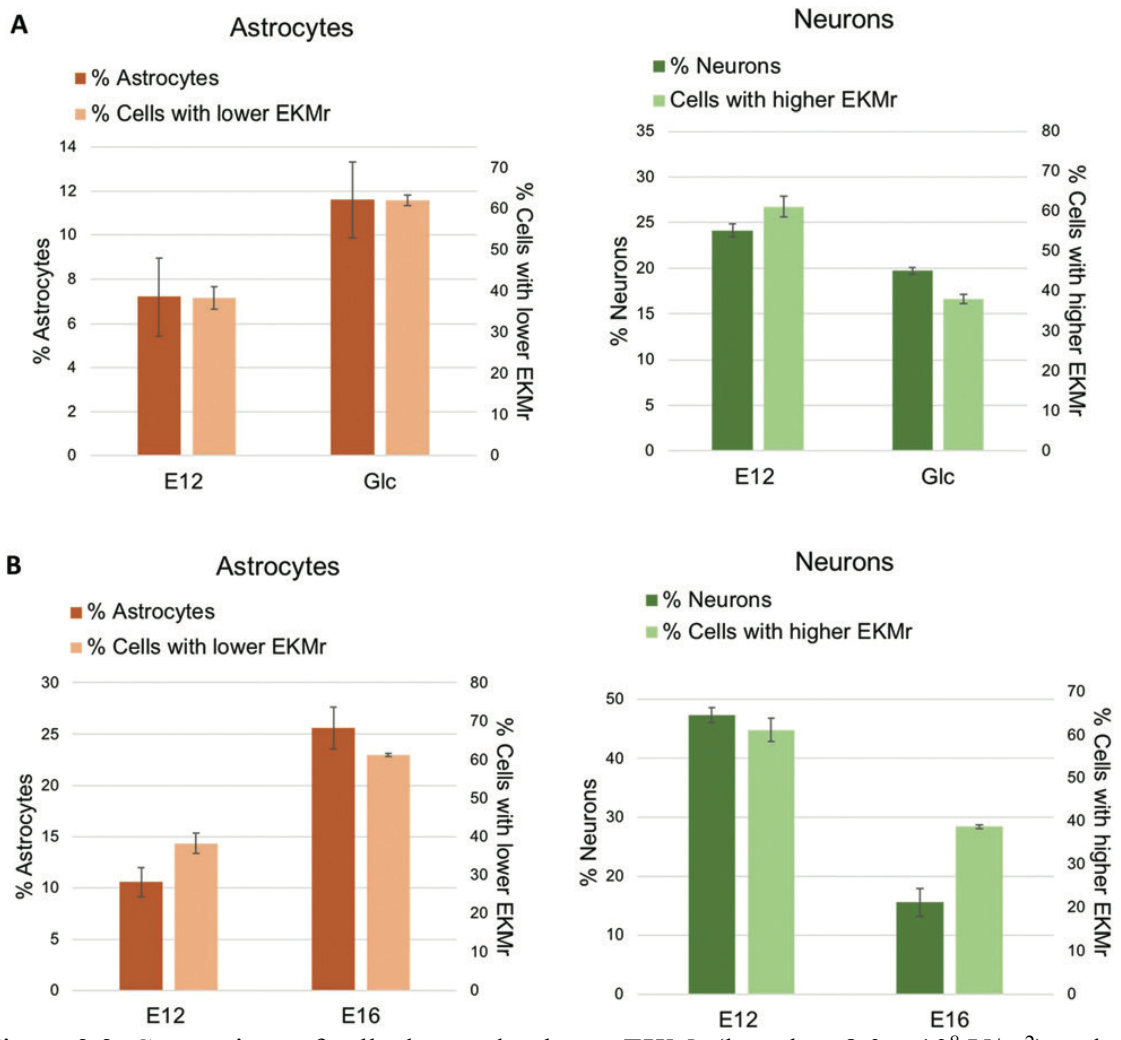

Figure 3.3. Comparison of cells detected at lower EKMr (less than 8.0×10^8 V/m^2) and higher EKMr region (larger than 8.0×10^8 V/m^2) with final fates of E12, Glc-treated E12 and E16 populations. (A) Differentiated astrocyte percentages (light orange) are compared with cells detected at lower EKMr (dark orange) region in E12 and Glc-E12 treated NSPCs. Differentiated neuron percentages (light green) are compared with cells detected at higher EKMr (Dark green) region in E12 and Glc-treated E12 NSPCs [24]. (B) Differentiated astrocyte percentages (light orange) are compared with cells detected at lower EKMr (dark orange) region in E12 and E16 NSPCs [14]. Differentiated neuron percentages (light green) are compared with cells detected at higher EKMr (Dark green) region in E12 and E16 NSPCs.

In this work, the percentages of neurons or astrocytes formed upon differentiation determined in previous studies with the abundance of the cells were compared in the

higher or lower EKMr bands in each set of NSPCs (Figure 3.3) [14,24]. A larger percentage of GlcNAc treated E12 or E16 cells with lower EKMr were captured than E12 cells. This is demonstrating the same trend of increasing astrocytes upon differentiation for E12 after treatment or with further embryonic development. The percentage of the cells captured with higher EKMr in GlcNAc treated E12 and E16 were smaller than E12 cells, which is consistent with the percentage reduction of neurogenic progenitors in these two populations. The different differentiated percentages of E12 for each comparison is due to small changes in the differentiation protocol across the different sets of experiments. Each comparison needs to be matched to be compared (especially for E12 and GlcNAc-treated E12). The abundance of cells captured at high or low EKMr are reflective of the neurogenic or astrogenic fate potential of NSPCs.

Unbiased high-resolution separation and characterization have been demonstrated for complex NSPC populations. Compared with the control cell population (HEK 293 cells), the NSPC populations all showed greater EKMr heterogeneity. It is currently impossible to assign biological significance to each given binned value represented within the histograms. However, all currently available assessments support the hypothesis that cells differ significantly for various values of EKMr. Functionally reducing the resolution by grouping the EKMr values results in distributions consistent with known ultimate fate assessments for each sample type. As single cell characterizations improve and on-chip/off-chip cell transport is addressed the open question of the significance of the ability to separate these cells can be answered. That

being said, these data support that these are complex mixtures and significant changes in the patterns of separation are consistent with known properties of those mixtures.

3.5 Conclusion

In summary, NSPCs were successfully separated and characterized in the DC-iDEP device. The presence of complex subpopulations of NSPCs with distinct final fates could be identified and differentiated by dielectrophoretic properties in the microdevice. The final fates of the populations are consistent with the distribution of EKMr of the cells detected. These results are promising toward clinical improvements for transplant safety and efficacy and the identified NSPCs are meaningful to the basic stem cell differentiation studies.

3.6 References

[1] Flanagan, Lisa A., et al. "Unique dielectric properties distinguish stem cells and their differentiated progeny." *Stem cells* 26.3 (2008): 656-665.

[2] Kang, Yuejun, et al. "DC-Dielectrophoretic separation of biological cells by size." *Biomedical microdevices* 10.2 (2008): 243-249.

[3] Stringari, Chiara, et al. "Phasor fluorescence lifetime microscopy of free and protein-bound NADH reveals neural stem cell differentiation potential." *PloS one* 7.11 (2012).

[4] Vrtovec, Bojan, et al. "Effects of intracoronary CD34+ stem cell transplantation in nonischemic dilated cardiomyopathy patients: 5-year follow-up." *Circulation research* 112.1 (2013): 165-173.

[5] Thomson, James A., et al. "Embryonic stem cell lines derived from human blastocysts." *science* 282.5391 (1998): 1145-1147.

[6] Gage, Fred H. "Mammalian neural stem cells." *Science*287.5457 (2000): 1433-1438.

[7] Temple, Sally. "The development of neural stem cells." *Nature*414.6859 (2001): 112-117.

[8] Arulmoli, Janahan, et al. "Static stretch affects neural stem cell differentiation in an extracellular matrix-dependent manner." *Scientific reports* 5.1 (2015): 1-8.

[9] Anderson, Aileen J., et al. "Preclinical efficacy failure of human CNS-derived stem cells for use in the pathway study of cervical spinal cord injury." *Stem Cell Reports* 8.2 (2017): 249-263.

[10] Marsh, Samuel E., et al. "HuCNS-SC human NSCs fail to differentiate, form ectopic clusters, and provide no cognitive benefits in a transgenic model of Alzheimer's disease." *Stem cell reports* 8.2 (2017): 235-248.

[11] Temple, Sally, and Lorenz Studer. "Lessons learned from pioneering neural stem cell studies." *Stem cell reports* 8.2 (2017): 191-193.

[12] Gage, Fred H., and Sally Temple. "Neural stem cells: generating and regenerating the brain." *Neuron* 80.3 (2013): 588-601.

[13] Groszer, Matthias, et al. "PTEN negatively regulates neural stem cell self-renewal by modulating G0-G1 cell cycle entry." *Proceedings of the National Academy of Sciences* 103.1 (2006): 111-116.

[14] Labeed, Fatima H., et al. "Biophysical characteristics reveal neural stem cell differentiation potential." *PloS one* 6.9 (2011).

[15] Qian, Xueming, et al. "Timing of CNS cell generation: a programmed sequence of neuron and glial cell production from isolated murine cortical stem cells." *Neuron* 28.1 (2000): 69-80.

[16] Blurton-Jones, Mathew, et al. "Neural stem cells improve cognition via BDNF in a transgenic model of Alzheimer disease." *Proceedings of the National Academy of Sciences*106.32 (2009): 13594-13599.

[17] Drago, Denise, et al. "The stem cell secretome and its role in brain repair." *Biochimie* 95.12 (2013): 2271-2285.

[18] Simon, Melinda G., et al. "Increasing label-free stem cell sorting capacity to reach transplantation-scale throughput." *Biomicrofluidics* 8.6 (2014): 064106.

[19] Adams, Tayloria NG, et al. "Separation of neural stem cells by whole cell membrane capacitance using dielectrophoresis." *Methods* 133 (2018): 91-103.

[20] Nourse, J. L., et al. "Membrane biophysics define neuron and astrocyte progenitors in the neural lineage." *Stem Cells* 32.3 (2014): 706-716.

[21] Staton, Sarah JR, et al. "Characterization of particle capture in a sawtooth patterned insulating electrokinetic microfluidic device." *Electrophoresis* 31.22 (2010): 3634-3641.

[22] Ding, Jie, et al. "Concentration of Sindbis virus with optimized gradient insulator-based dielectrophoresis." *Analyst* 141.6 (2016): 1997-2008.

[23] Jones, Paul V., et al. "Biophysical separation of Staphylococcus epidermidis strains based on antibiotic resistance." *Analyst* 140.15 (2015): 5152-5161.

[24] Yale, Andrew R., et al. "Cell surface N-glycans influence electrophysiological properties and fate potential of neural stem cells." *Stem cell reports* 11.4 (2018): 869-882.

[25] Weiss, Noah G., et al. "Dielectrophoretic mobility determination in DC insulator-based dielectrophoresis." *Electrophoresis* 32.17 (2011): 2292-2297.

[26] Crowther, Claire V., and Mark A. Hayes. "Refinement of insulator-based dielectrophoresis." *Analyst* 142.9 (2017): 1608-1618.

[27] Jones, Paul V., and Mark A. Hayes. "Development of the resolution theory for gradient insulator-based dielectrophoresis." *Electrophoresis* 36.9-10 (2015): 1098-1106

[28] LaLonde, Alexandra, et al. "Effect of insulating posts geometry on particle manipulation in insulator based dielectrophoretic devices." *Journal of Chromatography A* 1344 (2014): 99-108.

[29] Jorgenson, James W., and Krynn DeArman Lukacs. "High-resolution separations based on electrophoresis and electroosmosis." *Journal of chromatography A* 218 (1981): 209-216.

[30] Jones, Paul V., Sarah JR Staton, and Mark A. Hayes. "Blood cell capture in a sawtooth dielectrophoretic microchannel." *Analytical and bioanalytical chemistry* 401.7 (2011): 2103.

[31] Hilton, Shannon Huey, and Mark A. Hayes. "A mathematical model of dielectrophoretic data to connect measurements with cell properties." *Analytical and bioanalytical chemistry* 411.10 (2019): 2223-2237.

[32] Shaw, Gerry, et al. "Preferential transformation of human neuronal cells by human adenoviruses and the origin of HEK 293 cells." *The FASEB Journal* 16.8 (2002): 869-871.

[33] Daly, Emma, and Brian R. Saunders. "Temperature–dependent electrophoretic mobility and hydrodynamic radius measurements of poly (N-

isopropylacrylamide) microgel particles: structural insights." *Physical Chemistry Chemical Physics* 2.14 (2000): 3187-3193.

[34] Anderson, Theodore W. "On the distribution of the two-sample Cramer-von Mises criterion." *The Annals of Mathematical Statistics* (1962): 1148-1159.

CHAPTER 4

BIOPHYSICAL IDENTIFICATION OF SUBPOPULATIONS OF INSULIN VESICLES FROM BETA CELLS

4.1 Introduction

Insulin is a peptide hormone that plays a fundamental role in glucose homeostasis. It is stored in vesicles which are synthesized, stored and released from pancreatic beta cells. Prior to release, insulin is tightly packed at high concentration within insulin secretory granules (ISGs). The insulin vesicles are involved in signaling, along with their role in storage and processing [1]. Based on their appearance in electron transmission microscopy, the ISGs are dense core organelles in the beta cells, with sizes ranging from 300 to 350 nm. Within the vesicles and ISGs, the insulin molecules are stabilized by coordinating with zinc and calcium ions, forming crystals within the dense core. When needed, the vesicles fuse with the plasma membrane and release insulin as part of the regulation of glucose levels in the blood. The fusion process in exocytosis is considered to be reversible and defects of exocytosis can be a leading factor of diabetes 2. Understanding the precise proteins which are present in the ISGs will help determine the mechanisms of normal function and, by extension, the mechanisms of diabetes [2-4].

Changes in glucose concentration can be sensed by pancreatic beta cells, triggering the release of insulin. The signal is propagated through a glucose transporter, stimulation by the glucose. The triggering causes the closing of K^+ channels, opening of Ca^{2+} channels, and an increase of the ATP to ADP ratio. These contribute to the influx of Ca^{2+} and to the exocytosis of the insulin vesicles. The fusion process has also been

studied by examining the regulation of SNARE, synaptotagmin, some Rab GTPases and related proteins. Vesicle membrane is rich in synaptobrevin and plasma membrane has soluble SNAREs. The interaction of these proteins causes the fusion of the membranes. Some studies indicated that the vesicle is not fully merged and can depart intact during the fusion process [5].

As to the position of insulin vesicles in the beta cell, only a small fraction of the vesicles rest on the plasma membrane while some are close to the cell surface. Most of the insulin vesicles are non-motile and only a portion of them are motile. The vesicles that are remote from the plasma membrane transport along microtubules in the cell to become involved in the exocytosis process [6].

Insulin originates from beta cells only, even it can be activated and expressed in other cells. The beta cells have the special function of synthesis of insulin. The study of insulin vesicle proteome in their biogenesis, exocytosis, and maturation process is important to insulin secretion mechanism during diabetes and drug efficiency.

4.1.1 Significance of studying insulin vesicles in human pancreatic beta cell

There are two levels of significance for studying insulin vesicles. First is the irreplaceable role of pancreatic beta cell. The study of structure and mechanism human pancreatic beta cell contributes to the basic research mechanism studies for interdisciplinary and clinical healthcare applications. The techniques and knowledge for building a 3D model reflecting cellular and molecular interactions, signaling pathways, genotype and phenotype, how cell evolves can also be applied for other types of complex cells and tissue studies. Pancreatic beta cells also serve a role as a representative

mechanism for other cell types to be studied. All these factors are of significant importance for this type of cell to be a topic of interest. Insulin vesicle is an essential organelle for both insulin processing and exocytosis progression.

4.1.2 Insulin vesicle heterogeneity and proteome

Proteome identification of insulin vesicles varies based on purification methods. Analysis by SDS-PAGE and gradient purification identified about 150 proteins while affinity purification filtered the number to 50. The different protein profiles are deduced to be due to other interfering factors such as organelles including mitochondria and lysosomes. Only about 30 proteins are acknowledged to be related to ISGs and about 15 proteins in common were identified by multiple techniques, which indicates the unclear description of ISGs protein expression [5]. This is in need of improved purification and more advanced characterization method to identify proteins and complete proteome of insulin vesicles. Based on these purification methods, characterization techniques such as fluorescence imaging, X-ray tomography, and cryo-ET was combined to study the insulin vesicles for their abundance, localization, structure protypes and genotypes [7].

The maturation level, the vesicle anchoring location, the protein modification on vesicle membrane are the factors for insulin vesicle heterogeneity. It takes several days to form insulin crystals in insulin vesicles. Prohormone convertase and carboxypeptidase E are the proteases accelerates the maturation of insulin. They are stored in vesicles for several days before releasing by insulin vesicles with signaling. The process distinguishes the relative younger and older vesicles for determining their mature levels [1, 4, 5, 8].

4.1.3 Insulin vesicle purification techniques

The knowledge of ISGs proteome is incomplete because of contamination resulting from sample preparation and the weak sensitivity of the characterization methods. Potential contaminations include proteins from other organelles.

Based on the heterogeneity, techniques for insulin vesicle proteome separation and characterization has been developed. Early works separated pancreatic islet into multiple fractions. According to insulin activity of the fractions, secretory granule fraction with high insulin activity was further separated from the mixture with mitochondria by centrifugation. The granules were obtained from high density fraction [9]. Further improvements were reported using gradient purification based on the density differences of organelles in beta cell and affinity purification.

A more developed separation technique based on gradient centrifugation was introduced. A 2-step gradient purification method was used for ISGs purification [5]. They characterized 130 proteins in ISGs, with 110 of them characterized for first time. This result is significant because only 30 different proteins were identified in previous works. One more step gradient centrifugation was developed based on the previous work. The extra step separated immature and mature ISGs in lighter and heavier fractions of sucrose gradient. More importantly, it identified 140 proteins rich in mature ISGs and 81 proteins from immature ISGs and other contaminants [5].

The combination of gradient centrifugation and other techniques were also introduced. Hickey et al. combined density gradient centrifugation with immunoaffinity for ISGs purification. Synaptobrevin, an antibody specific to the membrane antigen of

ISGs, was used for its enrichment. LC-MS/MS was further used identifying ~50 proteins. The work provides an affinity purification approach for enriching ISGs and protein characterization [4].

In summary, insulin vesicle as an organelle of importance is involved in exocytosis process in pancreatic beta cells. Correctly and accurately identifying the proteome may potentially contribute to type 2 diabetes treatment. The challenges for accessing protein composition of ISGs includes the heterogeneity of the population as well as the contamination from other organelles. Gradient centrifugation and affinity purification could not meet the needs of characterization. DC-iDEP has shown high resolution separation for bacteria, virus, mammalian cells in previous work, thus, is introduced to study the subpopulations of insulin vesicles to assist their future basic and clinical studies.

4.2 Materials and Methods

4.2.1 Cell Culture

INS-1E cells (from AddexBio) were cultured according to previous literature [10]. Briefly, the cells were incubated in RPMI 1640 media with 10% fetal bovine serum (FBS) and were passaged when reached 80% confluency. The cells were rinsed with dialyzed phosphate-buffered saline and then incubated for 30 min in a Krebs-Ringer bicarbonate HEPES buffer for 30 min. A 25 mM glucose supplemented KRHB buffer was used for stimulating insulin release. The cells were obtained after treating with trypsin.

4.2.2 ISGs Enrichment and labeling

Cells were washed twice with PBS buffer and were homogenized in homogenization buffer (0.3 M Sucrose, 10mM MES, 1mM EGTA, 1mM $MgSO_4$, pH 6.3). After centrifugation at 600x g twice to collect the cell debris and lyse the cells, mitochondria, endoplasmic reticulum, and other subcellular compartments of similar density were removed by centrifugation at 5,400x g. The supernatant was centrifuged again at 35,000x g to get ISGs sediment. The sediment was suspended in HB and loaded on a density gradient column spinning at 160,000x g for 8 hours. It was identified by Enzyme Linked Immuno-Sorbent Assay as the most enriched insulin fraction. Dynamic light scattering was used for characterizing the size ranging from 200 – 500 nm. Identified fraction was spun at 35,000x g for 15 minutes to sediment the ISGs.

Insulin vesicles were first labeled with the primary antibody synaptotagmin V (Thermo Fisher Scientific, Catalog# PA5-44987; RRID: AB_2610517) and then stained with secondary antibody ((Invitrogen Catalog# A-11011; RRID: AB_143157)) Alexa568-conjugated goat anti-rabbit IgG. ISGs were washed 3 times with HB removing the extra antibodies and finally suspended in 0.3 M sucrose, 5 mM MES (2-(*N*-Morpholino) ethanesulfonic acid), pH 6.3.

4.2.3 ISGs separation

A 5% BSA (w/v) solution was used for primary treatment of the V2 type device for 15 min. A 0.3 M sucrose and 5 mM MES (pH=6.3) buffer was used to dissolve insulin vesicle samples and for DEP testing. The results obtained with each voltage were

based on more than 3 independent trials with multiple batches of incubated cells. Imaging conditions and simulations were described in Chapter 2 ‘imaging and simulation’ section.

4.3 Results

4.3.1 Insulin vesicle subpopulations characterized by DC-iDEP

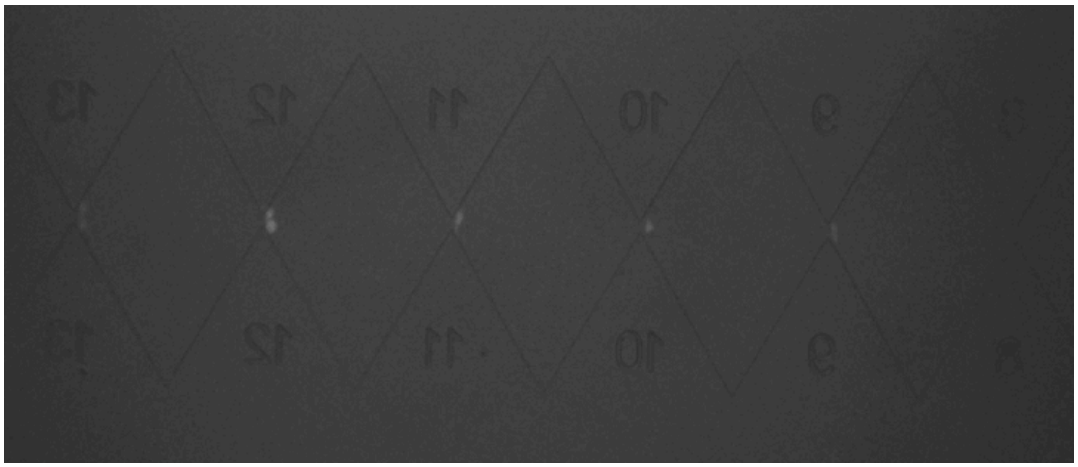

Figure 4.1. Image of insulin vesicle subpopulations captured in the DC-iDEP device. The labeled insulin vesicles subpopulations were concentrated at different gates (white). Image was recorded from gate 9 to gate 13.

Insulin vesicles were introduced into the type V2 microdevice to study their biophysical behaviors. The V2 device was used because it has smaller differences in the force ratios designed between each gate compared to previous versions. The separation can be achieved with higher resolution and the characterization of subpopulations can be identified with more accuracy.

The initial study was based on the original insulin vesicle sample with no special treatment. The vesicles were introduced from the inlet of the channel and they were kept static, balanced in the microchannel with no velocity before the first gate when voltages were applied. With potential applied, the vesicles were driven by EK force from inlet into the sawtooth area. The insulin vesicles were observed to be captured at gates of different

sizes (Figure 4.1). This is indicating the approximated equality of particle EK velocity and DEP velocity at that specific gate.

Varied voltages have been applied to obtain a full range of data and generate detailed information for insulin vesicle subpopulations (Figure 4.2). A high voltage up to 1800 V was applied on the device to determine the biophysical property, EKMr range and limit of the whole population. The intensity change was recorded according to where the vesicles are captured.

The population highest EKMr value emerged within the detection range of the device at this voltage applied. Then the voltage was decreased to 1500 V to further separated the subpopulations less than 15 $\times 10^9$ V/m^2. These subpopulations were mixed together in 1800 V observations. A peak with ~ 8 $\times 10^9$ V/m^2 appeared for the first time with some low EKMr populations still stacking together at the beginning gates with larger widths. Behaviors of insulin vesicles at 1200 V, 900 V and 600 V were also studied to separate stacked subpopulations at higher voltages. In these situations, with the spreading of low EKMr subpopulations giving clearer and higher resolution separation, some subpopulations after characterized at higher EKMr have moved to the outlet and were not within the detection range to give higher resolution of the peaks with lower EKMrs.

For the detected peaks, the peak found at 8 $\times$ 10^9 V/m^2 repeated as expected. This is indicating the measurements show good consistency and accuracy within detection range. Furthermore, a peak found at 11 $\times$ 10^9 V/m^2 were both found at 1200 V and 900 V trials and out of detection range at 600 V; an obvious peak at 6 $\times$ 10^9 V/m^2 was found at

900 V and 600 V; one more peak was found with EKMr of 3×10^9 V/m^2 with 600 V applied. The biophysical properties of insulin vesicles were used to characterize the subpopulation of bioparticles. The subpopulations of these particles were separated by DC-iDEP device. Multiple voltages were applied for monitoring the whole scheme and subtle differences between subpopulations. The results show good stability with high resolution separation.

4.3.2 Insulin vesicle from glucose treated pancreatic beta cell subpopulation characterization

Insulin vesicles obtained from 25 mM glucose-treated beta cells were studied with the same method that has been applied for insulin vesicles without treatment. Previous studies compared the concentration and imaging density differences of the two types of insulin vesicles with treated particles [11]. The experiments indicated two results: heterogeneity was observed for both untreated and treated insulin vesicle populations and there was a statistically significant difference between the two types of insulin vesicles based on the absorption and concentration.

To study the differences between the two populations, glucose treated insulin vesicles were introduced into the DC-iDEP device. The same voltages including 1800 V, 1500 V, 1200 V, 900 V, 600 V were applied for treated ISGs as tested for untreated sample (Figure 4.3). The strategy was to release and fractionate the full scheme at higher voltages with stacked peaks. The intensity of the insulin vesicles captured has been recorded with the localized EKMr scales. At 1800 V, the EKMr limit of treated vesicles are higher than untreated ones. This value has been extended to ~23×10^9 V/m^2. This is

indicating a more heterogeneity of the treated vesicles than untreated vesicles. With voltages decreases, peaks at 21 × 10^9 V/m^2 were determined with 1800 V and 1500 V; 4 × 10^9 V/m^2 were determined with 900 V, 600 V applied; Peak 8 × 10^9 V/m^2 was found with 1500 V, 1200 V, 900 V applied; 11 × 10^9 V/m^2 found with 1200 V and 900 V. The trends of the position changing of the same peak has been labeled with different color of arrows.

4.3.3 Comparison of insulin vesicles and treated insulin vesicles

The differences and similarities of the peaks of the treated vesicles were compared with the untreated vesicles (Figure 4.4). In brief, most of the treated vesicles show different biophysical behaviors than untreated ones. Untreated insulin vesicles showed 3 × 10^9 V/m^2 and 6 × 10^9 V/m^2 peaks. Treated insulin vesicles peak emerged at 4 × 10^9 V/m^2 and a new peak was found at 21 × 10^9 V/m^2, which has larger EKMr than any of the subpopulations in untreated samples. Two of the subpopulations are showing close EKMr ranges. They both showed subpopulation close to 8 × 10^9 V/m^2 and 11 × 10^9 V/m^2. The gate ranges and voltages used for extraction of each subpopulation has been listed together with each peak value, which can be used for future proteome and genome characterization.

There are several factors that can change the biophysical properties of the subpopulations after treatment. Conductivity can be measured by DEP and the changes of conductivity affects the DEP properties of the bioparticles. Existing literature has indicated that the membrane fluidity changes the conductance of the bioparticle. This

could be altered by a higher level of some surface protein expression and more enriched unsaturated lipids [12].

There are two major DEP behavior observations that are consistent with previous ISGs and glucose-treated ISGs distinguished by concentration and absorbance. First, the separation of ISGs subpopulations demonstrate the heterogeneity of each complex population. The subpopulations isolated in the microfluidic device were identified with EKMr values. Second, the distinguished distributions of the EKMr peaks in ISGs and glucose-treated ISGs with same condition (same voltage applied) indicate that there are differences between the two populations. With further statistical analysis, the different measurements will be compared and how different the two populations are. This biophysical characterization and isolation work lay the foundation for the future proteome studies when complimented with sample extraction techniques.

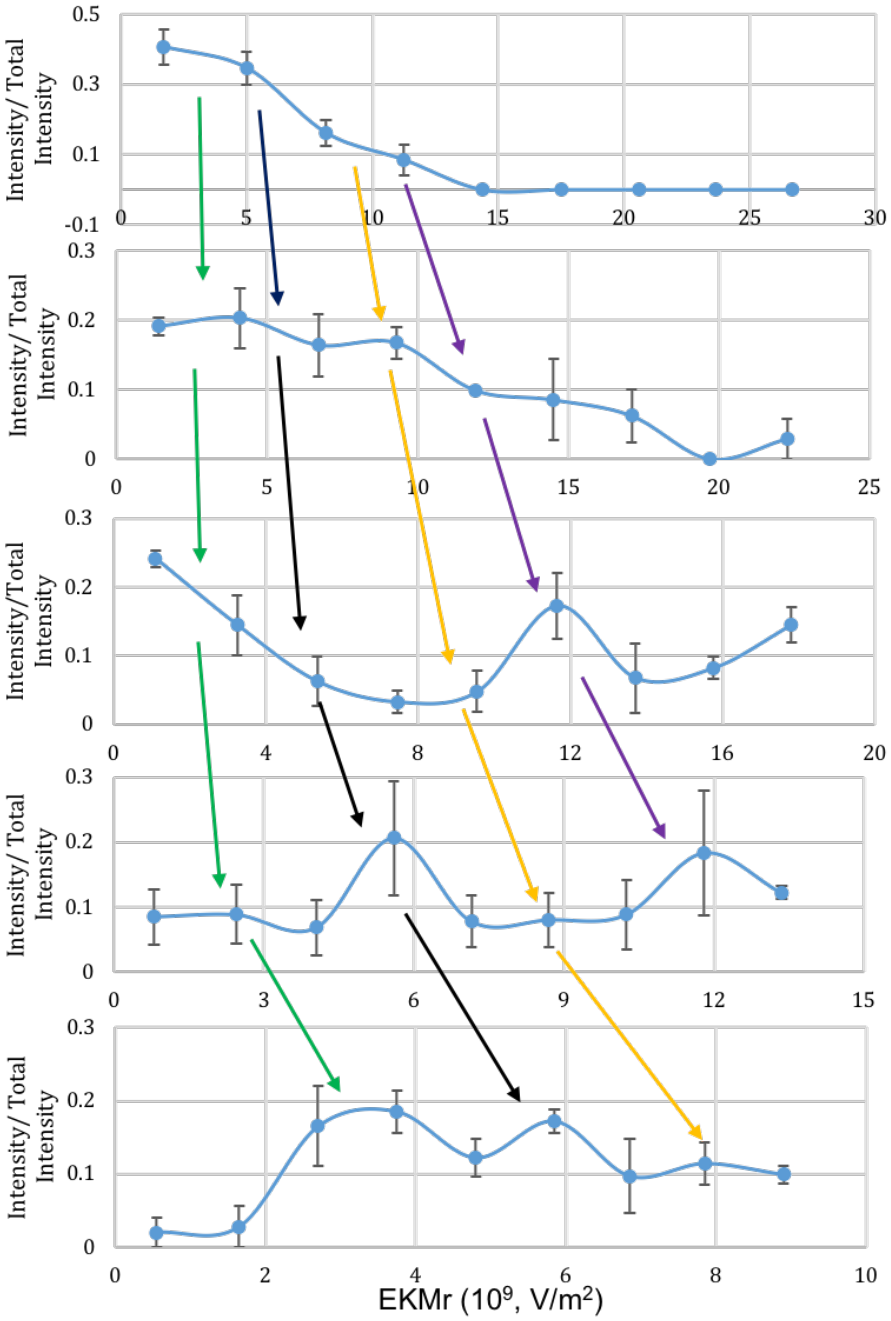

Figure 4.2. The biophysical property distributions of insulin vesicles with varied voltages applied. The normalized intensity of insulin vesicles captured were recorded with different EKMrs. From top to bottom, the voltage applied were 1800 V, 1500 V, 1200 V, 900 V, 600 V. Each color of arrow is representing a subpopulation found with a constant EKMr range. At 1800 V, full profile of insulin vesicle population biophysical distribution was recorded. The stacked subpopulations spread out and were separated with lower voltages applied. Error bars are based on SEM.

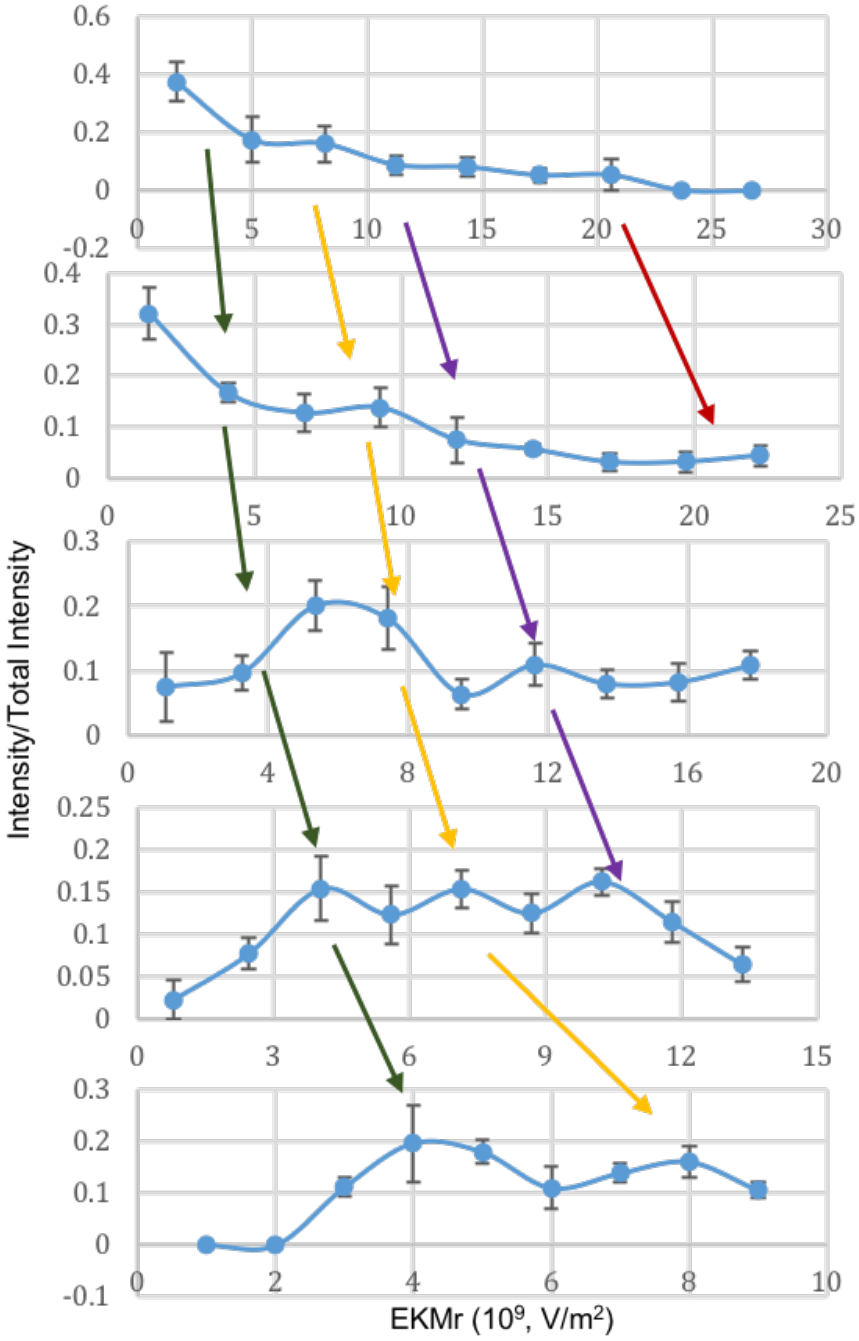

Figure 4.3. The biophysical property distributions of 25 mM glucose treated insulin vesicles with varied voltages applied. The normalized intensity of treated insulin vesicles captured were recorded with different EKMrs. From top to bottom, the voltage applied were 1800 V, 1500 V, 1200 V, 900 V, 600 V. Each color of arrow is representing a subpopulation found with a constant EKMr range. At 1800 V, full profile of insulin vesicle population biophysical distribution was recorded. The stacked subpopulations spread out and were separated with lower voltages applied. Error bars are based on SEM.

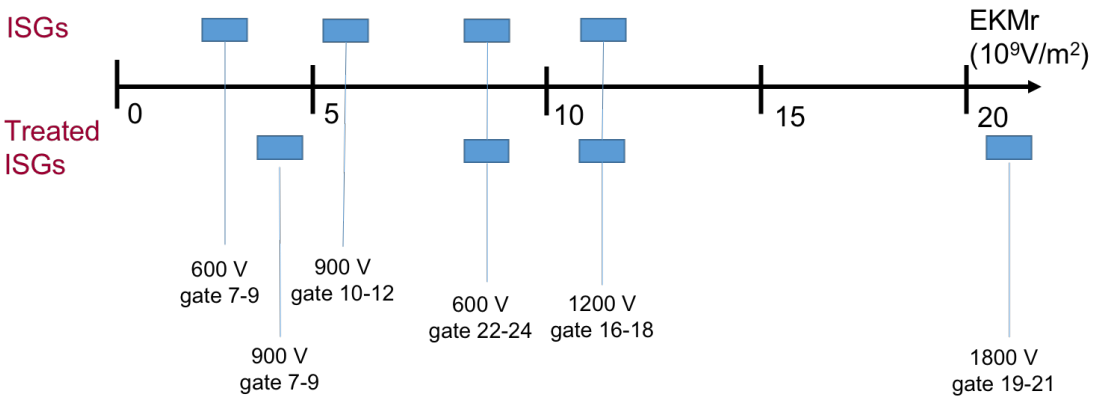

EKMr	Peaks found			
ISGs	3×10^9 V/m^2	6×10^9 V/m^2	8×10^9 V/m^2	11×10^9 V/m^2
Treated ISGs	4×10^9 V/m^2	8×10^9 V/m^2	11×10^9 V/m^2	21×10^9 V/m^2

Figure 4.4. Comparison of insulin vesicle and 25 mM glucose treated insulin vesicle subpopulations behaviors. An EKMr metric was used (top) to show where the peaks were found for the measurement. The inulin vesicle and glucose treated EKMr peaks are listed and compared (bottom).

4.4 Conclusion and Future Works

Insulin vesicles subpopulations were separated and thus identified by DC-iDEP and characterized by their biophysical properties. With varied potential applied, some more delicate subpopulation fingerprints were shown with higher resolution. The results of untreated insulin vesicles were compared with insulin vesicles from glucose-treated beta cells. The distributions showed significant differences with each other. This is consistent with the differences compared to treatment effect detected by granule density and absorbance. This is indicating the levels of specific surface protein is related with properties based on dielectrophoresis measurements as in previous work [1].

Future works include the extraction of insulin vesicle subpopulations from the device and characterizing them by techniques such as SEM and MS for more accurate and more complete proteome identification. The initial studies provide a promising method for purifying the insulin vesicles from other organelles and distinguish the biophysical properties related with genotypes and phenotypes. This success of the work would contribute to 3D structure of pancreatic beta cell model building, the mechanism study of disease progression, the evolvement of the cells and their molecular interactions.

4.5 References

[1] Suckale, Jakob, and Michele Solimena. "The insulin secretory granule as a signaling hub." *Trends in Endocrinology & Metabolism* 21.10 (2010): 599-609.

[2] Thurmond, Debbie C. "Regulation of insulin action and insulin secretion by SNARE-mediated vesicle exocytosis." *Mechanisms of Insulin Action*. Springer, New York, NY, 2007. 52-70.

[3] Khyade, Vitthalrao B. "Herbals and Their Compounds Targeting Pancreatic Beta Cells for the Treatment of Diabetes." *International Journal of Scientific Studies* 6.3 (2018): 1-44.

[4] Hickey, Anthony JR, et al. "Proteins associated with immunopurified granules from a model pancreatic islet β-cell system: proteomic snapshot of an endocrine secretory granule." *Journal of proteome research* 8.1 (2009): 178-186.

[5] Schvartz, Domitille, et al. "Improved characterization of the insulin secretory granule proteomes." *Journal of proteomics*75.15 (2012): 4620-4631.

[6] Rutter, Guy A., and Elaine V. Hill. "Insulin vesicle release: walk, kiss, pause… then run." *Physiology* 21.3 (2006): 189-196.

[7] Singla, Jitin, et al. "Opportunities and challenges in building a spatiotemporal multi-scale model of the human pancreatic β cell." *Cell* 173.1 (2018): 11-19.

[8] Hutton, J. C., E. J. Penn, and M. Peshavaria. "Isolation and characterisation of insulin secretory granules from a rat islet cell tumour." *Diabetologia* 23.4 (1982): 365-373.

[9] Lindall Jr, Arnold W., et al. "Isolation of an insulin secretion granule fraction." *The Journal of cell biology* 19.2 (1963): 317-324.

[10] Andrzejewski, Danielle, et al. "Activins A and B regulate fate-determining gene expression in islet cell lines and islet cells from male mice." *Endocrinology* 156.7 (2015): 2440-2450.

[11] White et al, Incretin Effect on Granule Density, in revision

[12] Moore, John H., et al. "Conductance-Based Biophysical Distinction and Microfluidic Enrichment of Nanovesicles Derived from Pancreatic Tumor Cells of Varying Invasiveness." *Analytical chemistry* 91.16 (2019): 10424-10431.

CHAPTER 5

HIGH RESOLUTION ISOLATION, CONCENTRATION AND CHARACTERIZATION OF PROTEINS

5.1 Introduction

The study of condensed phase solvated proteins in an electric field gradient are of great interest for both fundamental mechanisms of bioparticle dynamics and real-world general applications of protein manipulations. There remain several unsolved behaviors and unexplained properties of proteins in polar solvents. One of the most compelling and important manipulation is the separation of protein mixtures into pure and homogeneous fractions for each protein. Innumerable studies focused on simplifying heterogeneous mixtures into more pure fractions, typically in series using multiple mechanisms, have been studied and remain a core competency in every biology, biochemical and bioanalytical laboratory. These steps may include equilibrium-based biphasic systems (extractions, some chromatographies), gel entanglement or size exclusion mechanisms (filtration, other chromatographic mechanism), bulk properties (density, solubility) or electric field enhanced processes (gel and native electrophoresis). The overall goal of each of these processes is a purified fraction of solvated protein [1, 2]. The current study examines an additional capability for isolation, concentration, separation and characterization of proteins exploiting the higher order electrophysical properties of the protein-solvent system. [3] The mechanism promises extremely high fidelity and data presented is consistent with the theoretical resolving power of the system. Three proteins (Immunoglobulin G (IgG), α-chymotrypsinogen A and lysozyme) are chosen to

demonstrate the effects of electrophoresis juxtaposed with dielectrophoretic (encompassing all field gradient-induced forces) in a global gradient system. Each protein isolates and concentrates at a unique applied voltage such that its fundamental particle-solution-electric field interactions are quantified, all the while demonstrating a new separation scheme.

The ability to study proteins largely depends on isolating and concentrating fractions of completely pure material (purity such that the 3D location of every atom in the fraction is the same). Techniques have been used and developed for decades with continuously improved capabilities. However, all of these techniques merely exploit the first order moment (monopole) or equilibrium/mechanical interaction. Here differentiation is shown, which includes higher order electrical moments (dipole, quadrupole, etc.) and other related effects (interfacial polarization) which promises to be several orders of magnitude higher resolution and directly probes elements of the 3D structure (including entropic and temporal elements) which are only subtly different between two similar proteins [3].

This is a micro/nanoscale technique, generating concentrated bolus in pico/femtoliter volumes [2, 3]. Some characterization techniques commonly used in structural biology (EM, for example) need pure fractions of vanishingly small amounts of material (fmole/amole; 10^4-10^5 molecules), but common preparation schemes provide three to six orders of magnitude more than needed. While the ability to isolate and concentrate pure fractions of proteins in an ultra high-resolution format will find broad application for any protein preparation scheme, this is an exemplary demonstration of the

improved overall capability generated by optimizing separations and characterization schemes.

The separations occur by juxtaposing EP against DEP (and other gradient related forces), allowing each protein to reach its balance point or EKMr.

5.1.1 Protein separation significance

Protein has various well-known functions such as enzymatic action to facilitate catalysis, cell surface receptors for signaling, and transport for activation [4-6]. Proteomic analysis has attracted the interests of researchers towards providing biologically relevant function matched to genomic information. The identification of protein structure and function is still challenging for its complexity [7]. Efficient, specific and reliable protein purification methods are key steps for literally any proteomic study [8, 9]. Researchers are focusing their interest on specific proteins for purification and fractionation instead of general proteins [10].

In this chapter, some well characterized proteins were used for study. Lysozyme is a representative small protein where its function, structure, and dynamics are well-established. It functions as an enzyme to lyse bacteria, its presence can be a sign of disease, and it serves as model for folding mechanism studies [11, 12]. IgG is rich in human serum and works as an antibody involved in immune function [13]. α-chymotrypsinogen A was used as a protein model for studying the promotion effect of protein crystallization [14].

5.1.2 Protein separation techniques

5.1.2.1 Gel electrophoresis

Gel electrophoresis is a well-established method for protein sample mixture separation and is noted for its high sensitivity, multi protein detection and resolution [15].

Sodium dodecyl sulfate-polyacrylamide gel electrophoresis (SDS-PAGE) is a representative and reliable gel electrophoresis for separating proteins by size. SDS is an ionic surfactant that unfolds and denatures protein. Evenly distributed negative charges are given to the protein with the treatment by SDS, laying foundation on measuring the size of protein by the length. It includes one-dimensional and two-dimensional gel electrophoresis [16]. The technique has been applied for quantification, evaluating the purification, the molecular weight of the sample samples. Examples include separating hydrophobic proteins from hydrophilic proteins, for detecting phosphoproteins [17, 18].

Some commonly used techniques include tricine and glycine SDS-PAGE. The low concentration of acrylamide used not available in electrophoretic technique can be applied to measure hydrophobic proteins. The combination of the tricine and glycine SDS-PAGE broadens the protein measurement range to as high as 500 kDa. The tricine-SDS-PAGE can be applied to proteins larger than 30 kDa with very small proteins stacking at the front of the gel and the glycine-SDS-PAGE for small protein ranging less than 30 kDa. The protein band width composing less than 0.2 μg is preferentially stained, often with Coomassie staining [19, 20].

SDS-PAGE has been applied for protein quantification and heterogenous mixture studies in early works. Uytterhaegen et al. introduced an SDS-PAGE method for quantifying proteins [21]. This work monitored the amount of beef myofibrillar change

with aging. An SDS-PAGE method has been applied for separating the heavy chain from the embryonic myosin. This work demonstrates the embryonic myosin as a heterogenous mixtures [22].

However, there are also drawbacks for the method. Sample preparation, loading and staining complexity leads to fluctuation of the results. The oxidation of the proteins during separation also causes larger band width and lower resolution. The size estimation can be affected. This technique requires intense time and labor.

5.1.2.2 Size exclusion chromatography

Size exclusion chromatography (SEC) has been applied for protein separation because of its ability to provide molecular weight information from complex mixtures and preserve the native status of proteins. This is due to the fact that the separation is based on size and the proteins tested are non-denatured. Also, the silica support in the column makes it more efficiency and facilitates faster analysis than gel filtration [23, 24].

One of the drawbacks for this technique is the resolving capability. P. Lecchi et al. reported an SEC work for proteomics analysis. The work combined several other techniques including isoelectric focusing and 2D PAGE, which makes SEC capable of resolving for separating proteins [25]. Also, silica-based particles creating large plate numbers has been used for high performance SEC (HPSEC) to increase resolution [24]. A previous work showed the evaluation of proteins by HPSEC with 3 different pore sizes of particles [26]. The pH conditions were set up according to protein recovery and activity. The Protein mixtures including IgG, IgM, immunoglobulins were separated with good resolution. The hydrophobic coated silica particles showed high selectivity of different proteins.

SEC was also combined with other detection techniques for tracking protein aggregates. Large IgG aggregates were monitored using SEC combined with static light scattering detection. The was shown to be able to detect the existence of aggregates, not limited to recognizing oligomers and dimers [27].

5.1.2.3 Isoelectric focusing

Proteins are separated by isoelectric focusing (IEF) by their different isoelectric point (pI) values. The advantage is the high resolution of the technique over others. In IEF, pH gradients are created by ampholytes so that proteins can move to and concentrate in the corresponding pH zone according to their isoelectric point where the net charge is zero. This method can be applied for separating and identifying proteins that are closely related, enriching specific protein and measuring the heterogeneity of the mixtures [28, 29].

There are different types of isoelectric focusing. Micropreparative IEF is based on drop analysis between two electrodes. From anode to cathode, it enriches proteins either with increasing or decreasing PIs. It is suitable for purifying small amount of proteins preserving its non-denature conditions for further analysis. Egatz-Gomez et al. has used this technique for separating and monitoring four types of model proteins. The protein samples were recovered and analyzed in different fractions with simplicity [29].

IEF in immobilized pH gradients can be set by buffer monomers in gel, which provides higher resolution and capacity, easily controlled conductivity and ionic strength [30]. Harry Towbin et al. applied the technique for detecting the isoforms of protein by modification introduced by phosphorylation and acetylation. This is the first work for protein isoform analysis by 2D electrophoresis.

Capillary IEF has been used for its high sensitivity, direct detection and quantification, automation [31]. O'Neill et al. introduced a capillary IEF work combined with chemiluminescence, immunoassays for analyzing protein signaling by its phosphorylation state [32]. However for IEF, the pH gradient accuracy can easily be affected by the volume at the electrodes, the Joule heating effect [33]. Also, it is time consuming for analyzing proteins and forming protein precipitation.

5.2 Protein DEP Theory Evolution and Development

Small particles, including proteins, have long been considered a smaller version of particles well above the limit where diffusive forces dominate. With this consideration, they have been described by the Clausius-Mossotti factor which assumes a homogeneous solution and particle with no interfacial properties, just an infinitesimally small and abrupt change from solution permittivity and conductivity to those of the particle [34]. However, through separate works of Matyushov, Pethig and Heyden, there are a number of constructs which support a much larger force by considering interfacial polarization and detailed molecular properties of the bioparticles and local hydrating water molecules [34-36]. These evolving theories more closely reflect dielectric spectroscopic data from proteins and will undoubtable have a large impact on understanding other forms of electric field gradient-induced actions.

Three threads of underlying principles come into play for this study. First is the Clausius-Mossotti factor which describes an individually homogeneous particle/solution system in the presence of an electrical gradient. It predicts very small forces for small particles like proteins and is the currently accepted paradigm. Second is the basic

separations science associated with gradients showing that steep gradients give better separations, where in this study, due to the micro/nano scale of the system, the gradients are orders of magnitude higher than benchtop techniques. Third is a new theorical structure which includes interfacial polarization (the water/protein interface & multipole elements of the protein) in the force calculation that predicts reasonably large forces, as are observed here [1-3].

5.3 Materials and Methods

5.3.1 Microdevice Fabrication and Simulation

The device fabrication, imaging conditions and EKMr simulation has been described in Chapter 2 in the 'Microfluidic Device and Fabrication' section.

5.3.2 Protein sample preparation

The NHS-Rhodamine (Thermo Scientific, Rockford, IL, USA) was used for protein labeling according to the manuals & protocols. Briefly, 10 mg/ml NHS-Rhodamine in DMSO was freshly prepared and added to 1 mg/ml lysozyme (from chicken egg white, 3× crystallized, MP Biomedicals, LLC, Solon, Ohio, USA), IgG (≥ 95% SDS-PAGE, Sigma-Aldrich, St Louis, MO, USA) and α-chymotrypsinogen A (high purity, Bio Basic Inc., Amherst, NY, USA) 5 mM dissolved solution. The mixture was incubated for 1 h at room temperature after mixed with calculated volume of 10 mg/ml freshly dissolved NHS-Rhodamine. Dialysis was performed overnight to remove the unreacted dye. Lysozyme was finalized in 5 mM HEPES (Sigma-Aldrich, St Louis, MO, USA) solution with a conductivity of 115 μS/cm. IgG and α-chymotrypsinogen A were finalized in 5 mM HEPES and 2 mM phosphate (1:9, v/v) buffer solution with a

conductivity of 312 μS/cm. The final concentration of each protein was adjusted to 0.1 mg/ml prior to use.

5.3.3 Experimental

A microfluidic device was flushed with 5% BSA (bovine serum album) first for 15 min and then HEPES (5 mM, pH=7.3) buffer solution. The extra solution in the channel was removed by vacuum before introducing the protein samples. A 5 mM HEPES buffer solution (conductivity 115 μS/cm) was used for lysozyme testing and a mixture of 5 mM HEPES and 2 mM phosphate buffer (1:9, v/v) with conductivity of 312 μS/cm was used for α-chymotrypsinogen A and IgG testing. A global voltage up to 3000 V were applied between the inlet and outlet of the microfluidic device. The observations and intensities were recorded at 27 μm gate.

5.4 Results

5.4.1 Concentration and characterization of proteins by DC-iDEP

Non-linear electric field properties of proteins are probed and exploited in a DC-iDEP device. The electric field gradient was created by constraining the cross sectional area of the open channel with insulating bodies attached to the wall (see Figure 2.1) [37-40]. This study was performed at a single gate (27 μm), where the voltage was varied systematically and the intensity of the collected fluorescently labeled proteins was monitored. The three proteins were IgG (MW 150k), α -chymotripsinogen A (MW 25k), and lysozyme (MW 14.3k). These proteins were chosen because there was experimental data in the literature for free zone electrophoresis studies, which place the proteins in a similar environment to those of this platform and characterize similar properties [41-43].

Each protein began to collect at an applied potential unique to that protein. At higher values of applied potential, the intensity increased linearly. The point at which collection began to occur (onset voltage) indicates a balance of the linear electric field effects (electrophoresis, mono pole moment, first order electrokinetics) and higher order effects (dielectrophoresis, dipole and higher poles, higher order electrokinetics) for the buffer-protein-electric field system. The properties of the electric field may be obtained from finite element multiphysics calculation and the ratio of the two effects, as reflected by characteristic mobilities (electrokinetic and dielectrophoretic in current vernacular) is recorded [44]. At voltages above the onset voltage the dielectrophoretic forces dominate and no protein can pass the gate. Under this condition, more protein is transported to the capture zone as the potential is raised for a set period of time due to increased electrokinetic velocity induced by the higher field.

The nuanced structure of the electric field about the gates induces the collected proteins to form a characteristic arc where the forces are balanced across the width of the channel [44, 45]. When capture occurs, the intensity of the collected bolus continues to increase as more protein is transported electrophoretically until the voltage is removed and the particles diffuse away (Figure 5.1). Similar behavior occurs for all three proteins examined here, although at differing applied potentials. Here, the discussion below is noted that the concentration profile of the collected bands, as assessed along the longitudinal centerline of the device, are asymmetric and are steeper on the gate side than the more open area of the channel. Along these lines, the dielectrophoretic forces

dominate on the gate side of the collected bolus is noted, whereas the electrophoretic forces dominate on the more open side.

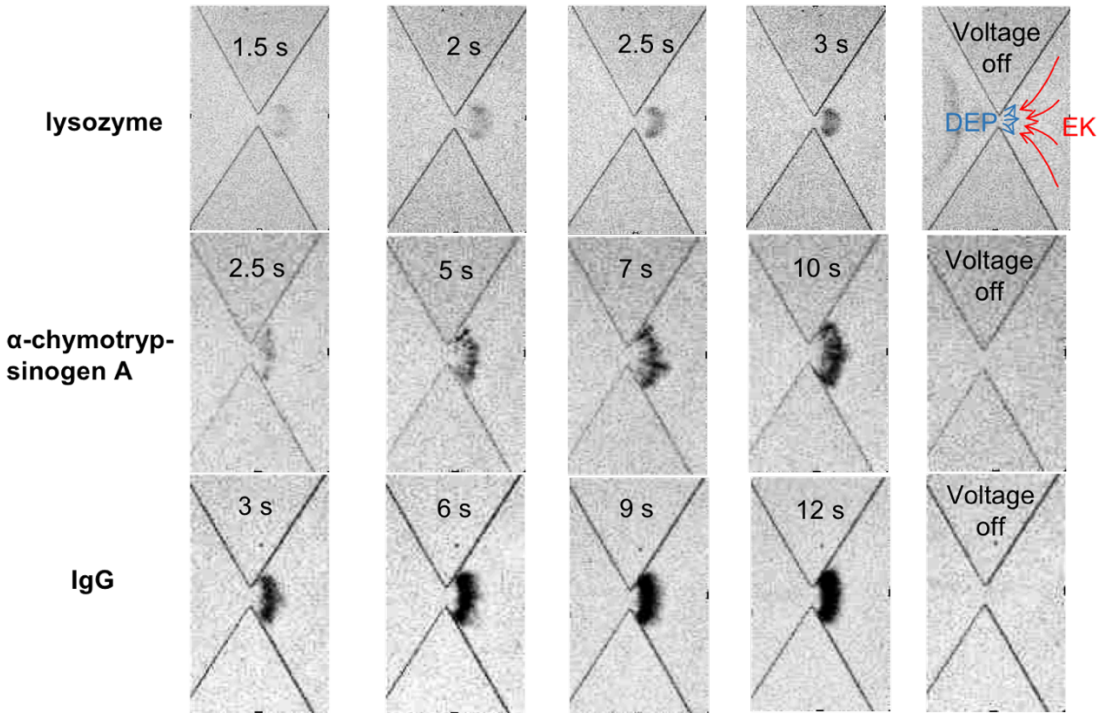

Figure 5.1. Images of lysozyme, α -chymotrypsinogen A, IgG captured at 27 μm gate. The process of capture and increasing concentration for lysozyme change was recorded with 2200 V applied over 3 s of potential applied. α -chymotrypsinogen A capture and concentration change was recorded within 10 s and IgG within 12 s of 1200 V applied. Note upon removal of the voltage, the proteins diffuse back into the bulk solution, showing the capture process is an applied potential dependent process. Images have been manipulated to increase visual clarity.

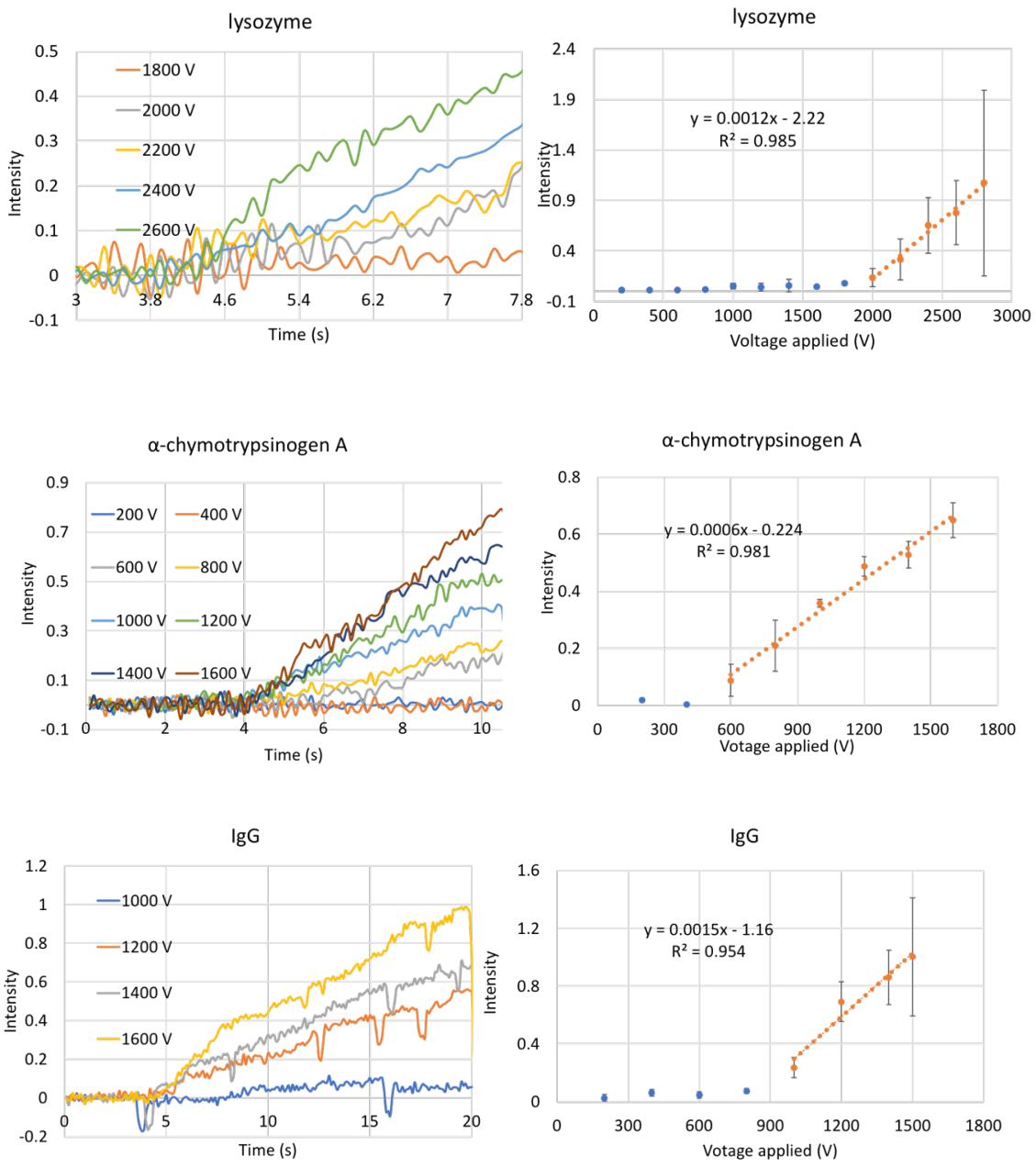

Figure 5.2. Time course plots (left) of intensity (normalized) for capture zone and single time point intensity versus applied external voltage (right) for three proteins on a DC-iDEP device. At sufficient voltage, at longer times (left) and higher voltages (right), more protein is collected. The linear portion of the variable voltage plots are used to obtain a more accurate 'onset' potential, the value where capture initiates and is mathematically related to the ratio of electrophoretic and dielectrophoretic mobility of the specific protein. Error bars are based on SEM.

5.4.2 New Scheme for high resolution protein separations

The intensity for a region of interest (ROI) of the collected proteins at a set time of applied potential were recorded and assessed (Figure 5.2). For values higher than the onset voltage, the linearity of the relationship of incrementally increased voltage and collected amount of protein was used to more accurately determine the onset voltage, with a characteristic variance determined [46]. The three proteins generated onset voltages which were significantly different and well differentiated. Using the calculated electric field properties, electrokinetic mobilities ratio values for each protein were determined [44]: lysozyme: 26.6 ± 3.8 × 10^9 V/m^2, α-chymotrypsinogen A: 5.3 ± 1.2 × 10^9 V/m^2, and IgG 11.1± 2.1 × 10^9 V/m^2 (Figure 5.3).

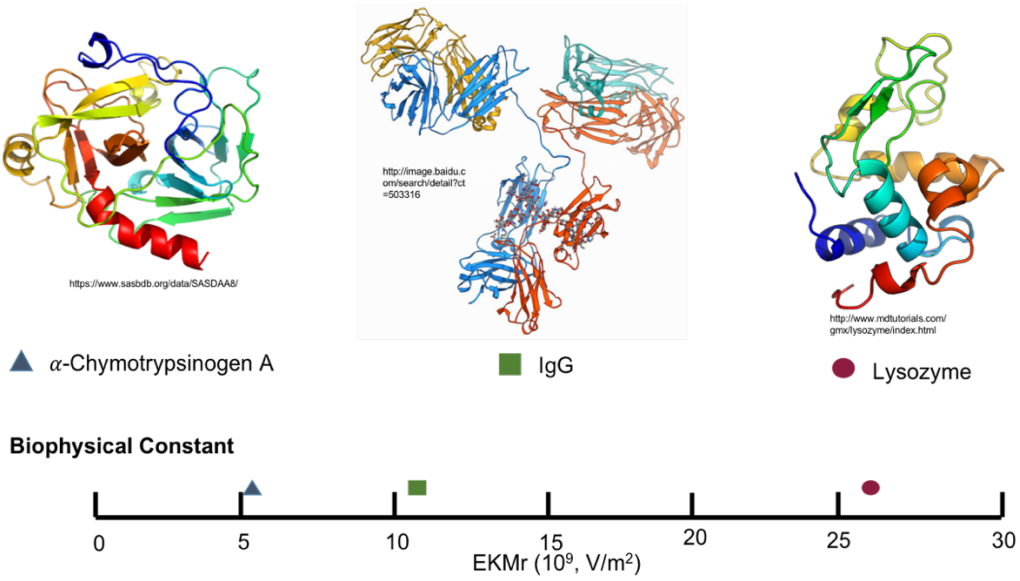

Figure 5.3. Characterization of lysozyme, α-chymotrypsinogen A, IgG by EKMr. The EKMr values of lysozyme, α -chymotripsinogen A, and IgG are compared on the EKMr scales. Blue triangle represents α -chymotripsinogen A, green square represents IgG, red circle represents lysozyme.

5.5 Conclusion and Future Directions

Proteins were successfully concentrated, differentiated and characterized by DC-iDEP. The lysozyme, α-chymotrypsinogen A, and IgG were distinguished by their biophysical properties. Their EKMr were identified to be 26.6 ± 3.8, 5.3 ± 1.2, and 11.1 ± 2.1×10^9 V/m^2, respectively. Future works include deeper characterization of the fundamental effects, application to a broader range of proteins, and integrating the system with high information content detection modalities such as mass spec and EM.

The updated theory guided behavior of proteins was demonstrated in the DC-iDEP device. Three protein including lysozyme, IgG and α-chymotrypsinogen A were differentiated by EKMr with high resolution based on their high order of electric properties. A new method for characterizing proteins is established.

5.6 References

[1] Pethig, Ronald. "Where is dielectrophoresis (DEP) going?." *Journal of The Electrochemical Society* 164.5 (2017): B3049-B3055.

[2] Matyushov, Dmitry V. "Dipolar response of hydrated proteins." *The Journal of chemical physics* 136.8 (2012): 02B618.

[3] Jones, Paul V., and Mark A. Hayes. "Development of the resolution theory for gradient insulator-based dielectrophoresis." *Electrophoresis* 36.9-10 (2015): 1098-1106.

[4] Shoichet, Brian K., et al. "A relationship between protein stability and protein function." *Proceedings of the National Academy of Sciences* 92.2 (1995): 452-456.

[5] Murphy, Mary G. "Dietary fatty acids and membrane protein function." *The Journal of nutritional biochemistry* 1.2 (1990): 68-79.

[6] Gimeno, Ruth E. "Fatty acid transport proteins." *Current opinion in lipidology* 18.3 (2007): 271-276.

[7] Lesley, Scott A. "High-throughput proteomics: protein expression and purification in the postgenomic world." *Protein expression and purification* 22.2 (2001): 159-164.

[8] Hilbrig, Frank, and Ruth Freitag. "Protein purification by affinity precipitation." *Journal of chromatography B* 790.1-2 (2003): 79-90.

[9] Franzreb, Matthias, et al. "Protein purification using magnetic adsorbent particles." *Applied microbiology and biotechnology*70.5 (2006): 505-516.

[10] Scopes, Robert K. *Protein purification: principles and practice*. Springer Science & Business Media, 2013.

[11] Merlini, Giampaolo, and Vittorio Bellotti. "Lysozyme: a paradigmatic molecule for the investigation of protein structure, function and misfolding." *Clinica chimica acta* 357.2 (2005): 168-172.

[12] Mckenzie, Hugh A., and Frederick H. White Jr. "Lysozyme and α-lactalbumin: structure, function, and interrelationships." *Advances in protein chemistry*. Vol. 41. Academic Press, 1991. 173-315.

[13] Vidarsson, Gestur, Gillian Dekkers, and Theo Rispens. "IgG subclasses and allotypes: from structure to effector functions." *Frontiers in immunology* 5 (2014): 520.

[14] Zhang, Chen-Yan, et al. "Effect of real-world sounds on protein crystallization." *International journal of biological macromolecules* 112 (2018): 841-851.

[15] Ünlü, Mustafa, Mary E. Morgan, and Jonathan S. Minden. "Difference gel electrophoresis. A single gel method for detecting changes in protein extracts." *Electrophoresis* 18.11 (1997): 2071-2077.

[16] Brunelle, Julie L., and Rachel Green. "One-dimensional SDS-polyacrylamide gel electrophoresis (1D SDS-PAGE)." *Methods in enzymology*. Vol. 541. Academic Press, 2014. 151-159.

[17] Rais, Isam, Michael Karas, and Hermann Schägger. "Two-dimensional electrophoresis for the isolation of integral membrane proteins and mass spectrometric identification." *Proteomics* 4.9 (2004): 2567-2571.

[18] Kinoshita, Eiji, Emiko Kinoshita-Kikuta, and Tohru Koike. "Separation and detection of large phosphoproteins using Phos-tag SDS-PAGE." *Nature protocols* 4.10 (2009): 1513.

[19] Schägger, Hermann. "Tricine–sds-page." *Nature protocols* 1.1 (2006): 16.

[20] Karpe, Fredrik, and Anders Hamsten. "Determination of apolipoproteins B-48 and B-100 in triglyceride-rich lipoproteins by analytical SDS-PAGE." *Journal of lipid research* 35.7 (1994): 1311-1317.

[21] Claeys, Erik, et al. "Quantification of beef myofibrillar proteins by SDS-PAGE." *Meat Science* 39.2 (1995): 177-193.

[22] Carraro, Ugo, and Claudia Catani. "A sensitive SDS-PAGE method separating myosin heavy chain isoforms of rat skeletal muscles reveals the heterogeneous nature of the embryonic myosin." *Biochemical and biophysical research communications* 116.3 (1983): 793-802.

[23] Lemmo, Anthony V., and James W. Jorgenson. "Two-dimensional protein separation by microcolumn size-exclusion chromatography-capillary zone electrophoresis." *Journal of Chromatography A* 633.1-2 (1993): 213-220.

[24] Irvine, G. Brent. "High-performance size-exclusion chromatography of peptides." *Journal of Biochemical and Biophysical Methods* 56.1-3 (2003): 233-242.

[25] Lecchi, Paolo, et al. "Size-exclusion chromatography in multidimensional separation schemes for proteome analysis." *Journal of biochemical and biophysical methods* 56.1-3 (2003): 141-152.

[26] Ahmed, Faizy, and Bijan Modrek. "Biosep-SEC-S high-performance size-exclusion chromatographic columns for proteins and peptides." *Journal of Chromatography A* 599.1-2 (1992): 25-33.

[27] Ahrer, K., et al. "Analysis of aggregates of human immunoglobulin G using size-exclusion chromatography, static and dynamic light scattering." *Journal of chromatography A*1009.1-2 (2003): 89-96.

[28] Righetti, Pier Giorgio, and James W. Drysdale. "Isoelectric focusing in gels." *Journal of Chromatography A* 98.2 (1974): 271-321.

[29] Egatz-Gomez, Ana, and Wolfgang Thormann. "Micropreparative isoelectric focusing protein separation in a suspended drop." *Electrophoresis* 32.12 (2011): 1433-1437.

[30] Bjellqvist, Bengt, et al. "Isoelectric focusing in immobilized pH gradients: principle, methodology and some applications." *Journal of biochemical and biophysical methods* 6.4 (1982): 317-339.

[31] Pritchett, Thomas J. "Capillary isoelectric focusing of proteins." *Electrophoresis* 17.7 (1996): 1195-1201.

[32] O'Neill, Roger A., et al. "Isoelectric focusing technology quantifies protein signaling in 25 cells." *Proceedings of the National Academy of Sciences* 103.44 (2006): 16153-16158.

[33] Vesterberg, Olof. "Isoelectric focusing of proteins in polyacrylamide gels." *Biochimica et Biophysica Acta (BBA)-Protein Structure* 257.1 (1972): 11-19.

[34] Pethig, Ronald. "Limitations of the Clausius-Mossotti function used in dielectrophoresis and electrical impedance studies of biomacromolecules." *Electrophoresis* 40.18-19 (2019): 2575-2583.

[35] Matyushov, Dmitry V. "Electrostatic solvation and mobility in uniform and non-uniform electric fields: From simple ions to proteins." *Biomicrofluidics* 13.6 (2019): 064106.

[36] Waskasi, M. and M. Heyden, Microscopic driving forces of protein dielectrophoresis. *Journal of Physical Chemistry B*, 2019. 123: p. In preparation.

[37] Clarke, Richard W., et al. "Trapping of proteins under physiological conditions in a nanopipette." *Angewandte Chemie International Edition* 44.24 (2005): 3747-3750.

[38] Lapizco-Encinas, Blanca H., Sandra Ozuna-Chacón, and Marco Rito-Palomares. "Protein manipulation with insulator-based dielectrophoresis and direct current electric fields." *Journal of Chromatography A* 1206.1 (2008): 45-51.

[39] Chou, Chia-Fu, et al. "Electrodeless dielectrophoresis of single-and double-stranded DNA." *Biophysical journal* 83.4 (2002): 2170-2179.

[40] Cummings, Eric B., and Anup K. Singh. "Dielectrophoresis in microchips containing arrays of insulating posts: theoretical and experimental results." *Analytical chemistry* 75.18 (2003): 4724-4731.

[41] Kvasnička, František. "Determination of egg white lysozyme by on-line coupled capillary isotachophoresis with capillary zone electrophoresis." *Electrophoresis* 24.5 (2003): 860-864.

[42] Otte, J. A. H. J., et al. "Separation of individual whey proteins and measurement of -lactalbumin and -lactoglobulin by capillary zone electrophoresis." *Netherlands Milk and Dairy Journal* 48 (1994): 81-81.

[43] Raacke, Ilse Dorothea. "Heterogeneity studies on several proteins by means of zone electrophoresis on starch." *Archives of biochemistry and biophysics* 62.1 (1956): 184-195.

[44] Crowther, Claire V., et al. "Isolation and identification of Listeria monocytogenes utilizing DC insulator-based dielectrophoresis." *Analytica chimica acta* 1068 (2019): 41-51.

[45] Staton, Sarah JR, et al. "Characterization of particle capture in a sawtooth patterned insulating electrokinetic microfluidic device." *Electrophoresis* 31.22 (2010): 3634-3641.

[46] Hilton, Shannon Huey, and Mark A. Hayes. "A mathematical model of dielectrophoretic data to connect measurements with cell properties." *Analytical and bioanalytical chemistry* 411.10 (2019): 2223-2237.

CHAPTER 6

SEPARATION AND CHARACTERIZATION OF SALMONELLA SEROTYPES

6.1 Introduction

There is an increasing array of methods to characterize microorganisms from whole genome sequencing to traditional culturing strategies [1,2]. For *Salmonella*, a common foodborne pathogen that can cause disease in humans, the characterization must allow tracking of the contamination source by using appropriate subtyping tools [3]. The 'gold standard' classifying subtle differences between salmonella strains is based on the *Kauffmann-White* nomenclature [4], representing a traditional phenotyping method that is logistically challenging, as it requires the use of more than 150 specific antisera and well trained personnel to interpret the results [5]. One emerging and unproven strategy is to directly assess the biophysical characteristics of the native and unlabeled cells towards correlating their properties with specific serotypes. In this study, two closely related serovars based on the similar antigens indicated in the *Kauffmann-White* categorization scheme are tested and were differentiated in their native state with simple electric field interactions.

The common microbe *Salmonella* is thought to be responsible for 450 deaths, 23,000 hospitalizations and 1.4 million illnesses each year in the United States [6]. The typical symptom is abdominal pain and is diagnosed as gastroenteritis, with severe infections becoming life threatening. Food safety incidents and recalls continue in recent years, mostly associated with processed products [7-10], and other food commodities (e.g., meat products, eggs, and vegetables) [3, 11-13]. These occurrences necessitate

accurate and relatively rapid subtyping tools for identifying the original source of contamination [14-16]. *Salmonella* is a diverse pathogen and there are over 2500 *Salmonella* serotypes (2007 data) which have been described.(Grimont and Weill 2007) Of these, 99% of human isolates belong to the subspecies *Salmonella enterica* subsp. *enterica* (also described equivalently as 'subspecies I').

The immunoreactivities to O and H antigens of each isolate define the serotype, where a substantial diversity exists within the antigens. A cell surface lipopolysaccharide structure makes up the O antigen and typically consists of four to six sugars. The various specific antigens can differ by the linkages between sugars, covalent bonds between the units, or differences in the sugars themselves. These are divided into "O group antigens" (specific sugar configuration of the O antigen structure) and "ancillary O antigens" (additional carbohydrates). On the other hand, a proteinaceous antigen, flagellin or H antigen, is located on the flagellum in a filamentous portion. The core structural elements of these proteins which provide the filamentous structure, C' and N' termini, are conserved. The middle region of flagellin is exposed on the surface and is antigenically variable. Like many taxonomic and categorization schemes, those associated with *Salmonella* are evolving and therefore include modern and systematic definitions along with archaic terms still in common usage. This will provide a framework for assigning the quantified differences in biophysical properties presented here to specific biochemical origins.

This chapter demonstrates a rapid biophysical differentiation of strains of *Salmonella,* sv. *Cubana*, sv. *Senftenberg*, sv. *I 11:a:*-, and sv. *Poona*, using constant

voltage gradient insulator-based dielectrophoresis (DC-iDEP) (Figure 6.1). The distinction is reflected by a different voltage at which each strain begins to capture, defining a specific characteristic and deterministic property for each strain. With some additional measurements, the specific forces regarding the electrokinetic and dielectrophoretic mobilities are determined. These values allow some insights into the molecular and structural origins of the differentiation [17]. This provides strong evidence that the simple measurement of the native and unlabeled cells may provide another valuable tool in the determination of serovars and basic science studies of *Salmonella.*

6.2 Materials and Methods

6.2.1 Bacterial Culture and Sample Preparation

sv. *Cubana* (ATCC 12007) sv. *Senftenberg*, sv. *I 11:a:*-, and sv. *Poona* (ATCC BAA-1673) were obtained from ATCC. Each strain was grown on triple sugar iron agar for 4 days at ambient temperature. 10 mL of sterile 3% tryptic soy broth was inoculated, and the serotype solutions were incubated in a shaker/incubator at 250 rpm (37 °C) for 19 h. The concentration of cells is about 10^9 CFU/mL. The cultures were stored at 4 °C. Microbial cultures are required at Biosafety Level 1 or 2 or 3. All the experiments were performed with Biosafety Level 2 space.

A volume of 100 µl of each culture was dissolved into 900 µl of 5 mM 4-(2-hydroxyethyl)-1-piperazineethanesulfonic acid (HEPES) buffer (pH=7.3) solution and centrifuged for 5 min at 2000 g. The supernatant was removed, and the washing procedure was repeated three times with HEPES buffer solution. The sample was suspended in 1 mL of 5 mM HEPES buffer solution prior to use.

6.2.2 Microdevice Design, Simulation and Fabrication

A microchannel described in a previous work [18] and used for other cellular studies [19-21]. It was described in Chapter 2.

6.2.3 Theory

The capture of the particles can be observed with the condition described in Chapter 2:

$$\frac{\nabla|\vec{E}|^2}{E^2} \cdot \vec{E} \geq \frac{\mu_{EK}}{\mu_{DEP}} \tag{5}$$

where $\nabla|\vec{E}|$ is the gradient of the electric field and E and $\vec{E}$ are the scalar and vector electric field, respectively. The ratio of EK to DEP mobilities $\frac{\mu_{EK}}{\mu_{DEP}}$ (EKMr) which relates size, conductivity, surface charge and other factors of the particle to the electric field properties are used to distinguish the subtle differences between the two strains of *Salmonella*. The specific cell features which are reflected in this term are under debate, but the magnitude of this measured property will not change [22]. The electric field and the gradient of the electric field combination ($\frac{\nabla|\vec{E}|^2}{E^2} \cdot \vec{E}$) are simulated to provide the EKMr for each strain.

The value of μ_{EK} was determined for both strains by particle tracking velocimetry [17, 21] at various applied voltages based on:

$$\vec{v}_{EK} = \mu_{EK}\, \vec{E} \tag{6}$$

where $\vec{v}_{EK}$ is the velocity of the particle in an open channel.

6.2.3 Experimental Procedure

The microdevice channel was treated with 5% (w/v) bovine serum album in 2 mM phosphate buffer at pH 7.4 and rinsed with 5 mM HEPES buffer solution before introducing the prepared bacterial sample. Dielectrophoresis behaviors of the two strains were observed by an Olympus IX70 inverted microscope with a ×4 or ×10 objective. Images and videos were recorded by QICAM cooled CCD camera (QImaging, Inc., Surrey, BC) and Streampix III image capture software (Norpix, Inc., Montreal, QC). A voltage between 0 – 3000 V was applied to platinum electrodes (0.404-mm external diameter, 99.9% purity, Alfa Aesar, Ward Hill, MA) connected to the inlet (+) and outlet (ground) to capture and study behaviors of Salmonella strains. Analysis and error assessment were based on 4 individual trials for each strain.

6.3 Results

6.3.1 Capture of salmonella serotypes by DC-iDEP

The biophysical behavior of sv. *Cubana*, sv. *Senftenberg*, sv. *I 11:a:-*, and sv. *Poona* were investigated in the DC-iDEP device. (Figure 6.1) Each strain was tested separately in various devices of the same design. All of the strains produced a pattern of collected cells appearing as distinct arcs near a 27 μm gate at appropriate applied voltages (Figure 6.1 left) [19-21]. Each strain showed different initial capture behavior. The strain dispersed as expected when the electric field was removed, which indicated the effective removal of the electrokinetic and dielectrophoretic forces on the particles.

The intensity within the capture area was recorded where the increased intensity reflected the collection of the cells (Figure 6.1 middle). The intensity curves of sv.

Cubana from 1200 – 3000 V and sv. *Poona* from 1200 – 2400 V in 200 V increments, sv. *Senftenberg* from 1400 V- 2800 V, *I 11:a:*- from 400 – 1800 V was plotted. The intensities increase with higher applied voltages for each strain.

Data were analyzed at a constant time (10 s after voltage applied) for sv. *Cubana*, sv. *Senftenberg*, sv. *I 11:a:*-, and sv. *Poona* (Figure 6.1 right). For the blue data points at lower voltages, where no capture occurred, no significant change of the intensity is observed and is comparable to the background. The orange data points at higher voltages, from 2000 V for sv. *Cubana* and sv. *Senftenberg*, from 1400 V for sv. *I 11:a:*-, and from 1600 V for sv. *Poona*, were used for plotting the linear regression line of the increased intensity reflective of cell accumulation. Error bars reflect standard error of the mean (SEM).

6.3.2 Ratio of EK to DEP mobility and EK mobility determination of salmonella serotypes

The slope and intercept of the linear fits were used to determine the rate of particle accumulation and onset voltage for capture (Figure 6.2) [17]. In this way, initial capture voltages were determined to be 1889 ± 228 V for sv. *Cubana* 1891.8 V ± 99.2 V for sv. *Senftenberg*, 1357.1 ± 226.4 V sv. *I 11:a:*-, and 1525 ± 196 V for sv. *Poona*. Using the multiphysics calculations to determine the field and gradient values, the EKMr was determined to be $2.7 \pm 0.3 \times 10^{10}$ V/m^2 for sv. *Cubana*, $2.7 \pm 0.1 \times 10^{10}$ V/m^2 for sv. *Senftenberg*, $1.9 \pm 0.3 \times 10^{10}$ V/m^2 for sv. *I 11:a:*-, and $2.2 \pm 0.3 \times 10^{10}$ V/m^2 for sv. *Poona*. These are well differentiated and sufficiently different to be considered statistically significant.

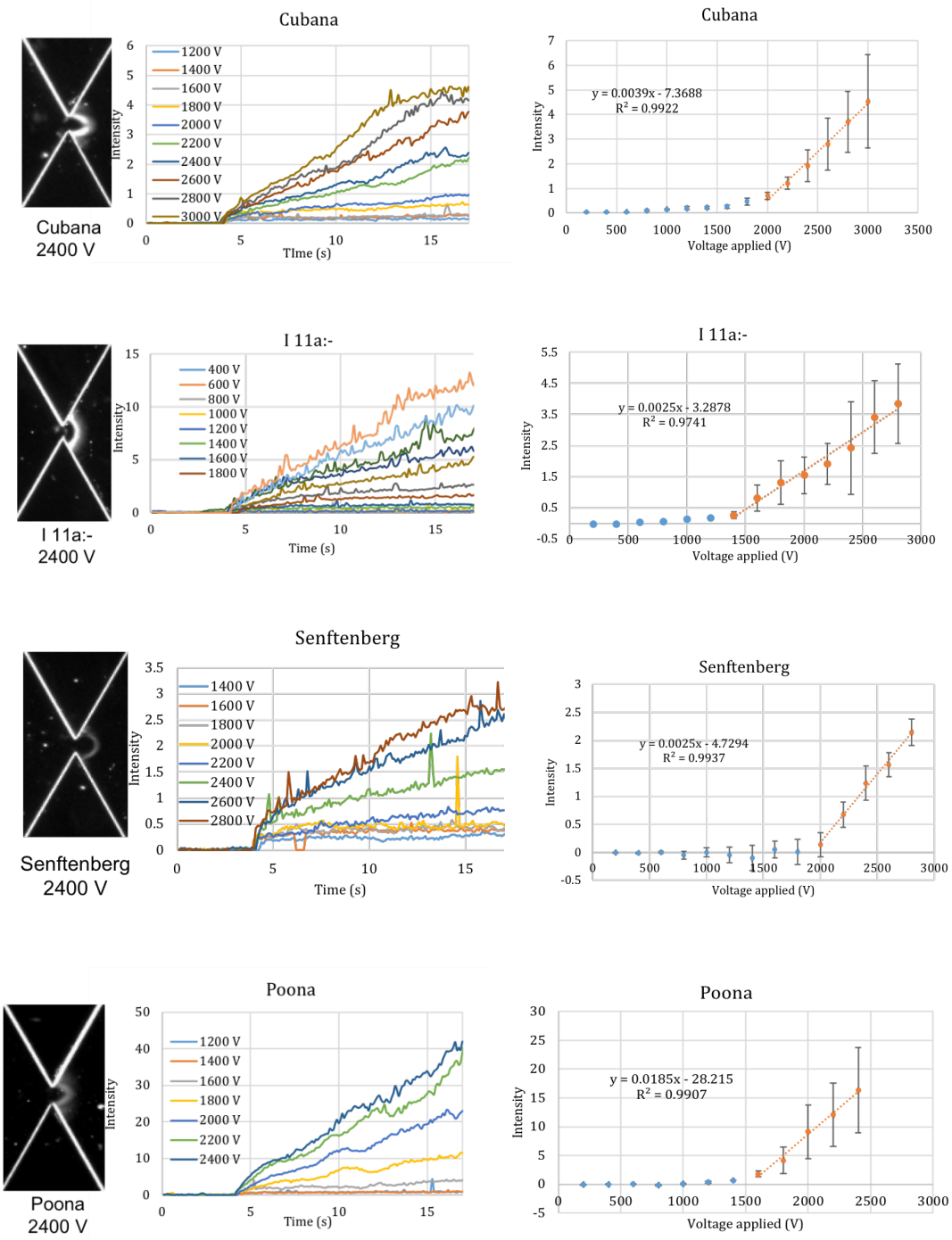

Figure 6.1. Capture of sv. *Senftenberg*, sv. *Cubana*, sv. *Poona*, and sv. *I 11:a:-* in DC-iDEP device. The capture images were taken at 2400 V at 27 µm gate (left). sv. *Senftenberg* intensity curves was shown from 1400 V to 2800 V, sv. *Cubana* from 1200 V to 3000 V, sv. *Poona* from 1200 V to 2400 V, sv. *I 11:a:-* from 400 V to 1800 V

(middle). sv. *Senftenberg*, sv. *Cubana*, sv. *Poona*, and sv. *I 11:a:-* concentration intensity change was recorded at 15 s with potential applied.

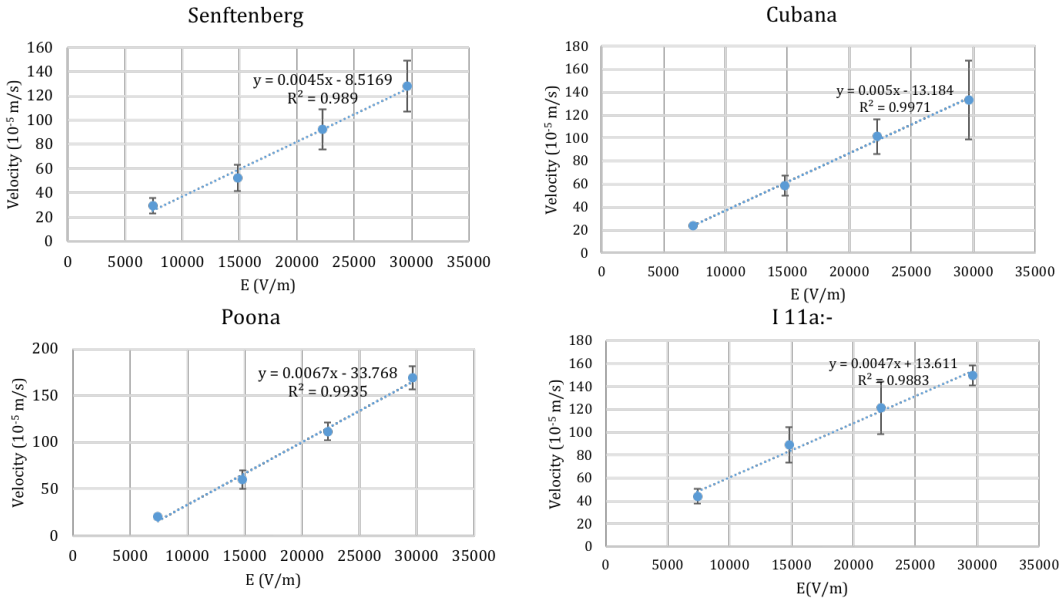

Figure 6.2. Plot of salmonella serotype velocity change with applied electric field. The velocity of sv. *Senftenberg*, sv. *Cubana*, sv. *Poona*, and sv. *I 11:a:-* was plotted and the EK mobility μ_{EK} can be calculated. $\vec{v}_{EK} = \mu_{EK}\,\vec{E}$.

The electrokinetic behaviors of the strains were determined according to eq. 6 by particle tracking to monitor the velocity while varying electric field strength. According to equation:

$$\vec{v}_{EK} = \mu_{EK}\,\vec{E}$$

the slopes of the linear fits determine the sv. *Cubana* μ_{EK} to be $5.0 \pm 0.5 \times 10^{-8}$ m^2/Vs, sv. *Senftenberg* to be $4.5 \pm 0.4 \times 10^{-8}$ m^2/Vs, sv. *I 11:a:-* to be $4.7 \pm 0.4 \times 10^{-8}$ m^2/Vs, and sv. *Poona* μ_{EK} to be $6.7 \pm 0.3 \times 10^{-8}$ m^2/Vs. With EKMr ($\frac{\mu_{EK}}{\mu_{DEP}}$) and μ_{EK} values,

$\mu_{DEP}$of sv. *Cubana* was calculated to be 1.8 ± 0.3 × 10^{-18} m^4/V^2s, *Senftenberg* to be 1.7 ± 0.2 × 10^{-18} m^4/V^2s, sv. *I 11:a:-* to be 2.5 ± 0.5 × 10^{-18} m^4/V^2s and for sv. *Poona* it was determined to be 3.0 ± 1.3 × 10^{-18} m^4/V^2s.

6.3.3 Differentiation of salmonella serotypes

The *Salmonella* strains were differentiated by mobility comparison (Figure 6.3). The EKMr were determined by the initial captured potential after simulation. The DEP mobility were obtained from the EK mobility and DEP mobility calculations. They can be distinguished by EKMr/DEP mobilities. The strains are demonstrated to have different biophysical behaviors distinguished by the DC-iDEP device.

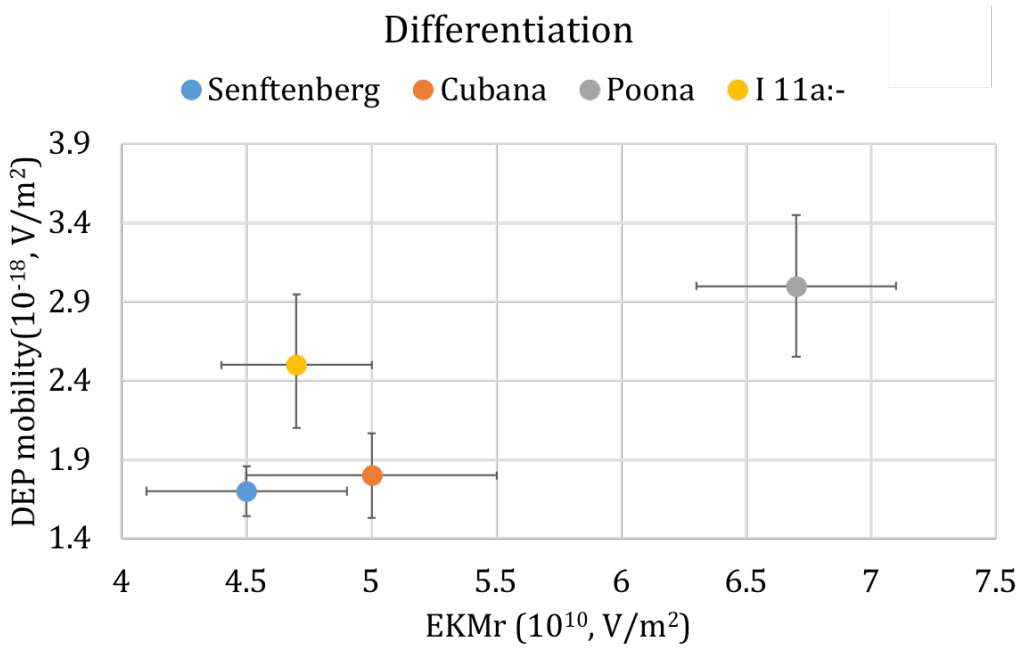

Figure 6.3. sv. *Senftenberg*, sv. *Cubana*, sv. *Poona*, and sv. *I 11:a:-* differentiation by their biophysical properties detected by DC-iDEP device. The four strains of salmonella can be distinguished by their EKMr and DEP mobility. Senftenberg: blue, Cubana: orange, Poona: grey, Ⅰ 11:a:-: yellow. Error bars represent SEM.

6.4 Discussion

Dielectrophoresis and cellular impedance spectroscopy have demonstrated a capability to differentiate cells based upon changes in the biochemical makeup of the cellular structure with labels [17, 20, 21, 23-31]. This approach of serotyping requires less expenses and expertise for producing antisera in agglutination test utilizing O and H antiserum and does not require expertise genomic information interpretation skills in whole genome sequencing for identifying *Salmonella* [32, 33].

The relationship between biophysical behaviors, zeta potential, and the mobilities has been described in a previous literature [17]. Zeta potential shows linearity with EK mobility and results in the difference of the onset voltage and the concentration slope. The differences in the conductivity of the serotypes could also affect the capture onset potential because the change of the DEP mobility. However, the conductivity and permittivity of the medium contribute little to the capture onset potentials for the behaviors of two serotypes but has a significant effect to the accumulation slope.

The electrokinetic mobility is significantly different between these strains, supporting the conclusion that the surface charge is changed [17]. This a reasonable result since the surface antigens are known to be different between sv. *Cubana* and sv. *Poona*. In addition, the dielectrophoretic mobility differs between the strains, showing that both surface and interior electrophysical properties differ, although it is impossible to assign a specific ratio to the relative effect from each [17]. The biophysical differences between the two strains are reasonable with regards to the biological and biochemical alterations noted in the nomenclature alone, without considering other undocumented effects. The

eventual impact of these results is yet to be understood in the serotyping laboratory; it is not known what other techniques will be enhanced by using this as a pre-screening or concentrating tool or if it will eventually develop into a standalone serotyping mechanism for well-known and vetted samples. An interesting question which remains to be answered is whether the magnitude of the differences in biophysical properties have any correlation with the total known and identified differences in the strains.

In developing and discussing this technique over many venues, some themes emerged which have proven instructive. First is that the effects of biologically important changes may not induce a measurable change in the cells using the electric field effects. The current study undermines this concept, along with many previous quantitative assessments [17, 19-21, 31]. The second theme is that the variation in the biological entities will be too great to decipher. Interestingly enough, this high-resolution capability provides a tool to investigate the origins and structure of that variability. Within any population of cells some will have a biologically significant change and others will have routine property variances which are not biological differentiators. This technique can allow for quantitative determination of biophysical-to-biological action connectivity.

6.5 Conclusion

This work demonstrates the differentiation of 4 strains of Salmonella, sv. *Cubana* sv. *Senftenberg*, sv. *I 11:a:-*, and sv. *Poona*, by DC-iDEP device. The variable capture conditions are accomplished without labels or otherwise altering the cells, the effects occur due to the native condition of the organisms with the setting of electric field properties. These results support the concept that biophysical separation and

concentration will potentially become a useful tool in the microbiology laboratory to aid in serotyping of Salmonella.

6.6 References

[1] Chiou, Chien-Shun, et al. "Usefulness of pulsed-field gel electrophoresis profiles for the determination of Salmonella serovars." *International journal of food microbiology* 214 (2015): 1-3.

[2] Ibrahim, George M., and Paul M. Morin. "Salmonella serotyping using whole genome sequencing." *Frontiers in microbiology* 9 (2018): 2993.

[3] Tang, Silin, et al. "Assessment and comparison of molecular subtyping and characterization methods for Salmonella." *Frontiers in microbiology* 10 (2019): 1591.

[4] Grimont, Patrick AD, and François-Xavier Weill. "Antigenic formulae of the Salmonella serovars." *WHO collaborating centre for reference and research on Salmonella* 9 (2007): 1-166.

[5] Diep, Benjamin, et al. "Salmonella serotyping; comparison of the traditional method to a microarray-based method and an in silico platform using whole genome sequencing data." *Frontiers in microbiology* 10 (2019): 2554.

[6] Centers for Disease Control and Prevention. "National Salmonella surveillance overview." *Atlanta, Georgia: US Department of Health and Human Services, CDC* (2011).

[7] Pillai, Suresh D., and Steven C. Ricke. "Review/Synthèse Bioaerosols from municipal and animal wastes: background and contemporary issues." *Canadian Journal of Microbiology*48.8 (2002): 681-696.

[8] Maciorowski, K. G., et al. "Incidence, sources, and control of food-borne Salmonella spp. in poultry feeds." *World's Poultry Science Journal* 60.4 (2004): 446-457.

[9] Park, S. Y., et al. "Environmental dissemination of foodborne Salmonella in preharvest poultry production: reservoirs, critical factors, and research strategies." *Critical reviews in environmental science and technology* 38.2 (2008): 73-111.

[10] Olaimat, Amin N., and Richard A. Holley. "Factors influencing the microbial safety of fresh produce: a review." *Food microbiology* 32.1 (2012): 1-19.

[11] Greig, J. D., and A. Ravel. "Analysis of foodborne outbreak data reported internationally for source attribution." *International journal of food microbiology* 130.2 (2009): 77-87.

[12] Wu, Shuang, et al. "Food safety hazards associated with ready-to-bake cookie dough and its ingredients." *Food Control*73 (2017): 986-993.

[13] Olaimat, Amin N., and Richard A. Holley. "Factors influencing the microbial safety of fresh produce: a review." *Food microbiology* 32.1 (2012): 1-19.

[14] Barco, Lisa, et al. "Salmonella source attribution based on microbial subtyping." *International Journal of Food Microbiology* 163.2-3 (2013): 193-203.

[15] Shi, Chunlei, et al. "Molecular methods for serovar determination of Salmonella." *Critical reviews in microbiology*41.3 (2015): 309-325.

[16] Hilton, Shannon Huey, and Mark A. Hayes. "A mathematical model of dielectrophoretic data to connect measurements with cell properties." *Analytical and bioanalytical chemistry* 411.10 (2019): 2223-2237.

[17] Staton, Sarah JR, et al. "Characterization of particle capture in a sawtooth patterned insulating electrokinetic microfluidic device." *Electrophoresis* 31.22 (2010): 3634-3641.

[18] Jones, Paul V., et al. "Differentiation of Escherichia coli serotypes using DC gradient insulator dielectrophoresis." *Analytical and bioanalytical chemistry* 406.1 (2014): 183-192.

[19] Jones, Paul V., et al. "Biophysical separation of Staphylococcus epidermidis strains based on antibiotic resistance." *Analyst* 140.15 (2015): 5152-5161.

[20] Crowther, Claire V., et al. "Isolation and identification of Listeria monocytogenes utilizing DC insulator-based dielectrophoresis." *Analytica chimica acta* 1068 (2019): 41-51.

[21] Pethig, Ronald. "Limitations of the Clausius-Mossotti function used in dielectrophoresis and electrical impedance studies of biomacromolecules." *Electrophoresis* 40.18-19 (2019): 2575-2583.

[22] Labeed, Fatima H., et al. "Assessment of multidrug resistance reversal using dielectrophoresis and flow cytometry." *Biophysical journal* 85.3 (2003): 2028-2034.

[23] Chin, Sue, et al. "Rapid assessment of early biophysical changes in K562 cells during apoptosis determined using dielectrophoresis." *international Journal of nanomedicine* 1.3 (2006): 333.

[24] Coley, Helen M., et al. "Biophysical characterization of MDR breast cancer cell lines reveals the cytoplasm is critical in determining drug sensitivity." *Biochimica et Biophysica Acta (BBA)-General Subjects* 1770.4 (2007): 601-608.

[25] Xiao, Xuan, Zhi-Cheng Wu, and Kuo-Chen Chou. "A multi-label classifier for predicting the subcellular localization of gram-negative bacterial proteins with both single and multiple sites." *PloS one* 6.6 (2011).

[26] Matarlo, Joe S., et al. "A methyl 4-oxo-4-phenylbut-2-enoate with in vivo activity against MRSA that inhibits MenB in the bacterial menaquinone biosynthesis pathway." *ACS infectious diseases* 2.5 (2016): 329-340.

[27] Fernandez, Renny E., et al. "Microbial analysis in dielectrophoretic microfluidic systems." *Analytica chimica acta*966 (2017): 11-33.

[28] Rohani, Ali, et al. "Single-cell electro-phenotyping for rapid assessment of Clostridium difficile heterogeneity under vancomycin treatment at sub-MIC (minimum inhibitory concentration) levels." *Sensors and Actuators B: Chemical*276 (2018): 472-480.

[29] Liu, Yameng, et al. "Identification of neural stem and progenitor cell subpopulations using DC insulator-based dielectrophoresis." *Analyst* 144.13 (2019): 4066-4072.

[30] Ashton, Philip M., et al. "Identification of Salmonella for public health surveillance using whole genome sequencing." *PeerJ* 4 (2016): e1752.

[31] Ng, Pauline C., and Ewen F. Kirkness. "Whole genome sequencing." *Genetic variation*. Humana Press, Totowa, NJ, 2010. 215-226.

CHAPTER 7

SUMMARY AND CONCLUSIONS

7.1 Summary

The technique of DC-iDEP has been developed and employed here towards identifying, characterizing and separating subpopulations of bioparticles with higher resolution. The separated subsets have potential roles in more efficacious transplantation and more accurate proteomic studies. The technique was also applied to differentiation of *Salmonella* serotypes and proteins aiming at developing a tool for simpler characterization of microorganisms and small particles.

This dissertation identified and characterized subpopulations of bioparticles by DC-iDEP in presented in several different chapters. The characterization and separation theory was introduced in Chapter 2 and is based on biophysical properties of particles, as specifically represented by EKMr. Neural stem and progenitor cells subpopulations were isolated and characterized in work presented in Chapter 3. NSPCs with different final fate demonstrated distinguishing distribution behaviors. Compared to controlled more homogenous HEK cells, NSPCs showed larger SD and %RSD. The cells detected at higher EKMr and lower EKMr are consistent with the final fate increasing or decreasing trend after GlcNAc treatment or further embryonic development. Insulin vesicle subpopulations were studied and the work was presented in Chapter 4. The stacked subpopulations captured at high voltages started to spread out across the channel with lower voltages applied. Subpopulations were identified and peaks were characterized by EKMr showing good consistency and accuracy. New development of DEP theory on

proteins were tested and verified in the work described in Chapter 5. Proteins were successfully concentrated and characterized by DC-iDEP indicating a potential role of DEP use for characterizing proteins. In Chapter 6, four strains of Salmonella serotypes as characterized by differing antigens were captured, characterized and distinguished by DC-iDEP for the first time. The serotypes of salmonella tested showed distinguishing behaviors. These results demonstrate DC-iDEP is a powerful tool of detecting and isolating bioparticles which are closely related based on their biophysical behaviors.

7.2 Future Directions

Achievements of identification and characterization has been accomplished with remaining interesting future works for genotype and phenotype studies of the separated subpopulations. Extraction of the bioparticles techniques from the channels are expected for further characterization of bioparticle proteomics by mass spectrometry.

Future works may be carried out in several different ways. One strategy is to take advantage of side channel designs for sample collection. Particles will be driven by pressure or air to side channels for separation and further characterization. Another strategy has been initially tested shown in Figure 7.1. This strategy is based on the poking and extraction of subpopulations at where they were concentrated. Even the material and extraction needle blocking are still challenges, the further development of the methods will enable more paralleled channel extraction to be possible. Also, on chip analysis could be performed by NanoSight to study the size distribution and concentration of the bioparticles. Laser scattering will be used to characterize the subpopulations profile differences.

These strategies aim at improving the throughput the microdevices and helps to overcome the difficulties of the inaccuracy of characterization induced by low sensitivity of mass spectrometry.

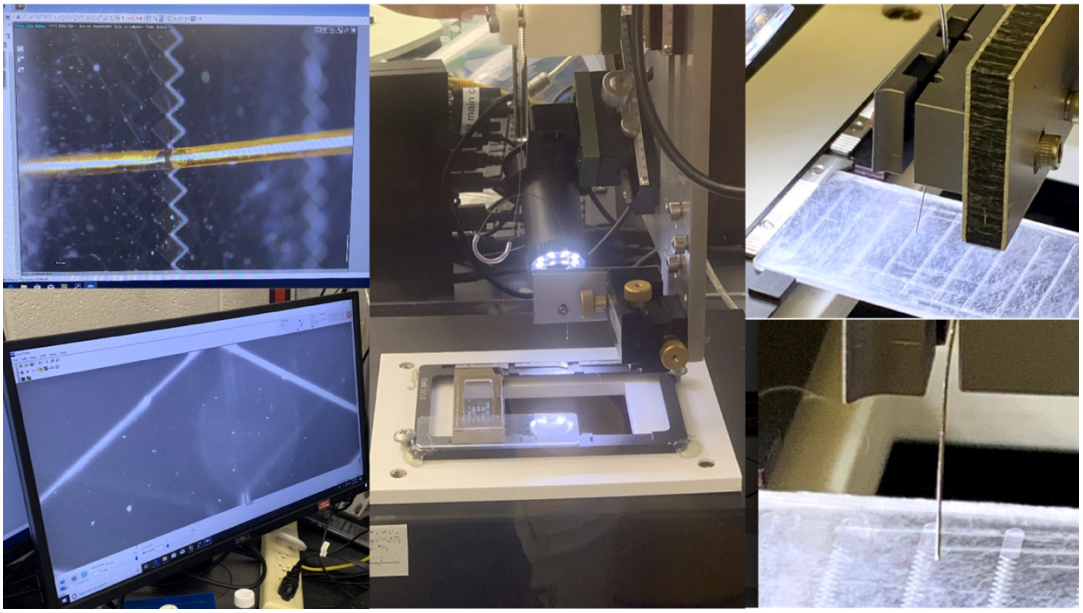

Figure 7.1 Future off-chip characterization device. A needle will be used for puncturing the covered PDMS exactly at where the bioparticles are concentrated. The extracted bio samples will be injected and analyzed by ultra-sensitive MS for high information collection including genotype and phenotype.

REFERENCES

[1] Darzynkiewicz, Zbigniew, et al. *Recent Advances in Cytometry, Part B: Advances in Applications*. Academic Press, 2011.

[2] Prince, M. E., et al. "Identification of a subpopulation of cells with cancer stem cell properties in head and neck squamous cell carcinoma." *Proceedings of the National Academy of Sciences* 104.3 (2007): 973-978.

[3] Holyoake, Tessa, et al. "Isolation of a highly quiescent subpopulation of primitive leukemic cells in chronic myeloid leukemia." *Blood, The Journal of the American Society of Hematology* 94.6 (1999): 2056-2064.

[4] Flow cytometry Thomas A. Fleisher, João Bosco de Oliveira, in Clinical Immunology (Third Edition), 2008

[5] Delves, Peter J., and Ivan Maurice Roitt. *Encyclopedia of immunology*. Academic Press, 1998.

[6] Pang, Roberta, et al. "A subpopulation of CD26+ cancer stem cells with metastatic capacity in human colorectal cancer." *Cell stem cell* 6.6 (2010): 603-615.

[7] Wicha, Max S., Suling Liu, and Gabriela Dontu. "Cancer stem cells: an old idea—a paradigm shift." *Cancer research* 66.4 (2006): 1883-1890.

[8] Prince, M. E., et al. "Identification of a subpopulation of cells with cancer stem cell properties in head and neck squamous cell carcinoma." *Proceedings of the National Academy of Sciences* 104.3 (2007): 973-978.

[9] Suetsugu, Atsushi, et al. "Characterization of CD133+ hepatocellular carcinoma cells as cancer stem/progenitor cells." *Biochemical and biophysical research communications*351.4 (2006): 820-824.

[10] Zhang, Shu, et al. "Identification and characterization of ovarian cancer-initiating cells from primary human tumors." *Cancer research* 68.11 (2008): 4311-4320.

[11] Fang, Dong, et al. "A tumorigenic subpopulation with stem cell properties in melanomas." *Cancer research* 65.20 (2005): 9328-9337.

[12] Colter, David C., et al. "Rapid expansion of recycling stem cells in cultures of plastic-adherent cells from human bone marrow." *Proceedings of the National Academy of Sciences*97.7 (2000): 3213-3218.

[13] Martín, Pilar, et al. "Characterization of a new subpopulation of mouse CD8alpha+ B220+ dendritic cells endowed with type 1 interferon production capacity and tolerogenic potential." *Blood* 100.2 (2002): 383-390.

[14] Rocheteau, Pierre, et al. "A subpopulation of adult skeletal muscle stem cells retains all template DNA strands after cell division." Cell 148.1-2 (2012): 112-125.

[15] Terstappen, L. W., Meredith Safford, and Michael R. Loken. "Flow cytometric analysis of human bone marrow. III. Neutrophil maturation." *Leukemia* 4.9 (1990): 657-663.

[16] Bhagat, Ali Asgar S., et al. "Microfluidics for cell separation." *Medical & biological engineering & computing* 48.10 (2010): 999-1014.

[17] Brown, Michael, and Carl Wittwer. "Flow cytometry: principles and clinical applications in hematology." *Clinical chemistry*46.8 (2000): 1221-1229.

[18] Nicoletti, I., et al. "A rapid and simple method for measuring thymocyte apoptosis by propidium iodide staining and flow cytometry." *Journal of immunological methods* 139.2 (1991): 271-279.

[19] Holyoake, Tessa, et al. "Isolation of a highly quiescent subpopulation of primitive leukemic cells in chronic myeloid leukemia." *Blood, The Journal of the American Society of Hematology* 94.6 (1999): 2056-2064.

[20] Fukusumi, T., et al. "CD10 as a novel marker of therapeutic resistance and cancer stem cells in head and neck squamous cell carcinoma." *British journal of cancer* 111.3 (2014): 506-514.

[21] Radbruch, Andreas, et al. "High-gradient magnetic cell sorting." *Methods in cell biology*. Vol. 42. Academic Press, 1994. 387-403.

[22] Owen, Charles S., and Norman L. Sykes. "Magnetic labeling and cell sorting." *Journal of immunological methods* 73.1 (1984): 41-48.

[23] Thiel, Andreas, Alexander Scheffold, and Andreas Radbruch. "Immunomagnetic cell sorting—pushing the limits." *Immunotechnology* 4.2 (1998): 89-96.

[24] Hansel, Trevor T., et al. "An improved immunomagnetic procedure for the isolation of highly purified human blood eosinophils." *Journal of immunological methods* 145.1-2 (1991): 105-110.

[25] Schmitz, Jürgen, and Andreas Radbruch. "Distinct antigen presenting cell-derived signals induce Th cell proliferation and expression of effector cytokines." *International immunology* 4.1 (1992): 43-51.

[26] Kato, Kimitaka, and Andreas Radbruch. "Isolation and characterization of CD34+ hematopoietic stem cells from human peripheral blood by high-gradient magnetic cell sorting." *Cytometry: The Journal of the International Society for Analytical Cytology* 14.4 (1993): 384-392.

[27] Vollenweider, Peter, et al. "Differential effects of hyperinsulinemia and carbohydrate metabolism on sympathetic nerve activity and muscle blood flow in humans." *The Journal of clinical investigation* 92.1 (1993): 147-154.

[28] Irsch, Johanns, et al. "Switch recombination in normal IgA1+ B lymphocytes." *Proceedings of the National Academy of Sciences* 91.4 (1994): 1323-1327.

[29] Kronick, Paul, and Richard W. Gilpin. "Use of superparamagnetic particles for isolation of cells." *Journal of biochemical and biophysical methods* 12.1-2 (1986): 73-80.

[30] Zhang, Qunzhou, et al. "A subpopulation of CD133+ cancer stem-like cells characterized in human oral squamous cell carcinoma confer resistance to chemotherapy." *Cancer letters*289.2 (2010): 151-160.

[31] Servida, Federica, et al. "Functional and morphological characterization of immunomagnetically selected CD34+ hematopoietic progenitor cells." *Stem Cells* 14.4 (1996): 430-438.

[32] Manent, Jan, et al. "Magnetic cell sorting for enriching Schwann cells from adult mouse peripheral nerves." *Journal of neuroscience methods* 123.2 (2003): 167-173.

[33] Singh, Sheila K., et al. "Identification of human brain tumour initiating cells." *nature* 432.7015 (2004): 396-401.

[34] Hoffmann, Beate, et al. "A new Medicago truncatula line with superior in vitro regeneration, transformation, and symbiotic properties isolated through cell culture selection." *Molecular plant-microbe interactions* 10.3 (1997): 307-315.

[35] Smith, Barry H., et al. "Three-dimensional culture of mouse renal carcinoma cells in agarose macrobeads selects for a subpopulation of cells with cancer stem cell or cancer progenitor properties." *Cancer research* 71.3 (2011): 716-724.

[36] Schild, G. C., et al. "Evidence for host-cell selection of influenza virus antigenic variants." *Nature* 303.5919 (1983): 706-709.

[37] Brakke, Myron K. "Density gradient centrifugation: a new separation technique1." *Journal of the American Chemical Society* 73.4 (1951): 1847-1848.

[38] Ford, T., J. Graham, and D. Rickwood. "Iodixanol: a nonionic iso-osmotic centrifugation medium for the formation of self-generated gradients." *Analytical biochemistry* 220.2 (1994): 360-366.

[39] Graham, J., T. Ford, and D. Rickwood. "The preparation of subcellular organelles from mouse liver in self-generated gradients of iodixanol." *Analytical biochemistry* 220.2 (1994): 367-373.

[40] Timonen, T., and E1 Saksela. "Isolation of human NK cells by density gradient centrifugation." *Journal of immunological methods* 36.3-4 (1980): 285-291.

[41] Schwitzguebel, Jean-Paul, and Paul-André Siegenthaler. "Purification of peroxisomes and mitochondria from spinach leaf by Percoll gradient centrifugation." *Plant Physiology* 75.3 (1984): 670-674.

[42] Tamir, Hadassah, and Charles Gilvarg. "Density gradient centrifugation for the separation of sporulating forms of bacteria." *Journal of Biological Chemistry* 241.5 (1966): 1085-1090.

[43] Filipski, Jan, Jean-Paul Thiery, and Giorgio Bernardi. "An analysis of the bovine genome by Cs2SO4—Ag+ density gradient centrifugation." *Journal of molecular biology* 80.1 (1973): 177-197.

[44] Autebert, Julien, et al. "Microfluidic: an innovative tool for efficient cell sorting." *Methods* 57.3 (2012): 297-307.

[45] Reece, Amy, et al. "Microfluidic techniques for high throughput single cell analysis." *Current opinion in biotechnology* 40 (2016): 90-96.

[46] Wu, Huei-Wen, et al. "An integrated microfluidic system for isolation, counting, and sorting of hematopoietic stem cells." *Biomicrofluidics* 4.2 (2010): 024112.

[47] Xu, Ye, et al. "Aptamer-based microfluidic device for enrichment, sorting, and detection of multiple cancer cells." *Analytical chemistry* 81.17 (2009): 7436-7442.

[48] Doh, Il, and Young-Ho Cho. "A continuous cell separation chip using hydrodynamic dielectrophoresis (DEP) process." *Sensors and Actuators A: Physical* 121.1 (2005): 59-65.

[49] Jones, Thomas B., and Thomas Byron Jones. *Electromechanics of particles*. Cambridge University Press, 2005.

[50] Nili, Hossein, and Nicolas G. Green. "Higher-order dielectrophoresis of nonspherical particles." *Physical Review E* 89.6 (2014): 063302.

[51] Hilton, Shannon Huey, and Mark A. Hayes. "A mathematical model of dielectrophoretic data to connect measurements with cell properties." *Analytical and bioanalytical chemistry* 411.10 (2019): 2223-2237.

[52] Staton, Sarah JR, et al. "Characterization of particle capture in a sawtooth patterned insulating electrokinetic microfluidic device." *Electrophoresis* 31.22 (2010): 3634-3641.

[53] Crowther, Claire V., et al. "Isolation and identification of Listeria monocytogenes utilizing DC insulator-based dielectrophoresis." *Analytica chimica acta* 1068 (2019): 41-51.

[54] Vahey, Michael D., and Joel Voldman. "An equilibrium method for continuous-flow cell sorting using dielectrophoresis." *Analytical chemistry* 80.9 (2008): 3135-3143.

[55] Gascoyne, Peter RC, et al. "Dielectrophoretic separation of cancer cells from blood." *IEEE transactions on industry applications* 33.3 (1997): 670-678.

[56] Song, Hongjun, et al. "Continuous-flow sorting of stem cells and differentiation products based on dielectrophoresis." *Lab on a Chip* 15.5 (2015): 1320-1328.

[57] Nourse, J. L., et al. "Membrane biophysics define neuron and astrocyte progenitors in the neural lineage." *Stem Cells* 32.3 (2014): 706-716.

[58] Kang, Yuejun, et al. "DC-Dielectrophoretic separation of biological cells by size." *Biomedical microdevices* 10.2 (2008): 243-249.

[59] Stringari, Chiara, et al. "Phasor fluorescence lifetime microscopy of free and protein-bound NADH reveals neural stem cell differentiation potential." *PloS one* 7.11 (2012).

[60] Vrtovec, Bojan, et al. "Effects of intracoronary CD34+ stem cell transplantation in nonischemic dilated cardiomyopathy patients: 5-year follow-up." *Circulation research* 112.1 (2013): 165-173.

[61] Thomson, James A., et al. "Embryonic stem cell lines derived from human blastocysts." *science* 282.5391 (1998): 1145-1147.

[62] Gage, Fred H. "Mammalian neural stem cells." *Science*287.5457 (2000): 1433-1438.

[63] Temple, Sally. "The development of neural stem cells." *Nature*414.6859 (2001): 112-117.

[64] Arulmoli, Janahan, et al. "Static stretch affects neural stem cell differentiation in an extracellular matrix-dependent manner." *Scientific reports* 5.1 (2015): 1-8.

[65] Anderson, Aileen J., et al. "Preclinical efficacy failure of human CNS-derived stem cells for use in the pathway study of cervical spinal cord injury." *Stem Cell Reports* 8.2 (2017): 249-263.

[66] Marsh, Samuel E., et al. "HuCNS-SC human NSCs fail to differentiate, form ectopic clusters, and provide no cognitive benefits in a transgenic model of Alzheimer's disease." *Stem cell reports* 8.2 (2017): 235-248.

[67] Temple, Sally, and Lorenz Studer. "Lessons learned from pioneering neural stem cell studies." *Stem cell reports* 8.2 (2017): 191-193.

[68] Gage, Fred H., and Sally Temple. "Neural stem cells: generating and regenerating the brain." *Neuron* 80.3 (2013): 588-601.

[69] Groszer, Matthias, et al. "PTEN negatively regulates neural stem cell self-renewal by modulating G0-G1 cell cycle entry." *Proceedings of the National Academy of Sciences* 103.1 (2006): 111-116.

[70] Labeed, Fatima H., et al. "Biophysical characteristics reveal neural stem cell differentiation potential." *PloS one* 6.9 (2011).

[71] Qian, Xueming, et al. "Timing of CNS cell generation: a programmed sequence of neuron and glial cell production from isolated murine cortical stem cells." *Neuron* 28.1 (2000): 69-80.

[72] Blurton-Jones, Mathew, et al. "Neural stem cells improve cognition via BDNF in a transgenic model of Alzheimer disease." *Proceedings of the National Academy of Sciences*106.32 (2009): 13594-13599.

[73] Drago, Denise, et al. "The stem cell secretome and its role in brain repair." *Biochimie* 95.12 (2013): 2271-2285.

[74] Simon, Melinda G., et al. "Increasing label-free stem cell sorting capacity to reach transplantation-scale throughput." *Biomicrofluidics* 8.6 (2014): 064106.

[75] Adams, Tayloria NG, et al. "Separation of neural stem cells by whole cell membrane capacitance using dielectrophoresis." *Methods* 133 (2018): 91-103.

[76] Nourse, J. L., et al. "Membrane biophysics define neuron and astrocyte progenitors in the neural lineage." *Stem Cells* 32.3 (2014): 706-716.

[77] Ding, Jie, et al. "Concentration of Sindbis virus with optimized gradient insulator-based dielectrophoresis." *Analyst* 141.6 (2016): 1997-2008.

[78] Jones, Paul V., et al. "Biophysical separation of Staphylococcus epidermidis strains based on antibiotic resistance." *Analyst* 140.15 (2015): 5152-5161.

[79] Yale, Andrew R., et al. "Cell surface N-glycans influence electrophysiological properties and fate potential of neural stem cells." *Stem cell reports* 11.4 (2018): 869-882.

[80] Weiss, Noah G., et al. "Dielectrophoretic mobility determination in DC insulator-based dielectrophoresis." *Electrophoresis* 32.17 (2011): 2292-2297.

[81] Crowther, Claire V., and Mark A. Hayes. "Refinement of insulator-based dielectrophoresis." *Analyst* 142.9 (2017): 1608-1618.

[82] Jones, Paul V., and Mark A. Hayes. "Development of the resolution theory for gradient insulator-based dielectrophoresis." *Electrophoresis* 36.9-10 (2015): 1098-1106

[83] LaLonde, Alexandra, et al. "Effect of insulating posts geometry on particle manipulation in insulator based dielectrophoretic devices." *Journal of Chromatography A* 1344 (2014): 99-108.

[84] Jorgenson, James W., and Krynn DeArman Lukacs. "High-resolution separations based on electrophoresis and electroosmosis." *Journal of chromatography A* 218 (1981): 209-216.

[85] Jones, Paul V., Sarah JR Staton, and Mark A. Hayes. "Blood cell capture in a sawtooth dielectrophoretic microchannel." *Analytical and bioanalytical chemistry* 401.7 (2011): 2103.

[86] Shaw, Gerry, et al. "Preferential transformation of human neuronal cells by human adenoviruses and the origin of HEK 293 cells." *The FASEB Journal* 16.8 (2002): 869-871.

[87] Daly, Emma, and Brian R. Saunders. "Temperature–dependent electrophoretic mobility and hydrodynamic radius measurements of poly (N-isopropylacrylamide) microgel particles: structural insights." *Physical Chemistry Chemical Physics* 2.14 (2000): 3187-3193.

[88] Anderson, Theodore W. "On the distribution of the two-sample Cramer-von Mises criterion." *The Annals of Mathematical Statistics* (1962): 1148-1159.

[89] Suckale, Jakob, and Michele Solimena. "The insulin secretory granule as a signaling hub." *Trends in Endocrinology & Metabolism* 21.10 (2010): 599-609.

[90] Thurmond, Debbie C. "Regulation of insulin action and insulin secretion by SNARE-mediated vesicle exocytosis." *Mechanisms of Insulin Action*. Springer, New York, NY, 2007. 52-70.

[91] Khyade, Vitthalrao B. "Herbals and Their Compounds Targeting Pancreatic Beta Cells for the Treatment of Diabetes." *International Journal of Scientific Studies* 6.3 (2018): 1-44.

[92] Hickey, Anthony JR, et al. "Proteins associated with immunopurified granules from a model pancreatic islet β-cell system: proteomic snapshot of an endocrine secretory granule." *Journal of proteome research* 8.1 (2009): 178-186.

[93] Schvartz, Domitille, et al. "Improved characterization of the insulin secretory granule proteomes." *Journal of proteomics*75.15 (2012): 4620-4631.

[94] Rutter, Guy A., and Elaine V. Hill. "Insulin vesicle release: walk, kiss, pause… then run." *Physiology* 21.3 (2006): 189-196.

[95] Singla, Jitin, et al. "Opportunities and challenges in building a spatiotemporal multi-scale model of the human pancreatic β cell." *Cell* 173.1 (2018): 11-19.

[96] Hutton, J. C., E. J. Penn, and M. Peshavaria. "Isolation and characterisation of insulin secretory granules from a rat islet cell tumour." *Diabetologia* 23.4 (1982): 365-373.

[97] Lindall Jr, Arnold W., et al. "Isolation of an insulin secretion granule fraction." *The Journal of cell biology* 19.2 (1963): 317-324.

[98] Andrzejewski, Danielle, et al. "Activins A and B regulate fate-determining gene expression in islet cell lines and islet cells from male mice." *Endocrinology* 156.7 (2015): 2440-2450.

[99] White et al, Incretin Effect on Granule Density, in revision

[100] Moore, John H., et al. "Conductance-Based Biophysical Distinction and Microfluidic Enrichment of Nanovesicles Derived from Pancreatic Tumor Cells of Varying Invasiveness." *Analytical chemistry* 91.16 (2019): 10424-10431.

[101] Pethig, Ronald. "Where is dielectrophoresis (DEP) going?." *Journal of The Electrochemical Society* 164.5 (2017): B3049-B3055.

[102] Matyushov, Dmitry V. "Dipolar response of hydrated proteins." *The Journal of chemical physics* 136.8 (2012): 02B618.

[103] Shoichet, Brian K., et al. "A relationship between protein stability and protein function." *Proceedings of the National Academy of Sciences* 92.2 (1995): 452-456.

[104] Murphy, Mary G. "Dietary fatty acids and membrane protein function." *The Journal of nutritional biochemistry* 1.2 (1990): 68-79.

[105] Gimeno, Ruth E. "Fatty acid transport proteins." *Current opinion in lipidology* 18.3 (2007): 271-276.

[106] Lesley, Scott A. "High-throughput proteomics: protein expression and purification in the postgenomic world." *Protein expression and purification* 22.2 (2001): 159-164.

[107] Hilbrig, Frank, and Ruth Freitag. "Protein purification by affinity precipitation." *Journal of chromatography B* 790.1-2 (2003): 79-90.

[108] Franzreb, Matthias, et al. "Protein purification using magnetic adsorbent particles." *Applied microbiology and biotechnology*70.5 (2006): 505-516.

[109] Scopes, Robert K. *Protein purification: principles and practice*. Springer Science & Business Media, 2013.

[110] Merlini, Giampaolo, and Vittorio Bellotti. "Lysozyme: a paradigmatic molecule for the investigation of protein structure, function and misfolding." *Clinica chimica acta* 357.2 (2005): 168-172.

[111] Mckenzie, Hugh A., and Frederick H. White Jr. "Lysozyme and α-lactalbumin: structure, function, and interrelationships." *Advances in protein chemistry*. Vol. 41. Academic Press, 1991. 173-315.

[112] Vidarsson, Gestur, Gillian Dekkers, and Theo Rispens. "IgG subclasses and allotypes: from structure to effector functions." *Frontiers in immunology* 5 (2014): 520.

[113] Zhang, Chen-Yan, et al. "Effect of real-world sounds on protein crystallization." *International journal of biological macromolecules* 112 (2018): 841-851.

[114] Ünlü, Mustafa, Mary E. Morgan, and Jonathan S. Minden. "Difference gel electrophoresis. A single gel method for detecting changes in protein extracts." *Electrophoresis* 18.11 (1997): 2071-2077.

[115] Brunelle, Julie L., and Rachel Green. "One-dimensional SDS-polyacrylamide gel electrophoresis (1D SDS-PAGE)." *Methods in enzymology*. Vol. 541. Academic Press, 2014. 151-159.

[116] Rais, Isam, Michael Karas, and Hermann Schägger. "Two-dimensional electrophoresis for the isolation of integral membrane proteins and mass spectrometric identification." *Proteomics* 4.9 (2004): 2567-2571.

[117] Kinoshita, Eiji, Emiko Kinoshita-Kikuta, and Tohru Koike. "Separation and detection of large phosphoproteins using Phos-tag SDS-PAGE." *Nature protocols* 4.10 (2009): 1513.

[118] Schägger, Hermann. "Tricine–sds-page." *Nature protocols* 1.1 (2006): 16.

[119] Karpe, Fredrik, and Anders Hamsten. "Determination of apolipoproteins B-48 and B-100 in triglyceride-rich lipoproteins by analytical SDS-PAGE." *Journal of lipid research* 35.7 (1994): 1311-1317.

[120] Claeys, Erik, et al. "Quantification of beef myofibrillar proteins by SDS-PAGE." *Meat Science* 39.2 (1995): 177-193.

[121] Carraro, Ugo, and Claudia Catani. "A sensitive SDS-PAGE method separating myosin heavy chain isoforms of rat skeletal muscles reveals the heterogeneous nature of the embryonic myosin." *Biochemical and biophysical research communications* 116.3 (1983): 793-802.

[122] Lemmo, Anthony V., and James W. Jorgenson. "Two-dimensional protein separation by microcolumn size-exclusion chromatography-capillary zone electrophoresis." *Journal of Chromatography A* 633.1-2 (1993): 213-220.

[123] Irvine, G. Brent. "High-performance size-exclusion chromatography of peptides." *Journal of Biochemical and Biophysical Methods* 56.1-3 (2003): 233-242.

[124] Lecchi, Paolo, et al. "Size-exclusion chromatography in multidimensional separation schemes for proteome analysis." *Journal of biochemical and biophysical methods* 56.1-3 (2003): 141-152.

[125] Ahmed, Faizy, and Bijan Modrek. "Biosep-SEC-S high-performance size-exclusion chromatographic columns for proteins and peptides." *Journal of Chromatography A* 599.1-2 (1992): 25-33.

[126] Ahrer, K., et al. "Analysis of aggregates of human immunoglobulin G using size-exclusion chromatography, static and dynamic light scattering." *Journal of chromatography A*1009.1-2 (2003): 89-96.

[127] Righetti, Pier Giorgio, and James W. Drysdale. "Isoelectric focusing in gels." *Journal of Chromatography A* 98.2 (1974): 271-321.

[128] Egatz-Gomez, Ana, and Wolfgang Thormann. "Micropreparative isoelectric focusing protein separation in a suspended drop." *Electrophoresis* 32.12 (2011): 1433-1437.

[129] Bjellqvist, Bengt, et al. "Isoelectric focusing in immobilized pH gradients: principle, methodology and some applications." *Journal of biochemical and biophysical methods* 6.4 (1982): 317-339.

[130] Pritchett, Thomas J. "Capillary isoelectric focusing of proteins." *Electrophoresis* 17.7 (1996): 1195-1201.

[131] O'Neill, Roger A., et al. "Isoelectric focusing technology quantifies protein signaling in 25 cells." *Proceedings of the National Academy of Sciences* 103.44 (2006): 16153-16158.

[132] Vesterberg, Olof. "Isoelectric focusing of proteins in polyacrylamide gels." *Biochimica et Biophysica Acta (BBA)-Protein Structure* 257.1 (1972): 11-19.

[133] Pethig, Ronald. "Limitations of the Clausius-Mossotti function used in dielectrophoresis and electrical impedance studies of biomacromolecules." *Electrophoresis* 40.18-19 (2019): 2575-2583.

[134] Matyushov, Dmitry V. "Electrostatic solvation and mobility in uniform and non-uniform electric fields: From simple ions to proteins." *Biomicrofluidics* 13.6 (2019): 064106.

[135] Waskasi, M. and M. Heyden, Microscopic driving forces of protein dielectrophoresis. *Journal of Physical Chemistry B*, 2019. 123: p. In preparation.

[136] Clarke, Richard W., et al. "Trapping of proteins under physiological conditions in a nanopipette." *Angewandte Chemie International Edition* 44.24 (2005): 3747-3750.

[137] Lapizco-Encinas, Blanca H., Sandra Ozuna-Chacón, and Marco Rito-Palomares. "Protein manipulation with insulator-based dielectrophoresis and direct current electric fields." *Journal of Chromatography A* 1206.1 (2008): 45-51.

[138] Chou, Chia-Fu, et al. "Electrodeless dielectrophoresis of single-and double-stranded DNA." *Biophysical journal* 83.4 (2002): 2170-2179.

[139] Cummings, Eric B., and Anup K. Singh. "Dielectrophoresis in microchips containing arrays of insulating posts: theoretical and experimental results." *Analytical chemistry* 75.18 (2003): 4724-4731.

[140] Kvasnička, František. "Determination of egg white lysozyme by on-line coupled capillary isotachophoresis with capillary zone electrophoresis." *Electrophoresis* 24.5 (2003): 860-864.

[141] Otte, J. A. H. J., et al. "Separation of individual whey proteins and measurement of -lactalbumin and -lactoglobulin by capillary zone electrophoresis." *Netherlands Milk and Dairy Journal* 48 (1994): 81-81.

[142] Raacke, Ilse Dorothea. "Heterogeneity studies on several proteins by means of zone electrophoresis on starch." *Archives of biochemistry and biophysics* 62.1 (1956): 184-195.

[143] Chiou, Chien-Shun, et al. "Usefulness of pulsed-field gel electrophoresis profiles for the determination of Salmonella serovars." *International journal of food microbiology* 214 (2015): 1-3.

[144] Ibrahim, George M., and Paul M. Morin. "Salmonella serotyping using whole genome sequencing." *Frontiers in microbiology* 9 (2018): 2993.

[145] Tang, Silin, et al. "Assessment and comparison of molecular subtyping and characterization methods for Salmonella." *Frontiers in microbiology* 10 (2019): 1591.

[146] Grimont, Patrick AD, and François-Xavier Weill. "Antigenic formulae of the Salmonella serovars." *WHO collaborating centre for reference and research on Salmonella* 9 (2007): 1-166.

[147] Diep, Benjamin, et al. "Salmonella serotyping; comparison of the traditional method to a microarray-based method and an in silico platform using whole genome sequencing data." *Frontiers in microbiology* 10 (2019): 2554.

[148] Centers for Disease Control and Prevention. "National Salmonella surveillance overview." *Atlanta, Georgia: US Department of Health and Human Services, CDC* (2011).

[149] Pillai, Suresh D., and Steven C. Ricke. "Review/Synthèse Bioaerosols from municipal and animal wastes: background and contemporary issues." *Canadian Journal of Microbiology*48.8 (2002): 681-696.

[150] Maciorowski, K. G., et al. "Incidence, sources, and control of food-borne Salmonella spp. in poultry feeds." *World's Poultry Science Journal* 60.4 (2004): 446-457.

[151] Park, S. Y., et al. "Environmental dissemination of foodborne Salmonella in preharvest poultry production: reservoirs, critical factors, and research

strategies." *Critical reviews in environmental science and technology* 38.2 (2008): 73-111.

[152] Olaimat, Amin N., and Richard A. Holley. "Factors influencing the microbial safety of fresh produce: a review." *Food microbiology* 32.1 (2012): 1-19.

[153] Greig, J. D., and A. Ravel. "Analysis of foodborne outbreak data reported internationally for source attribution." *International journal of food microbiology* 130.2 (2009): 77-87.

[154] Wu, Shuang, et al. "Food safety hazards associated with ready-to-bake cookie dough and its ingredients." *Food Control*73 (2017): 986-993.

[155] Olaimat, Amin N., and Richard A. Holley. "Factors influencing the microbial safety of fresh produce: a review." *Food microbiology* 32.1 (2012): 1-19.

[156] Barco, Lisa, et al. "Salmonella source attribution based on microbial subtyping." *International Journal of Food Microbiology* 163.2-3 (2013): 193-203.

[157] Shi, Chunlei, et al. "Molecular methods for serovar determination of Salmonella." *Critical reviews in microbiology*41.3 (2015): 309-325.

[158] Jones, Paul V., et al. "Differentiation of Escherichia coli serotypes using DC gradient insulator dielectrophoresis." *Analytical and bioanalytical chemistry* 406.1 (2014): 183-192.

[159] Pethig, Ronald. "Limitations of the Clausius-Mossotti function used in dielectrophoresis and electrical impedance studies of biomacromolecules." *Electrophoresis* 40.18-19 (2019): 2575-2583.

[160] Labeed, Fatima H., et al. "Assessment of multidrug resistance reversal using dielectrophoresis and flow cytometry." *Biophysical journal* 85.3 (2003): 2028-2034.

[161] Chin, Sue, et al. "Rapid assessment of early biophysical changes in K562 cells during apoptosis determined using dielectrophoresis." *international Journal of nanomedicine* 1.3 (2006): 333.

[162] Coley, Helen M., et al. "Biophysical characterization of MDR breast cancer cell lines reveals the cytoplasm is critical in determining drug sensitivity." *Biochimica et Biophysica Acta (BBA)-General Subjects* 1770.4 (2007): 601-608.

[163] Xiao, Xuan, Zhi-Cheng Wu, and Kuo-Chen Chou. "A multi-label classifier for predicting the subcellular localization of gram-negative bacterial proteins with both single and multiple sites." *PloS one* 6.6 (2011).

[164] Matarlo, Joe S., et al. "A methyl 4-oxo-4-phenylbut-2-enoate with in vivo activity against MRSA that inhibits MenB in the bacterial menaquinone biosynthesis pathway." *ACS infectious diseases* 2.5 (2016): 329-340.

[165] Fernandez, Renny E., et al. "Microbial analysis in dielectrophoretic microfluidic systems." *Analytica chimica acta*966 (2017): 11-33.

[166] Rohani, Ali, et al. "Single-cell electro-phenotyping for rapid assessment of Clostridium difficile heterogeneity under vancomycin treatment at sub-MIC (minimum inhibitory concentration) levels." *Sensors and Actuators B: Chemical*276 (2018): 472-480.

[167] Liu, Yameng, et al. "Identification of neural stem and progenitor cell subpopulations using DC insulator-based dielectrophoresis." *Analyst* 144.13 (2019): 4066-4072.

[168] Ashton, Philip M., et al. "Identification of Salmonella for public health surveillance using whole genome sequencing." *PeerJ* 4 (2016): e1752.

[169] Ng, Pauline C., and Ewen F. Kirkness. "Whole genome sequencing." *Genetic variation*. Humana Press, Totowa, NJ, 2010. 215-226.

APPENDIX A

PUBLISHED PORTIONS

Previously published work and publishable items that are listed below in each chapter. All co-authors have granted their permission for the use of the publications here.

Chapter 1

Liu, Yameng, et al. "Identification of neural stem and progenitor cell subpopulations using DC insulator-based dielectrophoresis." Analyst, 2019, 144, 4066.

Chapter 2

Liu, Yameng, et al. "Identification of neural stem and progenitor cell subpopulations using DC insulator-based dielectrophoresis." Analyst, 2019, 144, 4066.

Liu, Yameng, et al. "Differential Biophysical Behaviors of Closely Related Strains of Salmonella. " Frontiers Microbiology, 2020, Accepted, DOI: 10.3389/fmicb.2020.00302.

Chapter 3:

Liu, Yameng, et al. "Identification of neural stem and progenitor cell subpopulations using DC insulator-based dielectrophoresis." Analyst, 2019, 144, 4066.

Chapter 4:

Liu, Yameng, et al. “Biophysical identification of sub-populations of insulin granules from beta cells.” in preparation

Chapter 5:

Liu, Yameng, et al. "High resolution protein isolation, separation and characterization using high order electric field effects on a simple device." In preparation.

Chapter 6:

Liu, Yameng, et al. "Differential Biophysical Behaviors of Closely Related Strains of Salmonella. " Frontiers Microbiology, 2020, Accepted, DOI: 10.3389/fmicb.2020.00302.